ABSTRACT

A DESIGN OPTIMIZATION TECHNIQUE

APPLIED TO A SQUEEZE-FILM,

GAS, JOURNAL BEARING

By

Carl Leander Strodtman

Two different though related aspects of optimization of a compressible-fluid, squeeze-film journal bearing are treated. First, it is shown that the minimum clearance in the journal bearing can be maximized by the proper choice of the nominal clearance, the length-diameter ratio, and the excursion non-uniformity factor, for the case of fixed load force and volume. Second, it is shown that an optimum design can be selected by means of a merit function developed from the designer's value-judgement of the desired performance and cost. It is also shown that the merit function, multiplied by some suitable weighting function, can be used to select a maximax design. Although the merit function and the weighted merit function are applied to the squeeze-film journal bearing, it is believed that they constitute a design procedure of much greater generality.

A method of characterizing non-uniform driver excursion by means of its root-mean-square amplitude and a shape factor is developed.

Carl Leander Strodtman

An augmented, small-parameter solution of the squeeze-film partial differential equation including terms to the third power of the radial displacement is given. The results are compared to an alternating-direction, implicit, numerical method previously used.

A study of sensitivity to parameter changes is presented by means of a response surface defined by the second derivatives, near the optimum. Parameters not optimized are treated by employing sensitivity coefficients based on the first derivatives. Sensitivity is studied for both the clearance optimization and the merit optimization problems.

A DESIGN OPTIMIZATION TECHNIQUE APPLIED TO A SQUEEZE-FILM, GAS, JOURNAL BEARING

By

Carl Leander Strodtman

A THESIS

Submitted to
Michigan State University
in partial fulfillment of the requirements
for the degree of

DOCTOR OF PHILOSOPHY

Department of Mechanical Engineering

1968

ACKNOWLEDGEMENTS

The author wishes to thank his advisor, Dr. James V. Beck of the Michigan State University Mechanical Engineering Department, for his guidance and many helpful suggestions during the preparation of this thesis.

In addition, the author expresses thanks to the Instrument Division of Lear Siegler, Incorporated, for their financial support, for their sponsorship of the work done on this thesis, and for the use of their facilities, in particular, the digital computer.

Sincere thanks are given to Miss Anna D'Angelo and Miss Loretta Durkin for the typing of the manuscript and its numerous revisions.

Finally, the author wishes to express his appreciation to his wife, Marion, and to his children for their interest, encouragement, and forebearance throughout this graduate program.

TABLE OF CONTENTS

TABLE OF CONTENTS (Continued)

LIST OF TABLES

LIST OF FIGURES

LIST OF FIGURES (Continued)

LIST OF APPENDICES

LIST OF SYMBOLS

a	excursion amplitude at end of driver (microinches)
A	excursion shape factor ($A = b/a$)
b	excursion change at center of driver (microinches)
c	minimum clearance (microinches)
c'	minimum clearance normalized by δh_{1r}
d	fraction of maximum load at which design is optimized
f	$f_1(Z)$ evaluated at the boundaries
$f_1(Z)$	shape function of the excursion
$F(A)$	function defined on page 27
g_o, g_1, g_2	variables in differential equation for T_2
h	film thickness (microinch)
h_o	nominal film thickness (microinches)
h_1	variable in differential equation for T_1
H	film thickness normalized by h_o
H'	film thickness normalized by δh_{1r}
$\overline{H}$	time average film thickness
k_o, k_1, k_2, k_3	variables in differential equation for T_3
K	a constant, $K = (2\pi)^{1/3} p_a$
L	bearing length (inches)
m	mesh spacing in Z direction
M	merit function

M_n	merit factor
$\overline{M}_d$	weighted merit function
$M_{d,s}$	merit value of design optimized at a load equal to d, when loaded with s
n	mesh spacing in θ direction
p	pressure (lb_f per square inch)
p_a	ambient pressure (lb_f per square inch)
P	pressure normalized by p_a
Q	matrix of second derivatives
R	radius of the bearing (inches)
s	fraction of maximum load at which design is evaluated
S_k^M	sensitivity coefficient (see page 46)
t	time normalized by ω
T	film characteristic, $T = (PH)^2$
T_n	$n^{\underline{th}}$ component of T in expansion (Appendix A)
T'	film characteristic, $T' = (PH')^2$
w_n	weight exponent
W	average total bearing load (lb_f)
W_l	average bearing load per unit length (lb_f per inch)
W'	dimensionless average bearing load per unit length $W' = \frac{W_l}{2p_aR}$
x_i, x_j	generalized designation of a variable
$\overline{x}$	vector of $\Delta x_i/x_i$ values
z	longitudinal coordinate (inches)
z_L	half length of the bearing (inches)

z_{LC}	half length of the driver (inches)
Z	longitudinal coordinate normalized by R
Z_L	length-diameter ratio of bearing ($Z_L = \frac{L}{2R}$)
Z_{LC}	length-diameter ratio of driver
α	shape function, $\alpha = 1 + \frac{4A}{\pi} + \frac{A^2}{2}$
β	dimensionless "mass" parameter (see page 106)
$\delta h_1(z)$	amplitude of driver motion (microinches)
δh_{1m}	maximum drive amplitude (microinches)
δh_{1r}	root-mean-square drive amplitude (microinches)
δh_2	radial displacement (microinches)
ϵ_1	a reference drive amplitude normalized by h_o
ϵ_{1r}	root-mean-square drive amplitude normalized by h_o
ϵ'_{1r}	root-mean-square drive amplitude normalized by δh_{1r}
ϵ_2	eccentricity (radial displacement normalized by h_o)
ϵ'_2	eccentricity (radial displacement normalized by δh_{1r})
η_n	ratio of weight exponents (see page 64)
Θ	angular coordinate
μ	gas viscosity (lb_f - sec. per square inch)
ρ	gas density (lb_m per cubic inch)
σ	squeeze number (see page 11) also used in Chapter 5 for standard deviation of the load
σ'	squeeze number (see page 40)
τ	time (seconds)
ϕ	weight function (see page 95)
ω	drive frequency (radians per second)
*	a superscript asterisk denotes an optimum value

CHAPTER 1

INTRODUCTION

1.1 GAS BEARINGS

The use of a gas as a bearing lubricant has many advantages. There is an abundant supply of comparatively clean air available; gas bearings are very low friction devices having near infinite life; lubricating gases are comparatively free from adverse effects due to nuclear radiation; and for high temperature missile or low temperature cryogenic applications, gas bearings are useful because the gas viscosity does not change much over wide temperature ranges.

Gas bearings can be designed to have stiffnesses comparable to ball bearings and thus have wide applicability. Gas bearings have been used in textile spindles, machine tools, dental drills, jet engines, accelerometers, measuring instruments, and refrigerators. The first operational use of gas bearings was as gyroscope bearings for the German V-2 rockets. They are inherently well-suited in precision instruments due to their low noise when rotating and to zero friction when used as a null device. Because of the increased demand of the aero-space industry for bearings embodying the above advantages the study of gas bearings has recently been brought to a high level.

In the study of gas bearings to date, most of the work has related to basic understanding of their operation and design. Little has been done on the field of design optimization. This thesis will study one type of gas bearing only recently developed, the squeeze-film bearing. A primary objective is to show that the proper choice of parameters will maximize the minimum clearance in the bearing. A second objective is to develop a technique for design based on optimizing a series of functions developed from the designer's value judgement of the desired performance and cost.

Film lubrication occurs when two closely spaced parallel or nearly parallel surfaces are completely separated by a lubricating fluid. In order for such a film to support a load, the pressure forces in the film must be such that their resultant produces a net force. There are three main types of film bearings recognized, (1) those which depend on an external source of lubricant to create a pressure field in the film (hydrostatic or externally pressurized bearings), (2) those which depend on relative tangential motion of the bearing surfaces to create the pressure field (hydrodynamic or self-acting bearings), and (3) those which depend on relative normal motion of the bearing surfaces to create the pressure field (squeeze-film bearings). This paper will concern itself with the squeeze-film bearing using a compressible lubricant (gas), which should, more properly, be called the "steady-state, compressible-fluid squeeze-film bearing" to distinguish it from the transient bearing which is generated when two surfaces approach or recede from each other. It should also be distinguished from the incompressible fluid

squeeze-film bearing in that the compressibility of the lubricant plays a prime role in its operation.

In the absence of tangential velocity or of external pressurization, the squeeze-film gas bearing is able to support a load by virtue of a continuous high-frequency oscillation normal to the bearing surface.

The squeeze-film bearing can be thought of as a self-pressurizing bearing. Its advantages over the externally pressurized bearing include compactness, simplicity of construction, and ease in regulation. Further it seems to be relatively free of the stability problems associated with the externally pressurized bearing.

The high-frequency oscillation can be sustained by electrical means through a suitable transducer, hence a suitable oscillator for driving the transducer is required. To conserve driving power, the transducer is operated at one of its mechanical resonant frequencies.

The squeeze-film bearing, in its simplest form, is created between two plates, one plate vibrating normal to the other. If the plates are closely spaced in relation to their lateral extent and if the vibration is at a relatively high frequency (both conditions are usual), then the effect, due to the finite viscosity of the gas, is to trap the gas between the plates at a superambient density, i.e., more gas can flow in when the plates are separated during the vibration cycle than can flow out when the plates are close together. In

the limit as a parameter, known as the squeeze number, goes to infinity the trapped gas is completely isolated from the ambient and no external flow of gas occurs after an initial pump period. With the gas trapped between two closely spaced plates, the effect of a non-linearity due to Boyle's law is to create a non-zero cyclic average pressure on the plates.

Although described above in terms of a flat plate, the squeeze-film bearing can take many forms such as a round disk, journal, sphere or cone.

1.2 LITERATURE REVIEW

Gross[1] reports that the Frenchman G. Hirn[2] in 1854 was apparently the first to mention that air might be used as a lubricant but that this type bearing was not discussed again until Kingsbury[3] built an air-lubricated journal bearing in 1897.

The Englishman W. J. Harrison[4] in 1913 presented solutions for infinitely long gas-lubricated slider and journal bearings. It is only since about 1950 that the study of gas bearings has been noticeably accelerated.

Taylor and Saffman[5] in 1957, stated that the Reiner effect[6] was probably due to either non-parallel plates or to normal vibrations rather than due to a non-Newtonian or visco-elastic property of air. They showed that it was possible to develop an average load-carrying pressure distribution in a compressible film by a relative normal motion of two surfaces. This is probably the first reference to a compressible squeeze-film bearing.

One of the first analyses of squeeze effects for a gas bearing was that of Langlois[7], who considered the linearized problems for small periodic variations in the gap between infinitely long parallel plates and the gap between parallel disks. The case of periodic variation in the gap between parallel coaxial disks has also been considered experimentally and theoretically (numerical integration using a finite-difference scheme) by Salbu[8]. Malanoski and Pan[9] in the discussion of this paper, developed a mass content rule which allowed them to obtain the instantaneous film force and mean load-carrying capacity for large squeeze numbers. Their results were in excellent agreement with those of Salbu.

Pan[10] was the first to publish an asymptotic method for large squeeze numbers which is applicable to arbitrary bearing shapes and arbitrary modes of oscillation. These asymptotic techniques have been applied to determine the load support capacity of a number of different bearing shapes such as (1) the infinitely long journal bearing by Pan, Malonoski, Broussard, and Burch[11], the finite journal by Beck and Strodtman[12], the rotating sphere by Chiang, Malonoski, and Pan[13], the non-rotating sphere by Beck and Strodtman[14], and a variety of shapes by Pan and Broussard[15].

Other papers published include the following. A treatment of a high frequency instability for the infinitely long squeeze-film journal bearing is given by Beck and Strodtman[16]. A treatment of the same form of instability in the finite journal bearing is by Nolan[17]. An analysis has been developed by Elrod[18] of the effect of low frequency vibration in the bearing. This analysis has been

applied to spherical bearings by Pan and Chiang[19]. The asymptotic analysis for squeeze-film bearings including the effects of tangential motion (the hybrid bearing) has been rederived on the basis of singular perturbation theory by DiPrima[20]. Pan and Chiang[21] derived the turbine torques on the supported load for the cylindrical journal bearing. The case of coaxial disks where one member is driven and the other is free to respond was treated by Beck, Holliday, and Strodtman[22].

There appears to be no publication of optimization techniques applied to squeeze-film bearings.

1.3 DESIGN OPTIMIZATION AND PROBLEM STATEMENT

Although much has been written on optimization and on techniques for optimization, there does not seem to be any extensive field of literature on applications of these techniques to design problems, per se. Most of the applications use cost or profit as the objective function to be optimized. Sage[23] in his book "Optimum Systems Control" calls his objective function "a goal or a cost function", regardless of its nature. This is perhaps natural when one considers that cost is a common denominator in so much of man's activity.

Other applications speak of maximizing range (of a rocket), minimizing the error in estimation (of position of an object), or minimizing the energy to achieve some end state.

To attain an immediate goal it may be expedient to optimize the most important facet of a design. However, in the comprehensive

treatment of a design problem there is not one, but many features, often conflicting, which must be considered for optimization. Yet the very word "optimum" means "the best".

To resolve this conflict, it is proposed that a composite objective function be created. This composite function will embody the designer's value judgements as to the importance of the various features entering into the design and the relationship between these features and the design variables or parameters. For want of a better name this composite function will be called the figure-of-merit function or simply the merit function.

An examination of recent literature failed to show any previous work in this area. Starr[24] treated a similar problem in his quality function, although he used only a pure ratio between each feature and a standard feature. The fact that the design parameters can be used to define a merit function is one of the contributions of this thesis.

Another contribution is made in studying the optimization of minimum clearance in the squeeze-film journal bearing of finite length when carrying a given load of fixed volume.

The plan of this thesis is as follows:

1. The appropriate gas film equations for the squeeze-film bearing are stated and the equations for non-uniform driven excursion are derived.

2. The minimum clearance problem in the squeeze-film journal bearing is studied, the significant parameters are determined, and it is shown that the minimum clearance can be optimized.

3. The figure-of-merit function for a squeeze-film journal bearing used as an accelerometer element is developed and optimized.

4. A figure-of-merit function weighted in terms of the expected load is next developed. It is shown that this weighted merit function can also be optimized leading to what could be called an optimum of optimums or a maximax value.

Throughout the study, whenever specific application was required, the following practical design problem, called the demonstration problem, was used.

A single degree-of-freedom accelerometer is to be designed for an aerospace application. The accelerometer is to consist of a one gram (.0022 lb_m) proof-mass suspended in a squeeze-film journal bearing. The sensitive axis is along the axis of the journal bearing and sufficient restraints will be provided to withstand the maximum acceleration to be applied to the sensitive axis. Cross axis loading may be in any direction and may be any value up to thirty times the acceleration due to gravity. The proof-mass is to be completely contained within the squeeze-film transducer and is to consist of a cylinder of material with a density of .024 pounds

per cubic inch. The squeeze-film bearing problem, extracted from this specification, is to support a .0022 pound load having a volume of .0925 cubic inches in a 30g acceleration field (maximum load equal to .066 pounds) in the radial direction.

As a result of this study it was found that (1) the important parameters for maximizing the minimum clearance are the nominal clearance - drive amplitude ratio, the non-uniformity shape function of the excursion, and, to a lesser extent, the length-diameter ratio of the bearing; (2) a merit function based on the parameters above can be used to find an optimum combination of cost, radial displacement, length-diameter ratio, and drive amplitude; and (3) a weighted merit function can be used to show that a design optimized at less than the maximum load will not only work at all loads up to the maximum anticipated, but will have a higher merit rating than the design optimized at the maximum load.

CHAPTER 2

GOVERNING EQUATIONS

2.1 GAS FILM EQUATION

The equation describing the fluid dynamics of laminar gas films is called the Reynolds equation. For a bearing in which there is no relative tangential motion between mating surfaces and for the cylindrical coordinates z and θ, Reynolds equation may be written[1]

$$\frac{1}{R^2}\frac{\partial}{\partial\theta}\left[\rho\,\frac{h^3}{\mu}\frac{\partial p}{\partial\theta}\right] + \frac{\partial}{\partial z}\left[\rho\,\frac{h^3}{\mu}\frac{\partial p}{\partial z}\right] = 12\,\frac{\partial(\rho h)}{\partial\tau} \tag{2.1}$$

where ρ is the density of the gas film at a general location z and θ and at a general real time τ; h is the film thickness at (z,θ,τ); p is the pressure at (z,θ,τ); μ is the gas viscosity; and R is the bearing radius.

The assumption is generally made that the gas film is an isothermal, perfect gas, thus density is proportional to pressure and the viscosity may be treated as a constant. With this assumption then (2.1) becomes

$$\frac{1}{R^2}\frac{\partial}{\partial\theta}\left[ph^3\frac{\partial p}{\partial\theta}\right] + \frac{\partial}{\partial z}\left[ph^3\frac{\partial p}{\partial z}\right] = 12\mu\,\frac{\partial(ph)}{\partial\tau} \tag{2.2}$$

Equation (2.2) may be made dimensionless through substitution of the new variables

$$P = \frac{p}{p_a}$$

$$H = \frac{h}{h_o}$$

$$Z = \frac{z}{R}$$

$$t = \omega\tau$$

where

p_a is the ambient pressure

h_o is the nominal film thickness

ω is the squeeze frequency

Then (2.2) becomes

$$\frac{\partial}{\partial\theta}\left[PH^3\frac{\partial P}{\partial\theta}\right] + \frac{\partial}{\partial Z}\left[PH^3\frac{\partial P}{\partial Z}\right] = \sigma\frac{\partial(PH)}{\partial t} \qquad (2.3)$$

where

$$\sigma = \frac{12\,\mu\omega R^2}{p_a h_o^2}$$

a dimensionless group called the squeeze number.

The boundary conditions for use with (2.3) are

$$P(\pm Z_L,\theta) = 1 \qquad (2.4)$$

$$\frac{\partial P}{\partial\theta}(Z,0) = \frac{\partial P}{\partial\theta}(Z,\pi) = 0 \qquad (2.5)$$

where

$$Z_L = \frac{L}{2R}$$

Equation (2.3) may be greatly simplified when σ is large which is generally true in squeeze-film bearings. (Typically σ is 1000 or greater.) C.H.T. Pan[10] in 1966 first published an asymptotic solution of (2.3) allowing σ to go to infinity.

With the assumption of infinite squeeze number (2.3) becomes

$$\frac{\partial}{\partial\theta}\left[\frac{\bar{H}}{2}\frac{\partial(PH)^2}{\partial\theta} - (PH)^2\frac{\partial\bar{H}}{\partial\theta}\right] + \frac{\partial}{\partial Z}\left[\frac{\bar{H}}{2}\frac{\partial(PH)^2}{\partial\theta} - (PH)^2\frac{\partial\bar{H}}{\partial\theta}\right] = 0 \tag{2.6}$$

where $\bar{H}$ is the time average of H. Making the substitution

$$T = (PH)^2$$

reduces (2.6) to

$$\frac{\partial}{\partial\theta}\left[\frac{\bar{H}}{2}\frac{\partial T}{\partial\theta} - T\frac{\partial\bar{H}}{\partial\theta}\right] + \frac{\partial}{\partial Z}\left[\frac{\bar{H}}{2}\frac{\partial T}{\partial Z} - T\frac{\partial\bar{H}}{\partial Z}\right] = 0 \tag{2.7}$$

a second order, linear, partial differential equation in T, independent of time.

Since the asymptotic analysis used to derive (2.6) or (2.7) is valid only in the interior of the bearing, new boundary conditions where the bearing is exposed to the ambient are required. The boundary conditions at the ends of the bearing, (2.4), become (Pan[10])

$$T\left(\pm Z_L,\theta\right) = \left.\frac{\overline{H^3}}{\bar{H}}\right|_{\pm Z_L} \tag{2.8}$$

The derivative boundary conditions (2.5) are still valid but now take the form

$$\frac{\partial T(Z,0)}{\partial \theta} = \frac{\partial T(Z,\pi)}{\partial \theta} = 0 \qquad (2.9)$$

For a journal of uniform radius constrained to have radial displacement only, the film thickness for the bearing, when the driving member moves sinusoidally, is given by

$$h = h_o - \delta h_1(z) \sin \omega\tau - \delta h_2 \cos \theta \qquad (2.10)$$

where

$\delta h_1(z)$ is the amplitude of the excursion of the driving member at any location along the z axis

δh_2 is the displacement of the journal center above the bearing center measured in the plane defined by the journal center and $\theta = 0$. (See Figure 2.1)

Equation (2.10) may be made dimensionless by dividing through by h_o, and by using $t = \omega\tau$

$$H = \frac{h}{h_o} = 1 - \varepsilon_1 f_1(z) \sin t - \varepsilon_2 \cos \theta \qquad (2.11)$$

where

ε_1 is some reference excursion

$f_1(z)$ is a shape function for the excursion

ε_2 is the eccentricity of the bearing

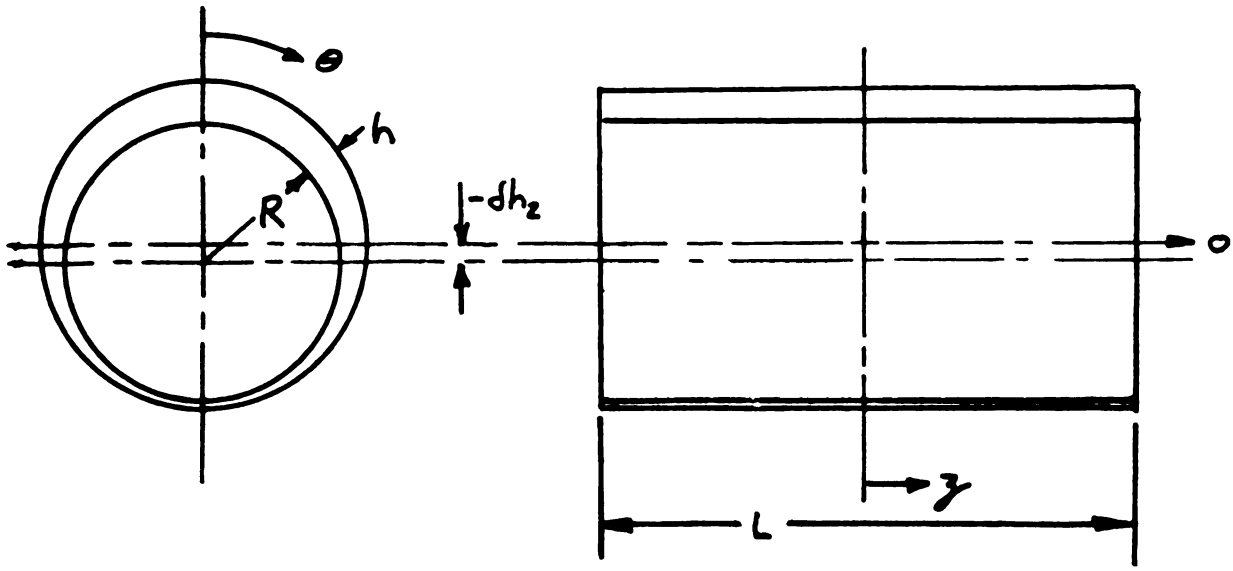

Figure 2.1 Configuration of the squeeze-film journal bearing

From (2.11) then

$$\bar{H} = 1 - \varepsilon_2 \cos\theta \tag{2.12}$$

and the boundary conditions (2.8) become

$$\begin{aligned} T\left(Z_L,\theta\right) &= \left(1 - \varepsilon_2 \cos\theta\right)^2 + \frac{3}{2}\varepsilon_1^2 f_1^2\left(Z_L\right) \\ T\left(-Z_L,\theta\right) &= \left(1 - \varepsilon_2 \cos\theta\right)^2 + \frac{3}{2}\varepsilon_1^2 f_1^2\left(-Z_L\right) \end{aligned} \tag{2.13}$$

for the journal bearing.

A solution to the asymptotic form of Reynolds equation has been approximated previously by two different methods, one numerical, the other analytical[12]. In the numerical approach, finite differences

were used in an alternating-direction, implicit method to generate a matrix of T values over the surface of the bearing. In the analytical approximation, the series

$$T \simeq T_o + \varepsilon_2 T_1 \tag{2.14}$$

was substituted into (2.7) and into the boundary conditions (2.9) and (2.13). A collection of like powers of ε_2 gave two partial differential equations, one in T_o, the other in T_o and T_1. The solution of these equations gave the answer

$$T \simeq 1 + \frac{3}{2}\varepsilon_1^2 - 2\varepsilon_2 \cos\theta \left[-\frac{3}{2}\varepsilon_1^2 \frac{\cosh Z}{\cosh Z_L} + 1 + \frac{3}{2}\varepsilon_1^2 \right] \tag{2.15}$$

valid when ε_2 is small and $f_1(z) = 1$ (uniform excursion). Later work produced the answer

$$T \simeq 1 + \frac{3}{2}\varepsilon_1^2 f^2 - 2\varepsilon_2 \cos\theta \left[-\frac{3}{2}\varepsilon_1^2 f^2 \frac{\cosh Z}{\cosh Z_L} + 1 + \frac{3}{2}\varepsilon_1^2 f^2 \right] \tag{2.16}$$

for non-uniform, but symmetrical, excursion where

$$f = \left| f_1(Z_L) \right| = \left| f_1(-Z_L) \right|$$

For this investigation it was concluded that (2.16) could be used only for preliminary investigations because of the restriction that ε_2 be small. The numerical method is valid for all ε_2 but requires a considerable amount of computer time for iterative solutions.

For these reasons the small parameter solution was expanded to include two additional terms in the series

$$T \simeq T_o + \varepsilon_2 T_1 + \varepsilon_2^2 T_2 + \varepsilon_2^3 T_3 \qquad (2.17)$$

The details of this work are given in Appendix A together with a comparison in Appendix B between this augmented, small-parameter analysis and the numerical results. The conclusions reached are that the T-values found using the augmented, small-parameter solution agree with the numerical solutions for values of ε_2 as large as -.8, and that the former requires significantly less computer time. In all that follows then, the small parameter solution was used for preliminary investigations or to find starting values and the final solution was made using the augmented, small-parameter equation. In the optimization procedure the solution of the partial differential equation (2.7) is required a large number of times. Without the augmented, small-parameter analysis, the total computer time may have been so large that the optimization procedure would not be practical.

In summary then the film characteristic, T, is a function of the variables

$$T = T(h_o, \delta h_1(z), \delta h_2, p_a, z, \theta, R, L) \qquad (2.18)$$

in the dimensioned form or of

$$T = T(\varepsilon_1, f_1(Z), \varepsilon_2, Z, \theta, Z_L) \qquad (2.19)$$

in the dimensionless form.

2.2 LOAD SUPPORT CAPABILITY

A bearing at equilibrium can support an average load W_1 , per unit length which is given by

$$W_1 = -\frac{1}{2\pi L}\int_0^{2\pi}\int_0^{2\pi}\int_{-\frac{L}{2}}^{\frac{L}{2}} p \cos\theta \, d\theta \, dz \, dt \tag{2.20}$$

In dimensionless terms (2.20) becomes

$$W' = \frac{W_1}{2p_a R} = -\frac{1}{8\pi Z_L}\int_0^{2\pi}\int_0^{2\pi}\int_{-Z_L}^{Z_L} P \cos\theta \, d\theta \, dZ \, dt \tag{2.21}$$

The sign of the force is chosen such that a displacement of the journal below the bearing center gives rise to a positive (upward) force.

The pressure, P , in (2.21) is obtained from the solution of the gas film equation and since $T = (PH)^2$,

$$P = \frac{T^{\frac{1}{2}}}{H} \tag{2.22}$$

Since H , given by (2.11), is the only factor of (2.21) containing

time and then in an especially simple manner, the integration of (2.21) over time may be performed explicity giving

$$W' = -\frac{1}{4Z_L}\int_0^{2\pi}\int_{-Z_L}^{Z_L}\frac{T^{\frac{1}{2}}\cos\theta\, d\theta\, dZ}{\left[\left(1-\epsilon_2\cos\theta\right)^2 - \epsilon_1^2 f_1^2\right]^{\frac{1}{2}}} \tag{2.23}$$

Again two methods of solution of (2.23) are available, numerical integration and a small parameter approximation. A two dimensional form of Simpson's rule was used for the numerical integration.

The small parameter solution, requiring now that ϵ_1^2 as well as ϵ_2 be small led to the answer[12]

$$W' = -\frac{\pi}{2}\epsilon_1^2\epsilon_2\left(1 + \frac{3\tanh Z_L}{2Z_L}\right) \tag{2.24}$$

for uniform excursion and to

$$W' = -\frac{\pi}{8}\frac{\epsilon_1^2\epsilon_2}{Z_L}\int_{-Z_L}^{Z_L}\left(2f_1^2 + 3f\frac{\cosh Z}{\cosh Z_L}\right)dZ \tag{2.25}$$

for non-uniform but symmetrical excursion.

In summary, the load support per unit length does not involve any variables other than those considered previously for the film

characteristic. In fact, the integration over the bearing area eliminates the dependency on position so that in dimensioned form

$$W' = \frac{W_1}{2p_a R} = W'\left(h_o, \delta h_1(z), \delta h_2, p_a, R, L\right) \tag{2.26}$$

and in dimensionless form

$$W' = W'(\varepsilon_1, f_1(Z), \varepsilon_2, Z_L) \tag{2.27}$$

2.3 NON-UNIFORM DRIVER EXCURSION

The high frequency, sinusoidal displacement of the driving member, in general, will not be uniform along the axial length. As suggested by (2.11) the excursion may be represented by some reference excursion multiplied by a non-uniformity shape function.

An assumption, substantiated by some unpublished experiments by William G. Holliday[25] is that the amplitude of some of the simpler radial motions of a thin-walled cylinder can be expressed by a cosine function as

$$\delta h_1 = a + b \cos \frac{\pi}{2} \frac{z}{z_{LC}} \tag{2.28}$$

Where a and b are two parameters to be treated at greater length below and z_{LC} is the half length of the driver. It is necessary to distinguish between the length of the driver and the length of the bearing since the two need not be equal. The length of the bearing is determined by the length over which the gas film extends. The driver excursion is defined over the length of the driver.

If a new variable, called the shape factor, is defined by the ratio

$$A = \frac{b}{a} \tag{2.29}$$

then (2.28) can be written

$$\delta h_1 = a\left(1 + A \cos \frac{\pi}{2} \frac{z}{z_{LC}}\right) \tag{2.30}$$

This accomplishes the separation of δh_1 into a reference amplitude, a , and a shape function.

If a is assumed to be a non-negative constant then a number of different drive shapes may be characterized by the magnitude of A as shown in Figure 2.2 , which depicts the range of displacement of one surface of the driving member.

Equation (2.30) suffers from two deficiencies. First, the excursion, a , at the end is not a good reference, since as the input power changes both the end excursion and the shape factor, A , change, and second if the excursion at the end should be zero, δh_1 is not defined.

It was postulated that a spatial root-mean-square excursion value would make a better reference. Limited experiments by W. G. Holliday[25] did in fact show that a good degree of correlation existed between the rms excursion and the input power.

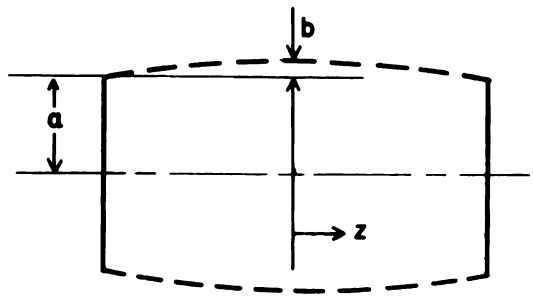

CASE 1 A > 0

A "no-node" or "barrel" mode

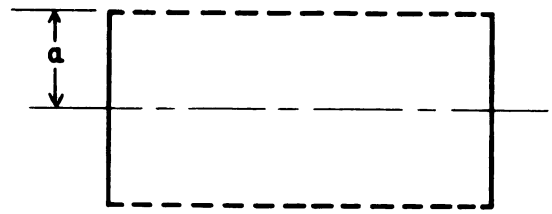

CASE 2 A = 0

uniform excursion

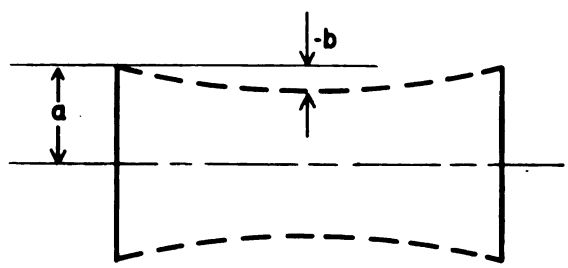

CASE 3 -1 < A < 0

A "no-mode" or "hour-glass" mode

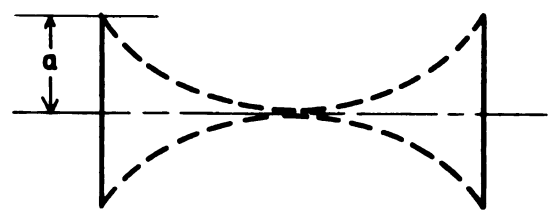

CASE 4 A = -1

A "one-node" mode

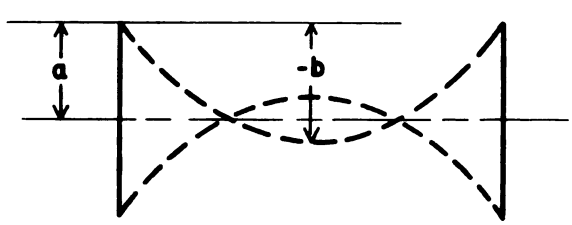

CASE 5 A < -1

A two node mode

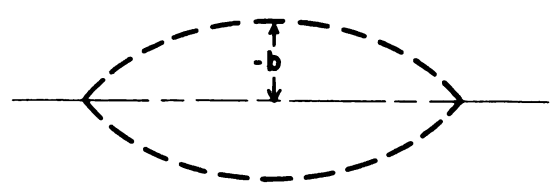

CASE 6 A = ∞

A special case of case 1 or case 5 depending on sign of b

Figure 2.2 Transducer amplitudes for various ranges of the non-uniformity factor.

Define

$$\delta h_{1r}^2 \equiv \frac{a^2}{2z_{LC}} \int_{-z_{LC}}^{z_{LC}} \left(1+A \cos \frac{\pi}{2} \frac{z}{z_{LC}}\right)^2 dz \tag{2.31}$$

After performing the indicated operations

$$\delta h_{1r} = a\left(\frac{A^2}{2} + \frac{4A}{\pi} + 1\right)^{\frac{1}{2}} = a\alpha^{\frac{1}{2}} \tag{2.32}$$

where

$$\alpha = 1 + \frac{4A}{\pi} + \frac{A^2}{2} \tag{2.33}$$

Then (2.30) can be written

$$\delta h_1 = \frac{\delta h_{1r}}{\alpha^{\frac{1}{2}}}\left(1+A \cos \frac{\pi}{2} \frac{z}{z_{LC}}\right) \tag{2.34}$$

since

$$a = \delta h_{1r} \alpha^{-\frac{1}{2}} . \tag{2.35}$$

In dimensionless terms (2.34) is

$$\frac{\delta h_1}{h_o} = \varepsilon_1 f_1(Z) = \frac{\varepsilon_{1r}}{\alpha^{\frac{1}{2}}}\left(1+A \cos \frac{\pi}{2} \frac{Z}{Z_{LC}}\right) \tag{2.36}$$

Thus for δh_1 given by (2.28) the shape function is identified as

$$f_1(Z) = \alpha^{-\frac{1}{2}} \left(1+A \cos \frac{\pi}{2} \frac{Z}{Z_{LC}}\right) = \left(\frac{A^2}{2} + \frac{4A}{\pi} + 1\right)^{-\frac{1}{2}} \left(1+A \cos \frac{\pi}{2} \frac{Z}{Z_{LC}}\right) \tag{2.37}$$

and the essential information identifying the shape is given by the value of A once the cosine distribution is assumed.

Note that if the excursion at the end of the driver is zero, $A = \infty$, but (2.32) can easily be shown in the limit as $A \to \infty$ to be

$$\delta h_{1r} = \frac{b}{\sqrt{2}} \tag{2.38}$$

Similarily (2.37) in the limit becomes

$$f_1(Z) = \sqrt{2} \cos \frac{\pi}{2} \frac{Z}{Z_{LC}} \tag{2.39}$$

For any given value of A, (2.37) defines an even function of Z so clearly $f_1(Z)$ is symmetrical.

Although in the development of (2.37) A was treated as a continuous variable only certain values of A correspond to mode shapes which are physically attainable. This point will be considered again in the subsequent work.

CHAPTER 3

OPTIMIZATION OF CLEARANCE

3.1 CLEARANCE EQUATIONS

Two highly desirable properties of a gas lubricated bearing are (1) a relatively large nominal clearance and (2) a small radial displacement, i.e., small eccentricity, regardless of load. Even relatively large nominal clearance in gas lubricated bearings must of necessity be small physical dimensions (of the order of 100-400 microinches). A large and uniform clearance would not have any preferred location tending to contact due to machinging tolerances or dirt particles. (At the other extreme, a very large eccentricity means that contact is always imminent and that a machining asperity or an extremely small dirt particle is capable of bridging the film thickness). Unfortunately, large nominal clearance and small eccentricity are incompatible requirements; however, it is possible to choose the nominal clearance such that the resulting eccentricity gives the maximum value of the minimum clearance. The problem is somewhat more complex that this because other independent variables are also important in the clearance optimization problem.

The minimum clearance, c , in the bearing corresponds to the minimum film thickness. In a journal constrained to have radial displacement only, c is a minimum at $\theta = \pi$ and when the

excursion is maximum. Thus the minimum value of h,

$$h = h_o - \delta h_1(z) \sin t - \delta h_2 \cos \theta \tag{3.1}$$

is

$$c = h_o - \delta h_{1m} + \delta h_2 \tag{3.2}$$

where δh_{1m} is the maximum value of $\delta h_1(z)$.

In the following, the minimum clearance, c, will be simply called "the clearance", but it should be distinguished from the nominal clearance, h_o.

In the previous chapter, the load support per unit length was shown to be a function of the dimensioned variables

$$W' = W'\left(h_o, \delta h_1(z), \delta h_2, p_a, R, L\right) \tag{3.3}$$

Also $\delta h_1(z)$ was represented as a reference excursion, δh_{1r} and a shape function characterized by the shape factor, A, so that finally

$$W' = W'\left(h_o, \delta h_{1r}, A, \delta h_2, p_a, R, L\right) \tag{3.4}$$

Quite frequently in the design of a bearing, the maximum load which the bearing will be expected to support is a predetermined value. In addition, in the accelerometer application, the volume of the load is contained completely within the bearing, thus for a material of fixed density, the volume of the load is also fixed. These two quantities may then be treated as equality constraints in the following work.

When a fixed load volume is considered, the volume acts as a constraint on the variables R and L ; however in the gas film computations R and L are also related through Z_L . It is thus convenient to replace R and L by the constraint relationship V and the length to diameter ratio, Z_L . Then

$$W' = W'\left(h_o, \delta h_1, A, \delta h_2, p_a, V, Z_L\right) \qquad (3.5)$$

The total dimensioned load, W , which a bearing is capable of supporting is given by

$$W = W_1 L = 2RL\, p_a\, W' \qquad (3.6)$$

If now W set equal to a constant is introduced as another constraint, and since the relationship for W introduces no new variables, (3.5) can be symbolically solved for the radial displacement giving

$$\delta h_2 = \delta h_2\left(W, V, h_o, \delta h_{1r}, A, p_a, Z_L\right) \qquad (3.7)$$

Of these variables, then, two, V and W , are constant constraints. The ambient pressure, p_a , enters linearly into the gas film equations such that a higher ambient pressure permits the bearing to carry a proportionately larger load. No further consideration was given p_a which was treated as a constant and set equal to atmospheric pressure.

To express δh_{1m} in terms of δh_{1r} and A consider the six cases shown in Figure 2.2.

CASE 1	$\delta h_{1m} = b + a = a(1 + A)$		$(A > 0)$
2	$\delta h_{1m} = a$		$(A = 0)$
3	$\delta h_{1m} = a$		$(-1 < A < 0)$
4	$\delta h_{1m} = a$		$A = -1$
5	$\delta h_{1m} = a$	for $b \geq -2a$	$(-2 \leq A < -1)$
	$\delta h_{1m} = \lvert b \rvert - 2a$	for $b < -2a$	$(A < -2)$
6	$\delta h_{1m} = b$		$(A = \infty)$

The first five cases may be expressed as $\delta h_{1m} = aF(A)$ where $F(A)$ is defined as follows

$A > 0$	$F(A) = A + 1$
$-2 \leq A \leq 0$	$F(A) = 1$
$A < -2$	$F(A) = \lvert A + 1 \rvert$

But from (2.35)

$$a = \delta h_{1r}\, \alpha^{-\frac{1}{2}} \tag{3.8}$$

Therefore

$$\frac{\delta h_{1m}}{\delta h_{1r}} = F(A)\, \alpha^{-\frac{1}{2}} \tag{3.9}$$

Equation (3.9) does not appear to cover case 6 since it is indeterminate as $A \to \infty$; however

$$\lim_{A \to \infty} \frac{\delta h_{1m}}{\delta h_{1r}} = \lim_{A \to \infty} \frac{\lvert A+1 \rvert}{\left[\frac{A^2}{2} + \frac{4A}{\pi} + 1 \right]^{\frac{1}{2}}} = \sqrt{2} \tag{3.10}$$

Figure 3.1 shows how the ratio $\frac{\delta h_{1m}}{\delta h_{1r}}$ varies in the range of A values of interest. Differentiation of (3.9) with respect to A for $-2 \leq A \leq 0$ gave the value of the maximum as 2.298 at $A = -\frac{4}{\pi}$ ($A = -1.2732$).

Putting (3.9) into the expression for clearance (3.2) gives

$$c = h_o - \frac{F(A)\delta h_{1r}}{\alpha^{\frac{1}{2}}} + \delta h_2 \left(W, V, h_o, \delta h_{1r}, A, p_a, Z_L \right) \tag{3.11}$$

as the expression for clearance to be maximized.

3.2 OPTIMIZATION OF SMALL PARAMETER EQUATION

For the case when the gas film is the same length as the driver, the small parameter load support equation (2.25) may be integrated, using the non-uniform excursion expression (2.36), to obtain

$$W' \simeq -\frac{\pi}{2} \varepsilon_{1r}^2 \varepsilon_2 \left[1 + \frac{3 \tanh Z_L}{2 \alpha Z_L} \right] \tag{3.12}$$

or in dimensioned terms

$$W' = \frac{W}{2RL\, p_a} = -\frac{\pi}{2} \frac{\delta h_{1r}^2\, \delta h_2}{h_o^3} \left[1 + \frac{3 \tanh Z_L}{2 \alpha Z_L} \right] \tag{3.13}$$

Equation (3.13) may be solved for δh_2 and put into the clearance equation (3.11) yielding

$$c = h_o - \frac{F(A)}{\alpha^{\frac{1}{2}}} \delta h_{1r} - \frac{W\, h_o^3}{\pi RL\, p_a\, \delta h_{1r}^2 \left[1 + \frac{3 \tanh Z_L}{2 \alpha Z_L} \right]} \tag{3.14}$$

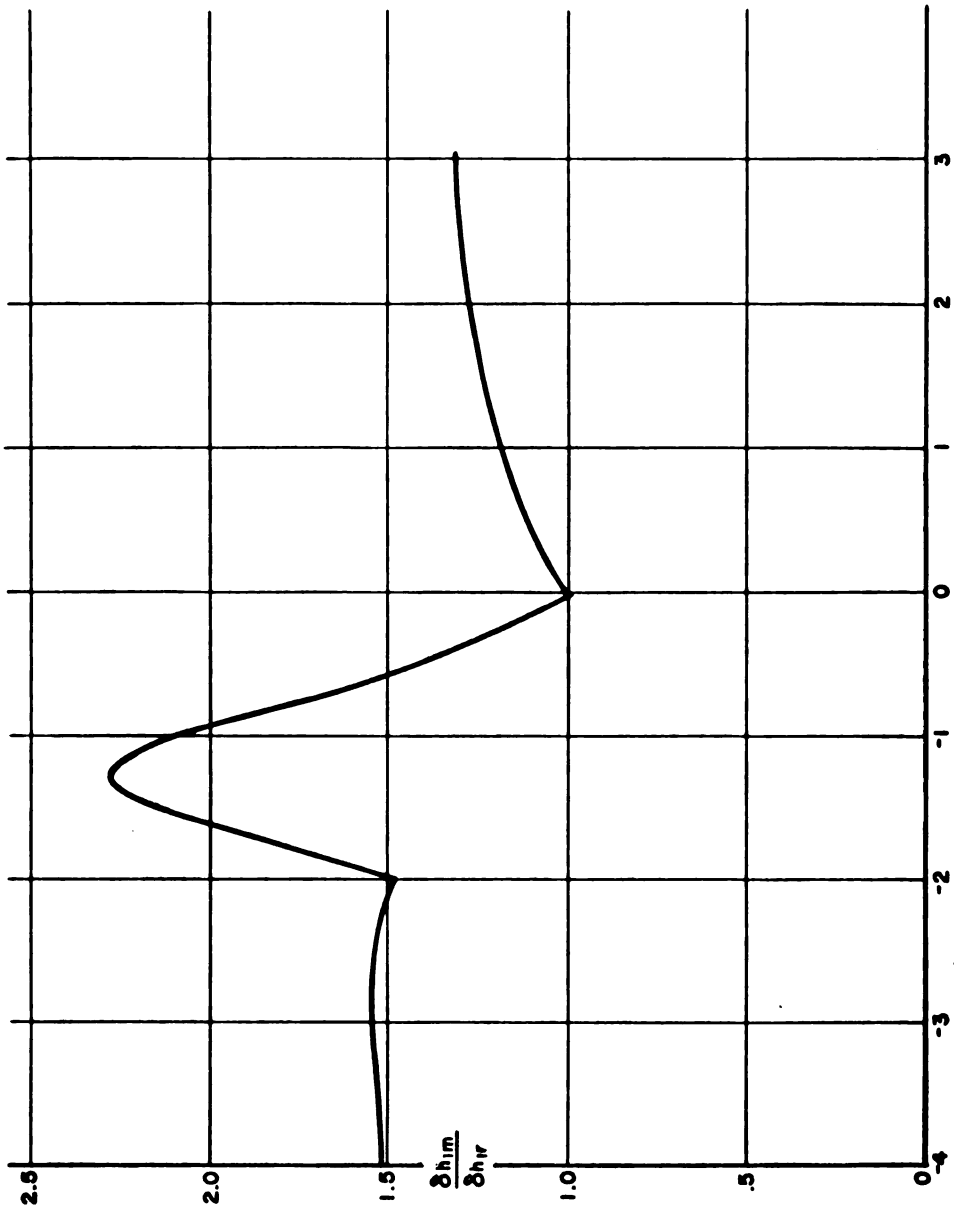

Figure 3.1 Ratio of maximum amplitude to rms amplitude as a function of the non-uniformity factor

as the clearance equation for values of $\frac{\delta h_{1r}^2}{h_o^2}$ and $\frac{\delta h_2}{h_o} << 1$. (This implies that $\frac{c}{h_o}$ must be near unity.)

Since constant volume was to be an equality constraint in the optimization it may be introduced by observing that the radius appearing in (3.14) may be given by

$$R = \left(\frac{V}{2\pi Z_L}\right)^{1/3} \tag{3.15}$$

and the length, L , by

$$L = 2R\, Z_L \tag{3.16}$$

Then

$$c\left(h_o, \delta h_{1r}, A, Z_L\right) = h_o - \frac{F(A)}{\alpha^{\frac{1}{2}}}\,\delta h_{1r} - \frac{W h_o^3}{\left(2\pi\right)^{1/3} p_a V^{2/3} Z_L^{1/3} \delta h_{1r}^2 \left[1 + \frac{3 \tanh Z_L}{2\alpha Z_L}\right]} \tag{3.17}$$

In order to gain some insight into the nature of the clearance function, it is instructive to study (3.17) by varying one parameter at a time; however to reduce the number of variables, divide (3.17) by δh_{1r} and define the new variables ε'_{1r} and ε'_2 to get

$$c' = \frac{c}{\delta h_{1r}} = \varepsilon'_{1r} - \frac{F(A)}{\alpha^{\frac{1}{2}}} + \varepsilon'_2 \tag{3.18}$$

where

$$\varepsilon_2' \equiv \frac{\delta h_2}{\delta h_{1r}} = \frac{-W\left(\varepsilon_{1r}'\right)^3}{KV^{2/3} Z_L^{1/3}\left[1 + \frac{3 \tanh Z_L}{2 \alpha Z_L}\right]} \tag{3.19}$$

$$\varepsilon_{1r}' \equiv \frac{h_o}{\delta h_{1r}}$$

$$K = (2\pi)^{1/3} p_a$$

Thus it is possible to plot a dimensionless clearance in terms of a dimensionless nominal clearance, so that the results to follow, although specific for W and V, are general in nominal clearance and excursion.

Figure 3.2 shows that for a fixed value of the load and the load volume, the clearance does have a definite maximum as a function of nominal clearance, and further that the maximum is a function of the non-uniformity of the excursion. Figure 3.2 also clearly shows the incompatibility of large nominal clearance and small eccentricity since as ε_{1r}' increases (large nominal clearance) so does ε_2' (large eccentricity).

Figure 3.3 shows for a fixed value of non-uniform excursion that the optimum clearance is also a function of Z_L, the length to diameter ratio of the bearing. The shape of the curves in Figure 3.3 suggest that Z_L may not be an important variable in determining the clearance. This is particularily true for ε_{1r}' near the

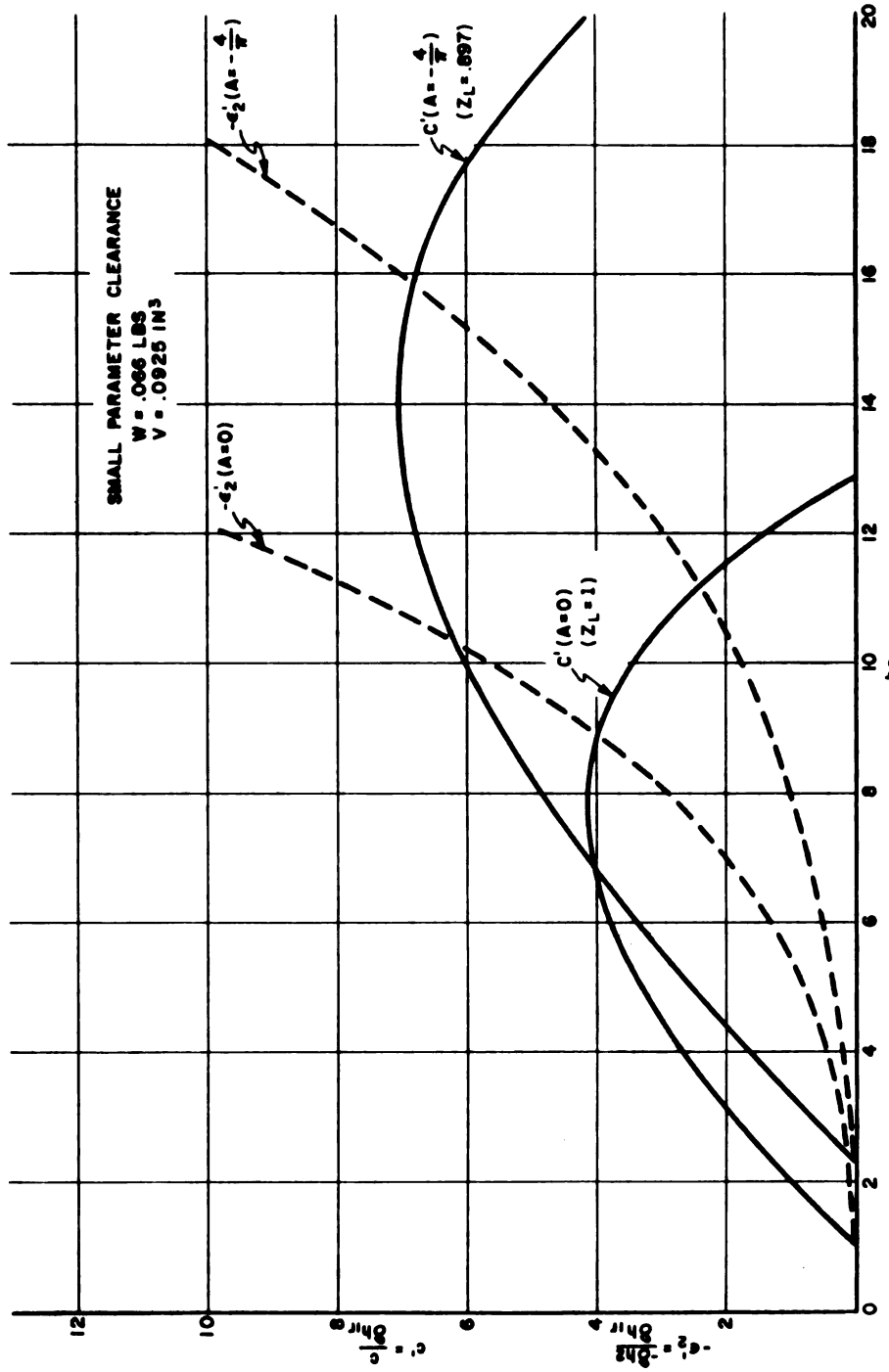

Figure 3.2 Clearance and radial displacement as functions of nominal clearance (small parameter equation)

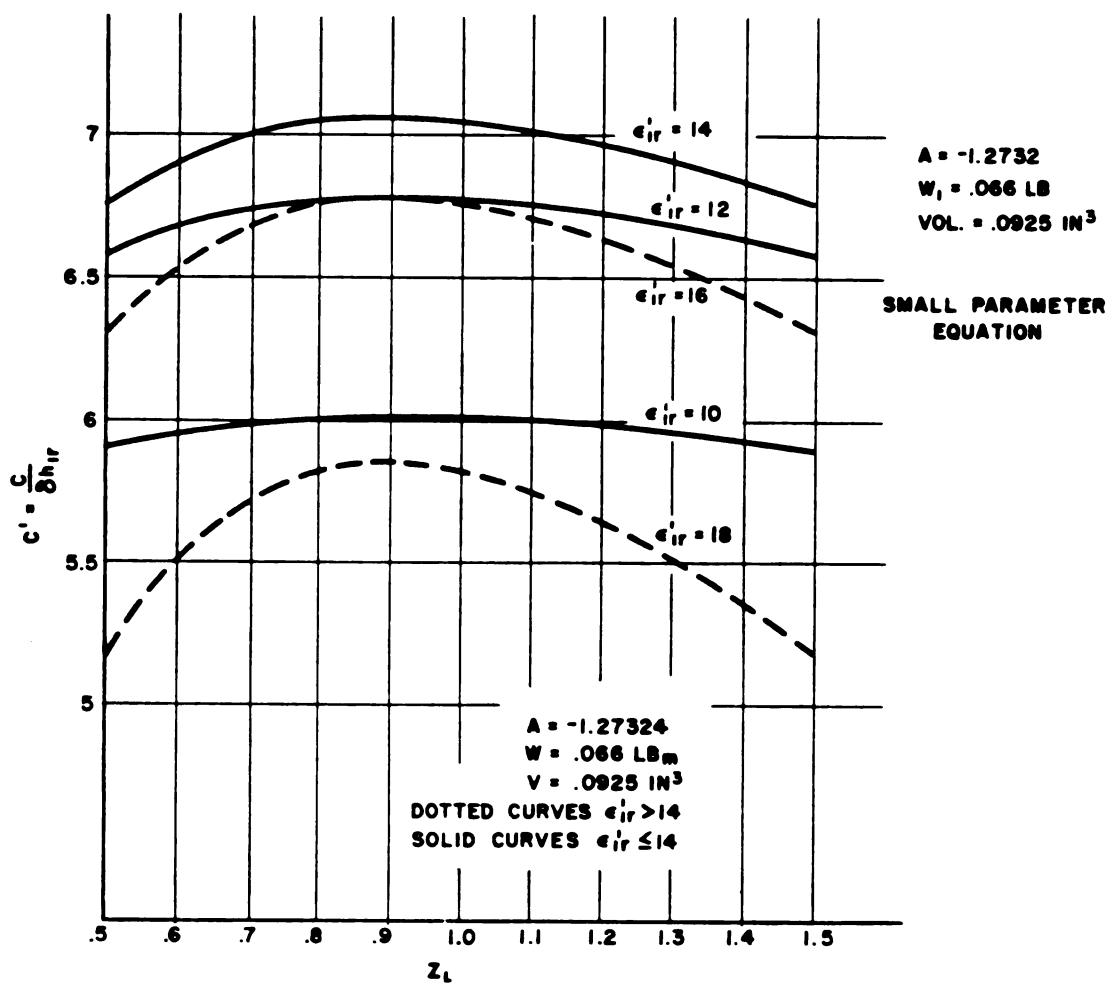

Figure 3.3 Clearance as function of length-diameter ratio (small parameter equation)

value of 14, the curve which yields the maximum clearance. For the dotted curves ($\varepsilon'_{1r} > 14$), the curvature becomes considerably more pronounced than for the solid curves ($\varepsilon'_{1r} \leq 14$) .

Figure 3.4 shows the contours of constant clearance plotted against the two most important variables, fixing Z_L at 0.897.

It is also possible to gain some insight into the maximum of (3.18) by the classical approach of setting the differential with respect to each of the three independent variables equal to zero. This procedure produces

$$\frac{\partial c'}{\partial Z_L} = \frac{W\left(\varepsilon'_{1r}\right)^3}{KV^{2/3}} \frac{\partial}{\partial Z_L}\left[Z_L^{-1/3}\left(1 + \frac{3 \tanh Z_L}{2 \alpha Z_L}\right)^{-1}\right] = 0 \tag{3.20}$$

$$\frac{\partial c'}{\partial\left(\varepsilon'_{1r}\right)} = 1 - \frac{3 W \left(\varepsilon'_{1r}\right)^2}{KV^{2/3} Z_L^{1/3}\left(1 + \frac{3 \tanh Z_L}{2 \alpha Z_L}\right)} = 0 \tag{3.21}$$

$$\frac{\partial c'}{\partial A} = \frac{d}{dA}\left[F(A)\right] \alpha^{-1/2} + F(A) \frac{d}{d\alpha}\left(\alpha^{-1/2}\right) + \frac{W\left(\varepsilon'_{1r}\right)^3}{KV^{2/3} Z_L^{1/3}} \frac{\partial}{\partial A}\left[1 + \frac{3 \tanh Z_L}{2 \alpha Z_L}\right]^{-1} = 0 \tag{3.22}$$

Performing the indicated differentiation of (3.22) with F(A) = 1, which assumes that A lies between -2 and 0 , gives

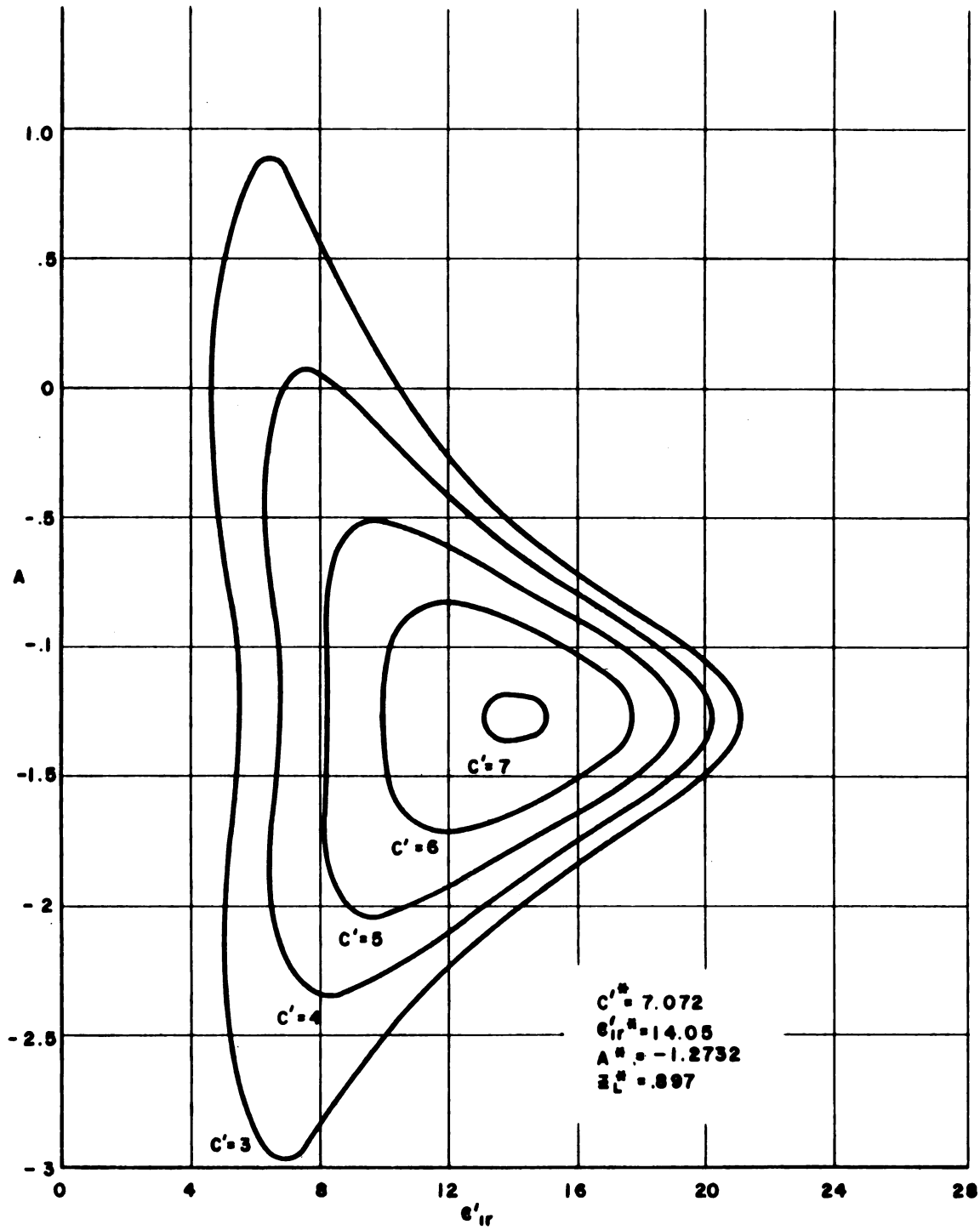

Figure 3.4 Contours of constant clearance (small parameter equation)

$$- \frac{1}{2}\left[\frac{A^2}{2} + \frac{4A}{\pi} + 1\right]^{-\frac{3}{2}}\left(A + \frac{4}{\pi}\right)$$

$$+ \frac{W(\epsilon'_{1r})^3}{KV^{2/3} Z_L^{1/3}}\left[1 + \frac{3 \tanh Z_L}{2Z_L\left(\frac{A2}{2} + \frac{4A}{\pi} + 1\right)}\right]^{-2} \frac{3 \tanh Z_L}{2Z_L}\left[\frac{A^2}{2} + \frac{4A}{\pi} + 1\right]^{-2}\left(A + \frac{4}{\pi}\right) = 0$$

(3.23)

This equation is satisfied by $A = -\frac{4}{\pi}$ for any value of W, Z_L, V, or ϵ'_{1r}. That the value of A lies in the assumed range justifies the original assumption. Further, Beck and Strodtman[12] showed for small parameters that the load support of a finite journal bearing with uniform excursion is composed of two components, one due to interior excursion (non-linearity of the load support equation), the other due to the excursion at the boundary, (pressure pump-up). It was also shown that the second component was a function of the length diameter ratio, Z_L, and for $Z_L \simeq 1$ was 1 1/2 times the first component. It has been shown that $\frac{\delta h_{1m}}{\delta h_{1r}}$ has a maximum at $A = -\frac{4}{\pi}$. This value of A is case 5 of Figure 2.2 with $|b| < 2a$ thus δh_{1m} occurs at the boundary, enhancing the total load support. It is reasonable to expect a maximum value for the clearance when the load support capability is maximum.

With the above value for A, since (3.20) is a function of A and Z_L only, one can solve for

$$\alpha\Big|_{A=-\frac{4}{\pi}} = \frac{\pi^2-8}{\pi^2} = \frac{3}{Z_L} \tanh Z_L - \frac{9}{2} \operatorname{sech}^2 Z_L$$

(3.24)

Newton-Raphson iteration gives

$$Z_L^* = 0.89664$$

where here and elsewhere the asterisk will be used to denote optimum quantities.

Using these values for Z_L and A in (3.21) gives

$$\varepsilon_{1r}'^* = \left[2.3501 \frac{KV^{2/3}}{W} \right]^{1/2} \tag{3.25}$$

For the assumed values of $V = 0.0925$ in^3 and $W = 0.066$ lbs,

$$\varepsilon_{1r}'^* = 14.054 \qquad \text{and} \qquad c'^* = 7.0719$$

That these values correspond to the maximum is evident from Figure 3.4 which is a contour map near the optimum. Further, in Section 3.4 it will be shown that the function defined by the second derivatives near the optimum is negative definite thus insuring that the optimum is a local maximum.

To relate the above optimum values to dimensioned quantities it is necessary to know δh_{1r}. Typical values for the rms excursion range from five to fifteen microinches. The optimum nominal clearance, h_o, will then be between 70 and 210 microinches and the minimum clearance, c, will be between 35 and 105 micro-inches. The lower limit of 70 microinches for the nominal clearance is less than usually used in squeeze-film bearings. It is near the limit of nominal clearance which can be reliably fabricated and measured.

The upper limit of 210 microinches is well within typical dimensions encountered. A bearing with the lower limit of 35 microinches for the minimum clearance may not be satisfactory since a very small asperity or foreign particle might bridge the gap and destroy the bearing.

It is also evident from (3.20) that if any other value of A is assumed for the excursion the corresponding maximums with respect to Z_L and ε'_{1r} only can be obtained from (3.24) and (3.21) respectively. It is also interesting to note that Z_L is independent of W and V thus only the optimum value of ε'_{1r} changes as W and V are varied.

The small parameter approach just described fails in one important respect. The optima predicted do not fulfill the small parameter restrictions; in particular $\frac{\delta h_2}{h_o}$ was required to small compared to unity. But at the optimum by using (3.21) and (3.19) one finds

$$\frac{\delta h_2}{h_o} = \frac{\varepsilon_2'}{\varepsilon'_{1r}} = -\frac{1}{3}$$

which is not small compared to unity.

3.3 OPTIMIZATION OF CLEARANCE USING THE AUGMENTED, SMALL-PARAMETER EQUATION

In the previous section, explicit solution of the clearance equation was analytically possible because a relatively simple expression for δh_2 was available. However, a more accurate

solution is obviously needed since the clearance predicted by the small parameter equation did not meet the small parameter requirements.

Equation (3.11) is still valid but δh_2 must be determined by a more accurate means. Two methods are available, (1) the finite difference solution and (2) the augmented, small-parameter equation. The latter was chosen because it uses less computer time with no significant difference in accuracy, in the range of interest for this problem. See Appendix B.

The programs written to solve for the load support by either method result in a W' corresponding to given values of ε_{1r}, ε_2, A, Z_L. To determine ε_2 corresponding to a given load it is necessary to iterate on ε_2 until the given W' is obtained within some given error bound. To start the iteration, the small parameter equation (3.12) was solved explicitly for ε_2 for the given load. Since for large loads or very small values of ε_1, the small parameter equation tends to overstate the value of ε_2, a check was necessary to insure that the resulting clearance was positive. If this condition was not satisfied, a value of ε_2 was selected which made the clearance slightly positive. The second value of ε_2 was always arbitrarily selected as 0.95 of the first. Linear interpolation to the desired W' gave a third value. Quadratic interpolation on the last three values was used for following steps to locate each new ε_2. As each ε_2 was located the corresponding W' was computed and compared to the desired W', the operation terminating as soon as the error criterion was satisfied.

The load support calculations were normalized by dividing all film dimensions by h_o, the nominal film thickness. But h_o is one of the independent variables in the clearance equation. To get around this inconvenience, it is desirable to work either with dimensioned clearances or, to simplify the problem by reducing the number of variables, to find a new normalizing parameter. In the previous section the use of $c' = \frac{c}{\delta h_{1r}}$ was immediately evident from (3.17). That the same normalization holds in general can be demonstrated from the gas film and load support equations.

Define a new variable $H' = \frac{h}{\delta h_{1r}}$. Substitute this new variable into (2.2) together with the other variables previously defined for P, Z, and t to get the analog of (2.3) in the form

$$\frac{\partial}{\partial\theta}\left[PH'^3\,\frac{\partial P}{\partial\theta}\right] + \frac{\partial}{\partial Z}\left[PH'^3\,\frac{\partial P}{\partial Z}\right] = \sigma'\,\frac{\partial(PH')}{\partial t} \qquad (3.26)$$

This is identical to (2.3) except that the squeeze number is redefined as

$$\sigma' = \frac{12\mu\,\omega\,R^2}{p_a(\delta h_{1r})^2}$$

Since the squeeze number was assumed to be very large, this normalization makes it even larger as $\delta h_{1r} < h_o$, and thus the asymptotic differential equation for the gas film characteristic is unchanged.

In the boundary conditions at the ends of the film

$$T' = \frac{\overline{H'^3}}{\overline{H'}} = \frac{\overline{\left(H \cdot \frac{h_o}{\delta h_{1r}}\right)^3}}{\overline{\left(H \cdot \frac{h_o}{\delta h_{1r}}\right)}} = \left(\frac{h_o}{\delta h_{1r}}\right)^2 \frac{\overline{H^3}}{\overline{H}} \tag{3.27}$$

thus the new boundary conditions are related to the old through the ratio of the normalizations. This means that the new T values (called $T' = (PH')^2$) computed from (2.7) will differ from the old by a factor of

$$\left(\frac{h_o}{\delta h_{1r}}\right)^2$$

Consider the load support, W', given by equation (2.21) with

$$P = \frac{(T')^{\frac{1}{2}}}{H'}$$

where

$$H' = \frac{h}{\delta h_{1r}} = \frac{h}{h_o} \cdot \frac{h_o}{\delta h_{1r}}$$

therefore

$$P = \frac{\left(\frac{h_o}{\delta h_{1r}}\right) T^{\frac{1}{2}}}{\left(\frac{h_o}{\delta h_{1r}}\right) H} = \frac{T^{\frac{1}{2}}}{H}$$

and the dimensionless pressure used for computing the load support is unchanged proving that W' is the same using either normalization.

Thus the clearance equation (3.18) derived originally from the small parameter equation is valid for the more general solution as well.

A steepest ascent method was used to find c'^* , the optimum dimensionless clearance, and the optimizing parameters $\varepsilon_1'^*$, Z_L^* , A^*, numerically, for given values of W, the total load in pounds and V, the load volume in cubic inches. However, in developing this program it was instructive to also develop curves comparable to those previously given for the small parameter treatment.

Figure 3.5 compares the small parameter solution with the augmented solution. It is evident that after the optimum clearance is reached, further increases in the nominal clearance-drive ratio, ε_{1r}' , result mainly in increasing ε_2' , the eccentricity, with only a slow decrease in the clearance. It is also evident that the two solutions correspond closely so long as ε_2' , which corresponds to δh_2 is small, and that the clearance curve in the more exact case has a flatter top. Although the solutions agree so far as clearance is concerned, the values of ε_{1r}' corresponding to the maximums of the two curves are quite far apart.

Figure 3.6 shows the contours of constant clearance for varying A and ε_{1r}' with Z_L fixed at 0.713. Again it appears that the optimum value of $\delta h_{1m} / \delta h_{1r}$ occurring at $A = -\frac{4}{\pi}$, determines the A^* value, certainly for the value of Z_L selected. Other computer runs confirmed that, indeed $A^* = -\frac{4}{\pi}$ for all values of Z_L that were checked.

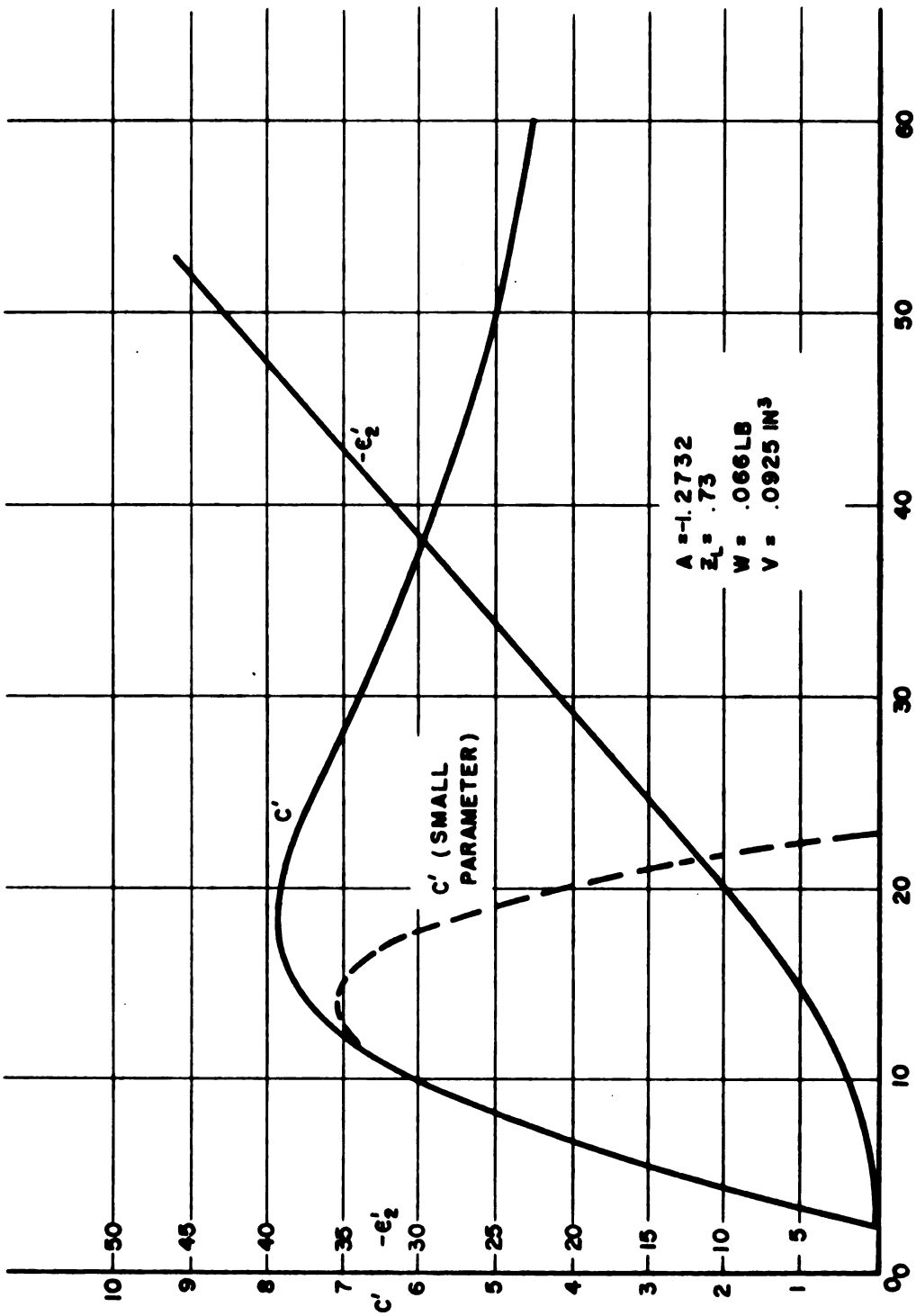

Figure 3.5 Clearance and radial displacement as functions of nominal clearance (augmented, small-parameter equation)

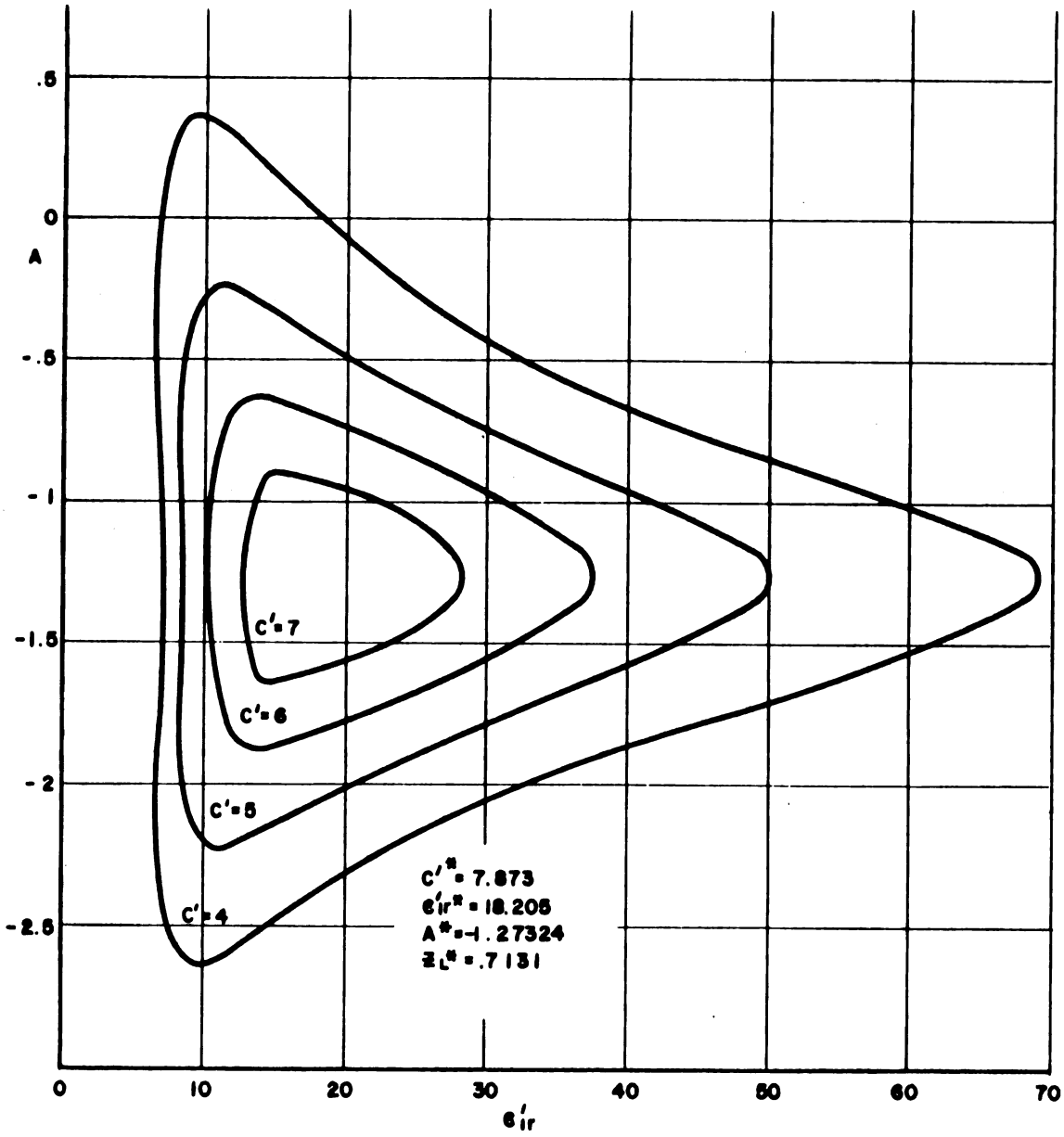

Figure 3.6 Contours of constant clearance (augmented, small-parameter equation)

The optimization program was run for the demonstration design of W = 0.066 lbs and volume of 0.0925 in^3 with the result $c'^* = 7.873$, $\varepsilon_{1r}'^* = 18.205$, $A^* = -1.2732$, $Z_L^* = 0.7131$.

Comparing these optimum values to those found previously from the small parameter equation, the nominal clearance, ε_{1r}', has increased 30 percent to 18.2. This represents a dimensioned nominal clearance of from 90 to 270 microinches depending on the drive amplitude. The minimum clearance has increased slightly more than 10 percent giving clearances between 40 and 120 microinches. It appears that the small parameter solution is not too far from the more exact solution.

The optimum length-diameter ratio of 0.713 is not convenient and many applications of the squeeze-film bearing use a Z_L between unity and 1.4.

3.4 SENSITIVITY TO PARAMETER CHANGES

To gain some insight into the fashion in which the optimum dimensionless clearance changes with changes in the independent variables, make a Taylor series expansion around the optimum giving

$$c' = c'^* + \sum_{i=1}^{3} \left.\frac{\partial c'}{\partial x_i}\right|^* \Delta x_i + \frac{1}{2!} \sum_{i=1}^{N} \sum_{j=1}^{N} \left.\frac{\partial^2 c}{\partial x_i \partial x_j}\right|^* \Delta x_i \Delta x_j + O\left(\Delta x_i\right)^3 \tag{3.28}$$

where Δx_i and Δx_j are the deviations from the optimum ($x_1 = \varepsilon_{1r}'$, $x_2 = Z_L$, $x_3 = A$).

One of the definitions of sensitivity widely used in feedback control theory is the following[26]

> Sensitivity is normally used to express the ratio of the percentage variation in some specific system quantity such as gain, impedance, etc., to the percentage variation in one of the system parameters. The sensitivity function is defined as

$$S_k^M = \frac{d\ \ell n\ M}{d\ \ell n\ x_i} = \frac{d\ M/M}{d\ x_i/x_i} = \frac{\text{Percentage change in M(due to change in } x_i)}{\text{Percentage change in } x_i}$$

> where M is a transfer function and x_i is a specified parameter.

At an interior optimum, where x_i is not constrained, $\frac{\partial c'}{\partial x_i} = 0$ leaving only the second derivatives and higher order terms, thus the definition given above is not applicable to this particular case. Following the ideas of Box [27] it is possible to fit a quadric surface in i dimensions to represent the response, $c'-c'^*$, for small deviations near the optimum.

Write (3.28) in the quadratic form

$$c'-c'^* = \bar{x}\, Q \bar{x}^T \tag{3.29}$$

where Q is the matrix of coefficients given by

$$Q = \begin{bmatrix} \frac{\partial^2 c'}{\partial x_1 \partial x_1}\Big|^*_{x_1 x_1} & \frac{\partial^2 c'}{\partial x_1 \partial x_2}\Big|^*_{x_1 x_2} & \frac{\partial^2 c'}{\partial x_1 \partial x_3}\Big|^*_{x_1 x_3} \\ \frac{\partial^2 c'}{\partial x_2 \partial x_1}\Big|^*_{x_2 x_1} & \frac{\partial^2 c'}{\partial x_2 \partial x_2}\Big|^*_{x_2 x_2} & \frac{\partial^2 c'}{\partial x_2 \partial x_3}\Big|^*_{x_2 x_3} \\ \frac{\partial^2 c'}{\partial x_3 \partial x_1}\Big|^*_{x_3 x_1} & \frac{\partial^2 c'}{\partial x_3 \partial x_2}\Big|^*_{x_3 x_2} & \frac{\partial^2 c'}{\partial x_3 \partial x_3}\Big|^*_{x_3 x_3} \end{bmatrix} \tag{3.30}$$

and

$$\bar{x} = \left[\frac{\Delta x_1}{x_1} , \frac{\Delta x_2}{x_2} , \frac{\Delta x_3}{x_3} \right] \tag{3.31}$$

The magnitude of the off-diagonal terms in (3.30) indicates the degree of interaction between the variables. (Called the "factor dependence" by Box.) In the diagonalized form, the diagonal members of (3.30) give the curvature of the surface in each of the dimensions considered and are thus a measure of the sensitivity of the system to changes in the variables.

Figure 3.7 shows the first derivatives near the optimum for the small parameter equation. The three curves in the top row (Figure 3.7 (a), (b), (c)) all are $\frac{\partial c'}{\partial \varepsilon'_{1r}} \varepsilon'_{1r}$ but, by being plotted versus ε'_{1r}, Z_L, and A respectively, have slopes which give the second derivatives required by the first row of (3.30) (except for the required normalizing factor).

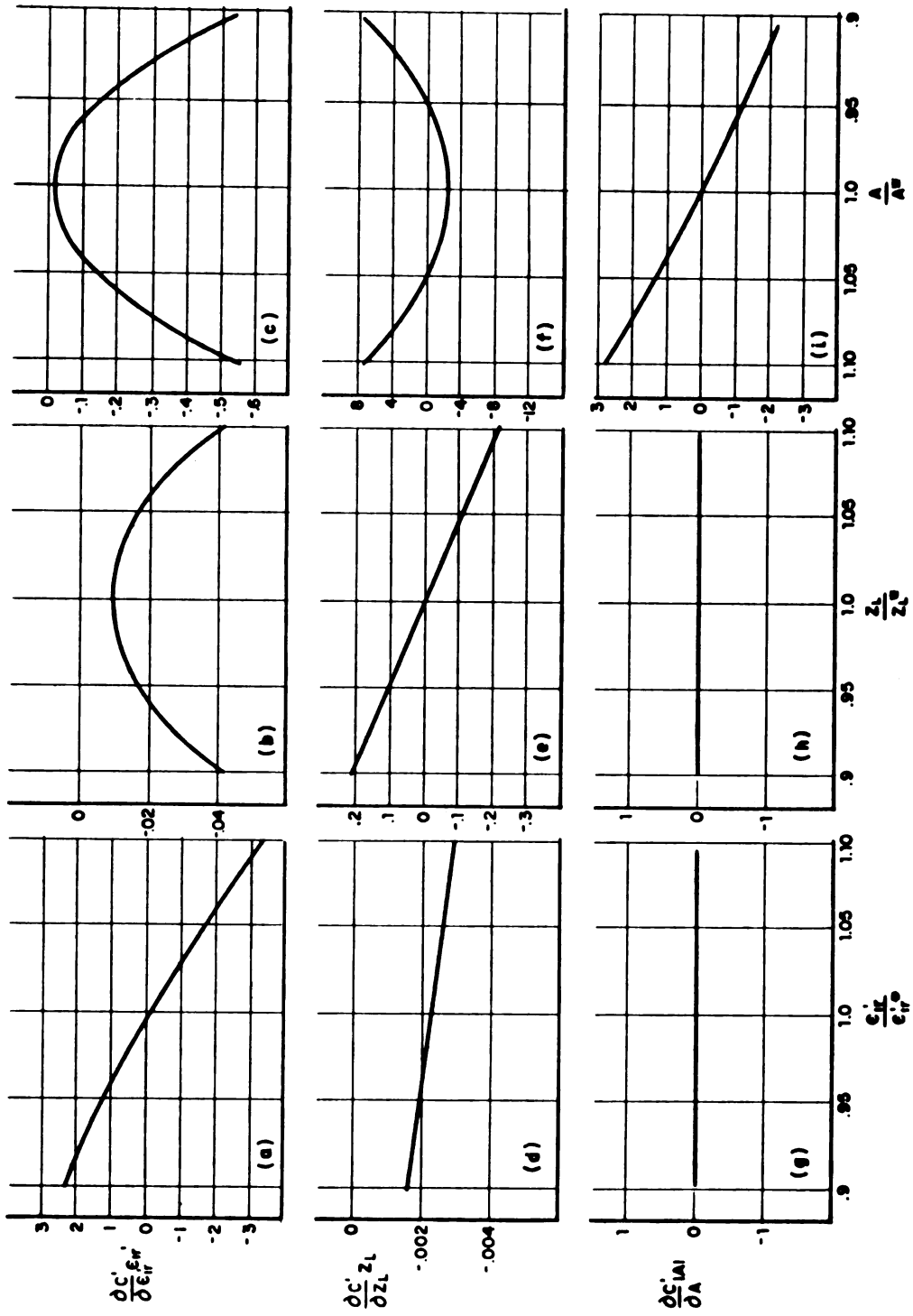

Figure 3.7 First derivatives of clearance near the optimum (small parameter equation)

This pattern is true for the other six curves also representing $\frac{\partial c'}{\partial Z_L} Z_L$ and $\frac{\partial c'}{\partial A} |A|$. Thus from Figure 3.7 (3.30) can be written for this particular problem as

$$Q = \begin{bmatrix} -28.1 & 0 & 0 \\ 0 & -2.14 & 0 \\ 0 & 0 & -24.8 \end{bmatrix} \tag{3.32}$$

evaluated at (14.05, .897, -1.2732), the optimum. It can be shown from (3.20), (3.21), and (3.22) that the off-diagonal terms of (3.32) are identically zero at the optimum.

Figure 3.8 shows the second derivatives of the dimensionless clearance as functions of the three independent variables. The curves are arranged so that the position of each corresponds to the location that the second derivative has in the Q matrix (3.30).

Figure 3.8 contains more information than is required by (3.30), or by (3.32) for the specific problem, in that (3.30) requires evaluation of the derivatives at the optimum only. Figure 3.8 shows the manner in which the second derivatives change away from the optimum. Note that only at the optimum are the pairs of mixed partial derivatives equal, i.e., $\frac{\partial^2 c'}{\partial \varepsilon'_{1r} \partial Z_L} = \frac{\partial^2 c'}{\partial Z_L \partial \varepsilon'_{1r}}$. This is not unexpected, in that in moving away from the optimum the mixed partials are no longer being evaluated at the same points on the surface, i.e., $\frac{\partial}{\partial \varepsilon'_{1r}} \left(\frac{\partial c'}{\partial Z_L} \Big| Z_L^* + \Delta Z_L \right) \Big|_{\varepsilon'^*_{1r}}$ in general, it is not the

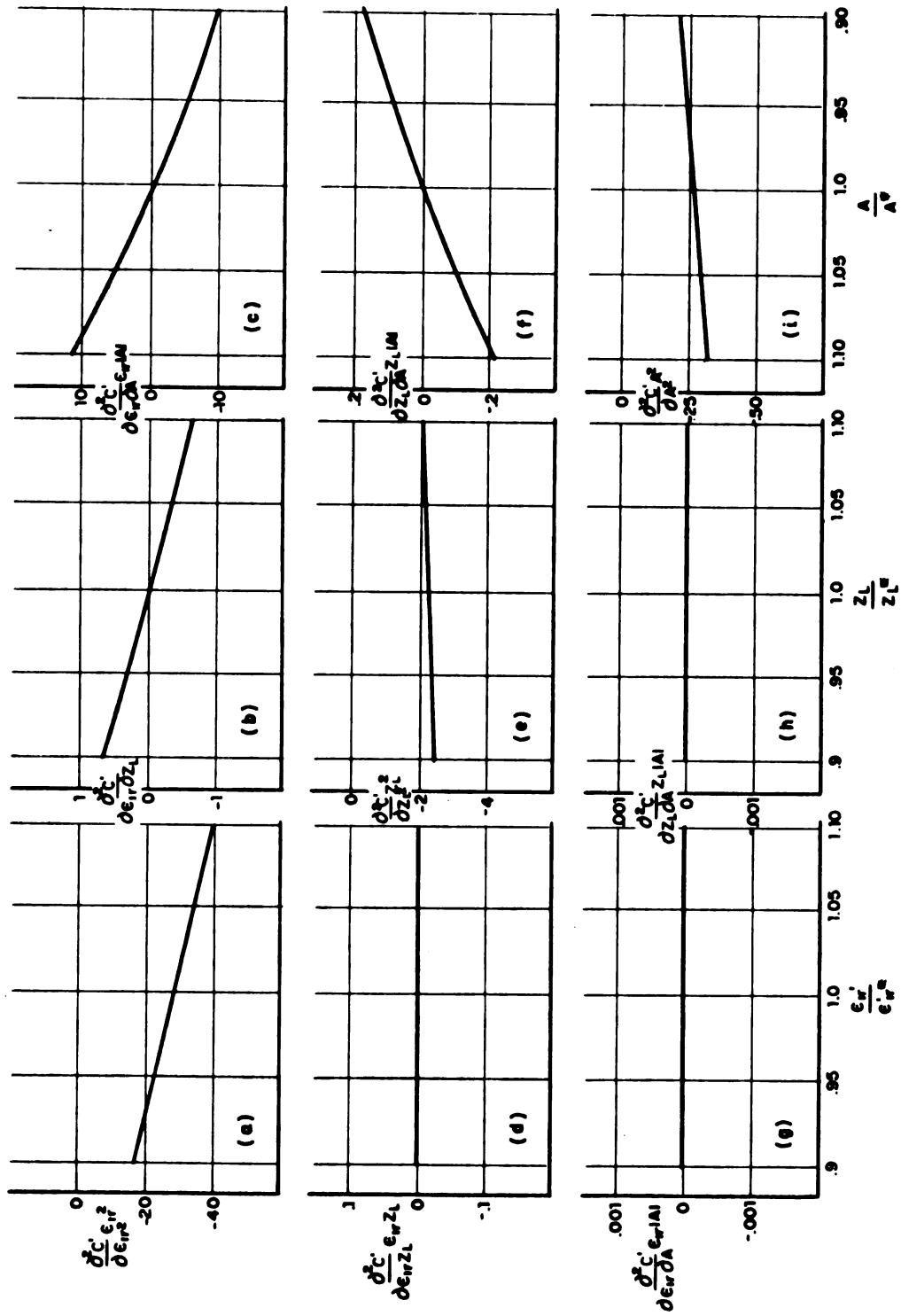

Figure 3.8 Second derivatives of clearance near the optimum (small parameter equation)

same as $\frac{\partial}{\partial Z_L}\left(\left.\frac{\partial c'}{\partial \varepsilon'_{1r}}\right|_{\varepsilon'^{*}_{1r} + \Delta\varepsilon'_{1r}}\right)\Bigg|_{Z_L^*}$

For a maximum it is necessary that (3.30) be negative definite. This insures that the quadric surface is ellipsoidal and not hyperbolic. The test for negative definiteness is that the principal minors of $-|Q|$ be positive.

It is immediately evident that (3.32) is negative definite. It is further evident that no cross coupling exits, i.e., each variable has the same effect regardless of the value of the other variables. In the geometrical sense the quadric surface developed from (3.32) is of the form

$$ax_1^2 + bx_2^2 + cx_3^2 = f(x_1,x_2,x_3) \qquad (3.33)$$

since only second derivatives of the form $\frac{\partial^2 f}{\partial x_i^2}$, (i = 1,2,3) exist and the mixed derivatives $\frac{\partial^2 f}{\partial x_i \partial x_j}$ (i = 1,2,3; j = 1,2,3, $i \neq j$) do not occur.

It is evident from Figure 3.7 and (3.32) that the nominal clearance-drive ratio, ε'_{1r}, has the largest influence on the curvature of the quadric surface followed closely by the non-uniformity factor, A. The length-diameter ratio, Z_L, has very little influence. Thus it can be concluded that the two most important variables are ε'_{1r} and A.

Figures 3.9 and 3.10 contain the same type information as Figure 3.7 and 3.8 except that the clearance is now computed from

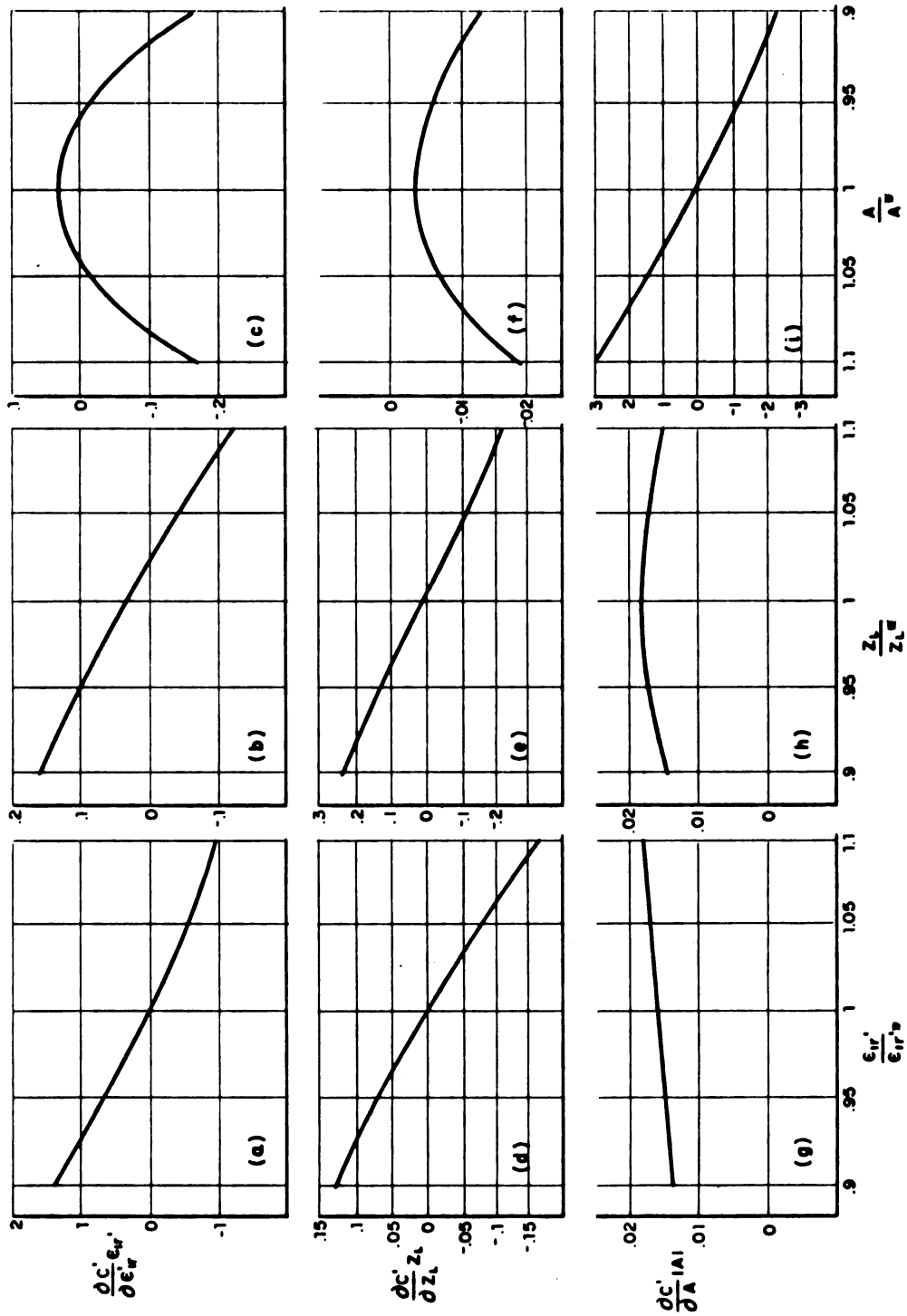

Figure 3.9 First derivatives of clearance near the optimum (augmented, small-parameter equation)

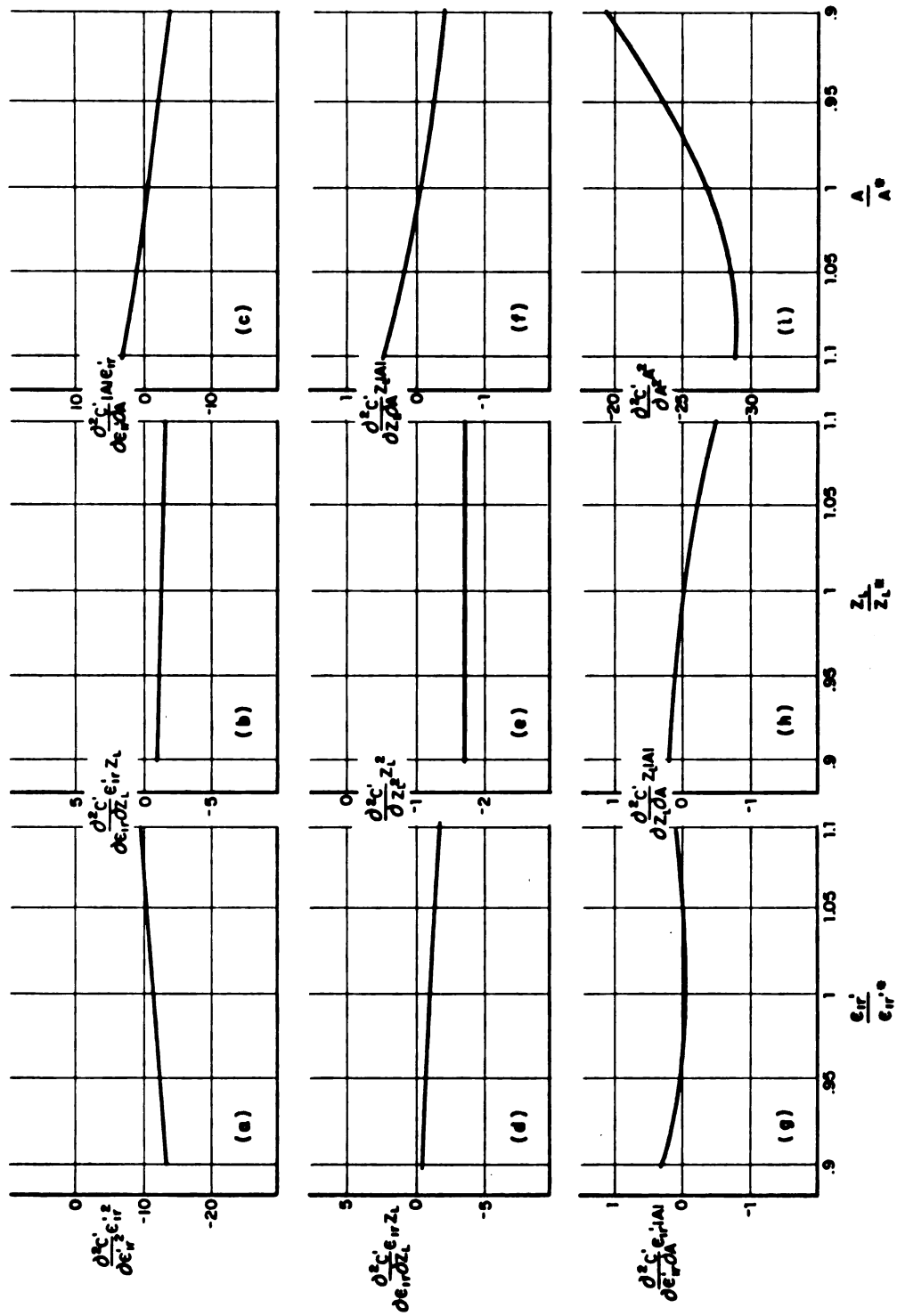

Figure 3.10 Second derivatives of clearance near the optimum (augmented, small-parameter equation)

the augmented equation. The matrix of approximate second derivatives analogous to (3.32) is

$$Q = \begin{bmatrix} -10.7 & -1.20 & -.157 \\ -1.16 & -1.78 & -.070 \\ -.01 & .018 & -26.8 \end{bmatrix} \tag{3.34}$$

evaluated at (18.2, .712, -1.2732), the optimum.

The off-diagonal terms at q_{13}, q_{23}, q_{31}, and q_{32} are essentially zero and could well be due to the inaccuracies in the finite difference procedure for computing the derivatives, to the finite error allowed in computing the eccentricity corresponding to a given load support and to the inability to determine the optimum exactly. Since no explicit solution is available for the clearance, c', it is not possible to show that these off-diagonal terms must be zero as was possible in the small parameter case. However since the clearance function is continuous and has continuous first derivatives, the order of differentiation at the optimum is immaterial. Thus the matrix (3.34) must be symmetrical. The terms at q_{23} and q_{32} are small and of opposite sign indicating a tendency to average to zero. The average of terms q_{13} and q_{31} is small compared to the diagonal terms. Thus q_{13} and q_{31} will be assumed to be zero.

The off-diagonal terms at q_{12} and q_{21} are clearly not zero and demonstrate that an interaction occurs between ε'_{1r} and Z_L.

By using the average of q_{12} and q_{21} as the value for these terms (3.34) can be written as

$$c' - c'^* = \bar{x} \begin{bmatrix} -10.7 & -1.18 & 0 \\ -1.18 & -1.78 & 0 \\ 0 & 0 & -26.8 \end{bmatrix} \bar{x}^T \tag{3.35}$$

The linear transformation

$$\bar{y} = \begin{bmatrix} 1 & .110 & 0 \\ 0 & 1 & 0 \\ 0 & 0 & 1 \end{bmatrix} \bar{x} \tag{3.36}$$

leads to the diagonalized form

$$c' - c'^* = \bar{y} \begin{bmatrix} -10.7 & 0 & 0 \\ 0 & -1.65 & 0 \\ 0 & 0 & -26.8 \end{bmatrix} \bar{y}^T \tag{3.37}$$

The matrix in (3.37) is clearly negative definite. It is evident that the shape factor, A, is the most important variable and that Z_L is of minor importance. A new variable

$$y = \frac{\Delta x_1}{x_1} + 0.11 \frac{\Delta x_2}{x_2} = \frac{\Delta \varepsilon_1}{\varepsilon'_{1r}} + 0.11 \frac{\Delta Z_L}{Z_L}$$

showing the interaction between ε'_{1r} and Z_L is also significant. Since the contribution of Z_L in y_1 is small, ε'_{1r} is still the more significant of the two variables.

Two other aspects of parameter sensitivity relate to (1) the influence of load or volume changes on the clearance and (2) the effect of load changes on the optimizing parameters.

For the first point the classical definition of sensitivity can be used with the results from (3.18)

$$\frac{\partial c'}{\partial W} \frac{W}{c'} = \frac{\partial \varepsilon'_2}{\partial W} \frac{W}{c'} \tag{3.38}$$

and

$$\frac{\partial c'}{\partial V} \frac{V}{c'} = \frac{\partial \varepsilon'_2}{\partial V} \frac{V}{c'} \tag{3.39}$$

For the small parameter equation ε'_2 is given explicitly by (3.19) resulting in

$$\frac{\partial c'}{\partial W} \frac{W}{c'} = - \frac{W(\varepsilon'_{1r})^3}{c' K V^{2/3} Z_L^{1/3} \left[1 + \frac{3 \tanh Z_L}{2 \alpha Z_L} \right]} = \frac{\varepsilon'_2}{c'} \tag{3.40}$$

and

$$\frac{\partial c'}{\partial V}\frac{V}{c'} = \frac{2}{3}\frac{W(\varepsilon_{1r}')^3}{c'KV^{2/3}\,Z_L^{1/3}\left[1+\dfrac{3\tanh Z_L}{2\,\alpha\,Z_L}\right]} = -\frac{2}{3}\frac{\varepsilon_2'}{c'} \tag{3.41}$$

Equations (3.40) and (3.41) evaluated at the optimum give -0.66243 and 0.44162 respectively. Thus a one percent change in W' results in a -0.66 percent change in c', whereas a one percent change in V changes c' by only 0.44 percent.

Numerical evaluation of (3.38) and (3.39) using the augmented, small-parameter equation gives

$$\frac{\partial c'}{\partial W}\frac{W}{c'} \simeq -.6482$$

and

$$\frac{\partial c'}{\partial V}\frac{V}{c'} \simeq .4318$$

for the optimum parameters. It appears that load and volume changes effect both the small parameter and the augmented, small parameter equations equally.

To investigate the second point, varying load values were used and the optimizing parameters were calculated numerically. Figure 3.11 shows the result of varying the load using the augmented equation. The small parameter analysis showed that once A was determined, Z_L^* was also determined, and that $\varepsilon_{1r}'^*$ was inversely proportional to square root of the load (3.25). It appears from

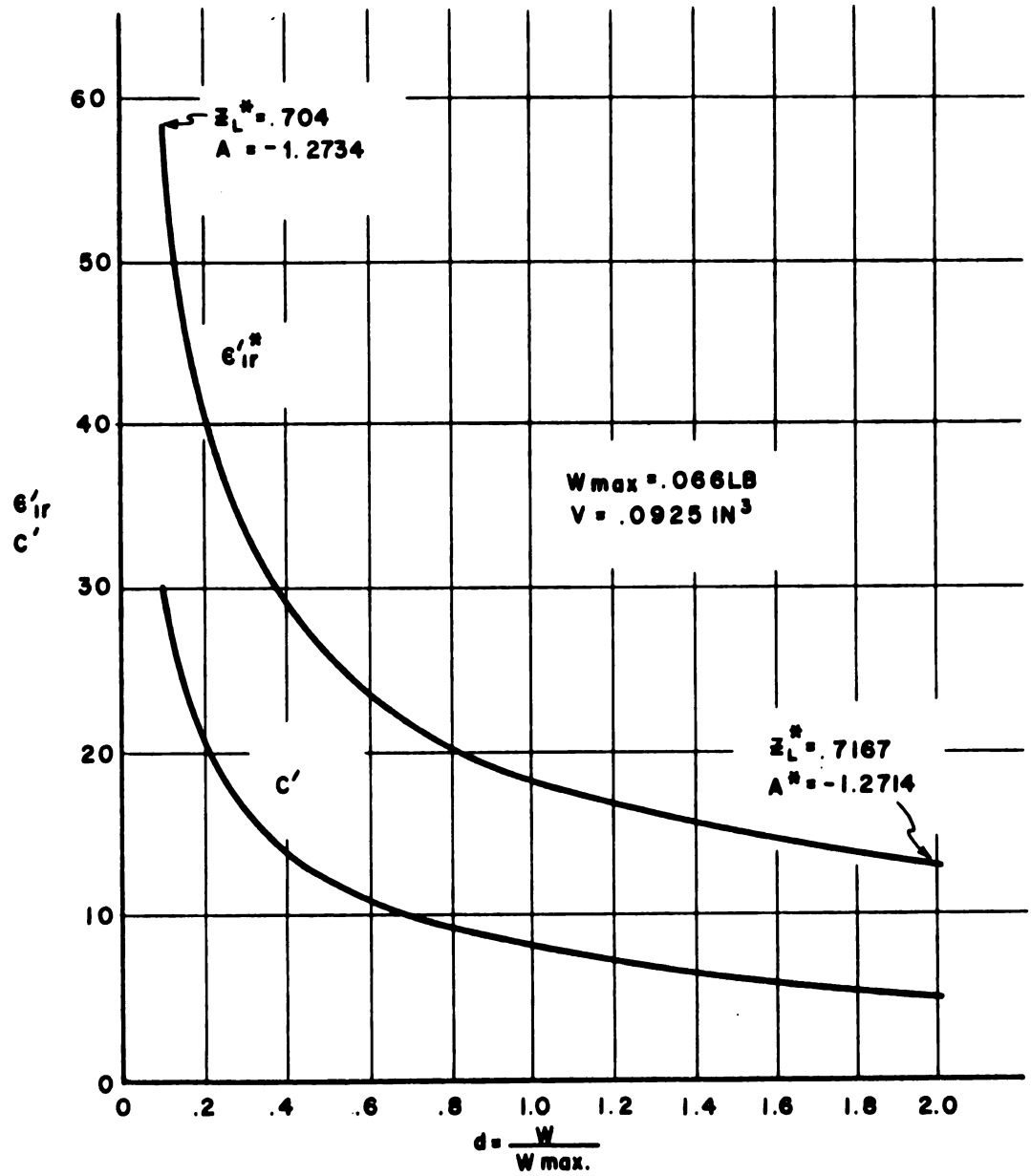

Figure 3.11 Optimum nominal clearance and optimum clearance as functions of load (augmented, small-parameter equation)

Figure 3.11 that $A = -\frac{4}{\pi}$ is near the optimum value for a wide variation in load (the difference may be due to computational error) and that Z_L^* is nearly a constant also, though not the same value as predicted by the small parameter equation. It is further interesting to note that the resulting $\varepsilon_{1r}'^*$ curve follows the equation

$$\varepsilon_{1r}'^* = \frac{K_1}{W^{\frac{1}{2}}} \tag{3.42}$$

with $K_1 = 4.69 \pm 0.03$; whereas the small parameter equation (3.25) predicts $K_1 = 3.61$ for the volume of 0.0925 cubic inches. From (3.42) then

$$\frac{\partial \varepsilon_{1r}'^*}{\partial W} \frac{W}{\varepsilon_{1r}'^*} = -\frac{1}{2} \frac{K_1}{W^{3/2}} \frac{W}{\varepsilon_{1r}'^*} = -\frac{1}{2} \tag{3.43}$$

giving the sensitivity of the optimum dimensionless nominal clearance to load changes for constant volume.

CHAPTER 4

FIGURE-OF-MERIT

4.1 MERIT FUNCTIONS

It is now desired to develop some method of rating competing designs so that the computer can be used to select the design with the highest rating. One common method of rating is strictly on a cost basis, dollars being used as a measure of minimum cost or as a measure of maximum profit. A dollar measure is not always easy to apply. Performance of the design must be translated into dollars - often a formidable task. What is proposed here is a figure-of-merit rating (or simply merit rating), M , which may involve cost as well as certain other design considerations which may at first seem non-comparable.

The idea of merit rating by a merit function owes its origin to the utility function as used by VonNeumann and Morgenstern[28], and others[29]. If a preference can be expressed then some mathematical expression should be capable of describing this preference. Merit differs from utility in that the latter assigns a numerical value which is the order of preference whereas the merit function as proposed here assigns a functional value to the preference. In a design problem, particularily when rating the performance of competing designs, the problem can be reduced to a series of dichotomies. One extreme of each being acceptable, the other completely unacceptable.

In a continuum, there will always be cases between these two extremes and it is in this "in-between region" that design decisions between conflicting requirements must be made. If the value of unity is assigned to the acceptable extremity and zero to the other, than the in-between region can take on the intermediate values by means of some, perhaps arbitrarily determined, relation.

An example of these conflicting requirements occurs in the squeeze-film bearing between the desire to have a large nominal clearance and a small eccentricity. Once having established a merit rating for each requirement then optimization techniques can determine the compromise which yields the highest merit value.

The proposed merit rating procedure appears to be part of the field of decision theory. The only reference which was found that approached the same method of rating appeared in Starr[24]. He employed the simple ratio of the rated design quality to a standard design quality in what he termed a "quality" function. A weighting exponent was to be used with each ratio. As conceived by Starr, both the rated design quality and the standard design quality were to be value judgements by the members of the design team. It would seem that the quality function could only be used to choose the optimum quality after the design is completed, the measurements taken and the value judgements made. An examination of the quality function offers no direction as to how an optimum design might be achieved.

The proposed merit function, M, will be made up of the product of individual merit factors, M_n. Each M_n is a functional

relationship relating one of the output characteristics or requirements of the design to the independent variables determining that characteristic. Each merit factor will be given a positive weight exponent, w_n , which will permit emphasizing ($w^n < 1$) or de-emphasizing ($w^n > 1$), the accompanying merit factor. The general form of the merit function for a design is then

$$M = \prod_{n=1}^{N} M_n^{w_n}\left(x_i\right) \qquad \left(i = 1,2,\cdots I\right) \qquad (4.1)$$

The argument for multiplying the merit factors is that this insures that if any one factor is zero, the product is zero also. (This may seem drastic, but what merit does a design have which is perfect in all respects except that it costs so much to produce there is no market? or one whose performance is so poor that the design fails its intended purpose?). Further, since each factor ranges from zero to one, the product does also, and additional factors may be appended still keeping the total product between zero and one. Also, one or more factors may be eliminated by setting the appropriate exponent equal to zero.

In order to make the optimization of the merit function meaningful, it is desirable to define or specify each merit factor carefully. The desired result is to have the merit function a strictly concave function in the vicinity of the optimum, thus assuring second derivatives with respect to all variables and a negative definite matrix of second derivatives. This is a necessary condition for the function to have a maximum on the interval. It is also

desired to have a merit function which has first derivatives with respect to all variables equal to zero on the open interval, thus insuring that the optimum is not at one limit. This is desired since any variable going to its limit means that that variable does not enter into the optimization and could just as well be eliminated by setting it equal to its limit value.

Some requirements for attaining the desired properties in the merit function can be given for some of the simpler cases.

It is assumed that the merit function will be single-valued, continuous and have continuous first derivatives in each of its variables. It is also assumed that the range of the merit function will be zero to unity and that the domain of the variables is closed and finite.

Consider (4.1) written in the logarithmic form

$$\log M = \sum_{n=1}^{N} w_n \log M_n(x_i) \tag{4.2}$$

then, assuming that an interior optimum exists,

$$\frac{\partial}{\partial x_i} \log M = \sum_{n=1}^{N} w_n \frac{\partial}{\partial x_i} \log M_n(x_i) = 0 \quad (i = 1,2,\cdots I) \tag{4.3}$$

It is evident from (4.3) that the individual values of the w_n are not important in determining the optimum but rather only their ratio.

Thus in (4.3) w_n can be replaced by η_n where

$$\eta_n = \frac{w_n}{w_{n-1}} \tag{4.4}$$

with the definition, $\eta_1 \equiv 1$.

Consider now a particularly simple case of a merit function made up of two factors each of which is a function of the same independent variable on the interval (a,b), i.e.,

$$M = M_1(x_1)\, M_2^{\eta_2}(x_1) \tag{4.5}$$

Then if on (a,b)

$$\frac{1}{M}\frac{\partial M}{\partial x_1} = \frac{1}{M_1}\frac{\partial M_1}{\partial x_1} + \eta_2 \frac{1}{M_2}\frac{\partial M_2}{\partial x_1} = 0 \tag{4.6}$$

since $\eta_2 > 0$, $M_1 \geq 0$, $M_2 \geq 0$, (4.6) requires that the two first derivatives be of opposite sign at the optimum.

The simplest pair of candidate functions which fulfill this requirement is two linear functions, one increasing and the other decreasing in x_1.

The other requirement for a maximum is that

$$\frac{1}{M}\frac{\partial^2 M}{\partial x_1^2} = \frac{1}{M_1}\frac{\partial^2 M_1}{\partial x_1^2} + 2\eta_2 \frac{1}{M_1 M_2}\left(\frac{\partial M_1}{\partial x_1}\frac{\partial M_2}{\partial x_1}\right) + \eta_2(\eta_2 - 1)\frac{1}{M_2^2}\left(\frac{\partial M_2}{\partial x_1}\right)^2 + \eta_2 \frac{1}{M_2}\frac{\partial^2 M_2}{\partial x_1^2} < 0 \tag{4.7}$$

For the simplest pair of functions, the two linear functions, the two second derivatives vanish leaving

$$2\,\frac{1}{M_1M_2}\left(\frac{\partial M_1}{\partial x_1}\,\frac{\partial M_2}{\partial x_1}\right) + (\eta_2-1)\,\frac{1}{M^2}\left(\frac{\partial M_2}{\partial x_1}\right)^2 < 0 \qquad (\eta_2 \neq 0) \tag{4.7a}$$

Since the two first derivatives are of opposite sign, the first term of (4.7a) will be negative. The sign of the second term is determined by (η_2-1). If $0 < \eta_2 \leq 1$, then the sign of the second term will be negative also and clearly (4.7a) is negative. This is somewhat more restrictive than needed as the final requirement is

$$\left|\frac{\partial M_1}{M_1\partial x_1}\,\frac{\partial M_2}{M_2\partial x_1}\right| > \frac{(\eta_2-1)}{2}\left(\frac{\partial M_2}{M_2\partial x_1}\right)^2 \tag{4.7b}$$

In the event strict monotonicity is not required, both functions can be zero simultaneously over part of the interval even though one is an increasing function and the other decreasing. When this happens, the product function will be zero over the entire interval. Another problem with non-strict monotonicity is that the functions may simultaneously be constant over part of the interval. Although the requirement of (4.6) will be satisfied, the second derivative (4.7) will be zero and not negative-definite as required for a maximum.

Since it is not desired to restrict the candidate functions to linear functions, any other pairs of function can be used provided the requirements of (4.6) and (4.7) are met.

If considering more than two functions of a single variable, those which strictly increase may be grouped together and treated as a single, strictly increasing function. Those which strictly decrease may be similarily grouped. Since neither of the resulting pair need be linear, the tests of (4.6) and (4.7) must be met by the resulting merit function.

If now we consider a function of two variables

$$M = M_1 (x_1, x_2) M_2^{\eta_2}(x_1, x_2) \tag{4.8}$$

Then for an interior optimum on the interval [a,b]

$$\left.\begin{aligned} \frac{1}{M}\frac{\partial M}{\partial x_1} &= \frac{1}{M_1}\frac{\partial M_1}{\partial x_1} + \eta_2 \frac{1}{M_2}\frac{\partial M_2}{\partial x_1} = 0 \\ \frac{1}{M}\frac{\partial M}{\partial x_2} &= \frac{1}{M_1}\frac{\partial M_1}{\partial x_2} + \eta_2 \frac{1}{M_2}\frac{\partial M_2}{\partial x_2} = 0 \end{aligned}\right\} \tag{4.9}$$

Write (4.9) in the form

$$\left.\begin{aligned} \frac{1}{M}\frac{\partial M}{\partial x_1} &= \frac{\partial \log M}{\partial x_1} = \frac{\partial}{\partial x_1}\log M_1 + \eta_2 \frac{\partial}{\partial x_1}\log M_2 = 0 \\ \frac{1}{M}\frac{\partial M}{\partial x_2} &= \frac{\partial \log M}{\partial x_2} = \frac{\partial}{\partial x_2}\log M_1 + \eta_2 \frac{\partial}{\partial x_2}\log M_2 = 0 \end{aligned}\right\} \tag{4.10}$$

Try an iterative solution of (4.10) for x_1 and x_2 where, for the k+1 iteration,

$$\frac{\partial}{\partial x_1}\log M_1^{k+1}\left(x_1^k + \delta x_1^{k+1},\ x_2^k + \delta x_2^{k+1}\right) = \frac{\partial \log M_1^k}{\partial x_1} + \frac{\partial^2 \log M_1^k}{\partial x_1^2}\delta x_1^{k+1} + \frac{\partial^2 \log M_1^k}{\partial x_1 \delta x_2}\delta x_2^{k+1} + \cdots \tag{4.11}$$

$$\frac{\partial}{\partial x_1}\log M_2^{k+1} = \frac{\partial \log M_2^k}{\partial x_1} + \frac{\partial^2 \log M_2^k}{\partial x_1^2}\delta x_1^{k+1} + \frac{\partial^2 \log M_2^k}{\partial x_1 \partial x_2}\delta x_2^{k+1} + \cdots \tag{4.12}$$

$$\frac{\partial}{\partial x_2}\log M_1^{k+1} = \frac{\partial \log M_1^k}{\partial x_2} + \frac{\partial^2 \log M_1^k}{\partial x_2^2}\delta x_2^{k+1} + \frac{\partial^2 \log M_1^k}{\partial x_1 \partial x_2}\delta x_1^{k+1} \tag{4.13}$$

$$\frac{\partial}{\partial x_2}\log M_2^{k+1} = \frac{\partial \log M_2^k}{\partial x_2} + \frac{\partial^2 \log M_2^k}{\partial x_2^2}\delta x_1^{k+1} + \frac{\partial^2 \log M_2^k}{\partial x_1 \partial x_2}\delta x_2^{k+1} \tag{4.14}$$

Putting (4.11), (4.12), (4.13) and (4.14) into (4.10) gives

$$\begin{bmatrix} \nabla x_1 \\ \nabla x_2 \end{bmatrix} = \begin{bmatrix} \frac{\partial^2 \log M_1^k}{\partial x_1^2} + \eta_2 \frac{\partial^2 \log M_2^k}{\partial x_1^2} & \frac{\partial^2 \log M_1^k}{\partial x_1 \partial x_2} + \eta_2 \frac{\partial^2 \log M_2^k}{\partial x_1 \partial x_2} \\ \frac{\partial^2 \log M_1^k}{\partial x_1 \partial x_2} + \eta_2 \frac{\partial^2 \log M_2^k}{\partial x_1 \partial x_2} & \frac{\partial^2 \log M_1^k}{\partial x_2^2} + \eta_2 \frac{\partial^2 \log M_2^k}{\partial x_2^2} \end{bmatrix} \begin{bmatrix} \delta x_1^{k+1} \\ \delta x_2^{k+1} \end{bmatrix}$$

(4.15)

where $$\nabla x_i = \frac{\partial \log M_1^{k+1}}{\partial x_i} - \frac{\partial \log M_1^k}{\partial x_i} + \eta_2 \left(\frac{\partial \log M_2^{k+1}}{\partial x_i} - \frac{\partial \log M_2^k}{\partial x_i} \right)$$

For (4.15) to have a unique solution it is necessary that the square matrix, which will be called Q, be other than zero. Since (4.15) is to be iterated for a maximum, at which point the left side will be zero; it is necessary that Q be negative definite. This is to insure that a positive value of δx_i will decrease the value the left hand side of (4.15) when x_i is less than the optimum. It is evident that Q is identical to the matrix of the quadratic form obtained by expanding (4.8) in a Taylor series about the optimum.

It should also be noted that if the set of equations (4.15) is solved by Cramer's rule, the determinant of Q will be the denominator in the solution. Thus if Q is near zero, small changes in Q will have a large effect on the answer. This then constitutes an "ill-conditioned" set of equations.

The simplest candidate functions for M_1 and M_2 are linear

functions in x_1 and x_2.

Assume

$$\begin{aligned} M_1 &= ax_1 + bx_2 + e \\ M_2 &= cx_1 + dx_2 + f \end{aligned} \tag{4.16}$$

What requirements must be placed in the coefficients of equation (4.16) in order that it meet the requirements of (4.9) and that Q of (4.15) be negative definite?

Using (4.9) one obtains

$$\left.\begin{aligned} \frac{1}{M}\frac{\partial M}{\partial x_1} &= \frac{a}{M_1} + \eta_2 \frac{c}{M_2} = 0 = aM_2 + c\eta_2 M_1 \\ \frac{1}{M}\frac{\partial M}{\partial x_2} &= \frac{b}{M_1} + \eta_2 \frac{d}{M_2} = 0 = bM_2 + d\eta_2 M_1 \end{aligned}\right\} \tag{4.17}$$

Evaluating Q from the square matrix of (4.15) gives

$$Q = -\frac{1}{M_1^2 M_2^2}\begin{bmatrix} a^2M_2^2 + \eta_2 c^2 M_1^2 & abM_2^2 + \eta_2 cdM_1^2 \\ abM_2^2 + \eta_2 cdM_1^2 & b^2M_2^2 + \eta_2 d^2 M_1^2 \end{bmatrix} \tag{4.18}$$

Since M_1 and M_2 are to be non-negative, (4.17) can be satisfied only if a and c are of opposite sign as well as b and d of opposite sign. This says that if M_1 is an increasing linear function of x_i then M_2 must be a decreasing function of the same variable. Expanding the determinant of (4.18) leads to the requirement

$$(ad - bc)^2 > 0 \tag{4.19}$$

Equation (4.19) says that Q given by (4.18) will be negative definite for any values of the coefficients in (4.16) except those which make Q equal zero. However, so far, there is no restriction on the domain of x_1 and x_2 . Being assured that the merit function is negative definite, it is necessary to impose conditions that insure that at least a local optimum occurs on the open intervals defined by x_1 and x_2 . Rolle's theorem in one dimension states that a continuous function on a closed, finite interval which has a continuous first derivative will have its first derivative zero some place on the interior of the interval provided the values of the function at each end are equal to each other. By extending this to a plane and requiring all four of the combinations of boundary points to be equal, an interior optimum of M is assured.

The requirements for an interior maximum of the merit function when made up of two linear factors of the form given by (4.16) on the intervals $0 \leq x_1 \leq 1$, $0 \leq x_2 \leq 1$ is then

(1) $ac < 0$

(2) $bd < 0$

(3) $ad - bc \neq 0$

(4) $M(0,0) = M(1,0) = M(0,1) = M(1,1) = k$

If equation (4.2) is expanded in general for N merit factors with I variables, (4.15) takes the general form

$$\begin{bmatrix} \nabla x_1 \\ \nabla x_2 \\ \vdots \\ \nabla x_I \end{bmatrix} = \begin{bmatrix} \sum_{n=1}^{N} \eta_n \frac{\partial^2 \log M_n^k}{\partial x_1^2} & \sum_{n=1}^{N} \eta_n \frac{\partial^2 \log M_n^k}{\partial x_1 \partial x_2} & \cdots & \sum_{n=1}^{N} \eta_n \frac{\partial^2 \log M_n^k}{\partial x_1 \partial x_I} \\ \sum_{n=1}^{N} \eta_n \frac{\partial^2 \log M_n^k}{\partial x_2 \partial x_1} & \sum_{n=1}^{N} \eta_n \frac{\partial^2 \log M_n^k}{\partial x_2^2} & \cdots & \sum_{n=1}^{N} \eta_n \frac{\partial^2 \log M_n^k}{\partial x_2 \partial x_I} \\ \vdots & & & \\ \sum_{n=1}^{N} \eta_n \frac{\partial^2 \log M_n^k}{\partial x_I \partial x_1} & \cdots & \cdots & \sum_{n=1}^{N} \eta_n \frac{\partial^2 \log M_n^k}{\partial x_I^2} \end{bmatrix} \begin{bmatrix} \delta x_1^{k+1} \\ \delta x_2^{k+1} \\ \vdots \\ \delta x_I^{k+1} \end{bmatrix}$$

(4.20)

where $$\nabla x_i = \sum_{n=1}^{N} \eta_n \left(\frac{\partial \log M_n^{k+1}}{\partial x_i} - \frac{\partial \log M_n^k}{\partial x_i} \right)$$

Equation (4.20) assumes that an interior optimum exists. An I-dimensional form of Rolle's theorem will be required to insure an interior optimum. Then, if the square matrix of (4.20) is negative definite, the optimum is at least a local maximum.

It is very time consuming to apply the requirements of (4.20) to candidate functions but in general it appears that at least the following requirements must be met by either the individual merit factors or by the final merit function.

1. Each merit factor must be continuous, single-valued, and have continuous first derivatives.

2. Each merit factor must be dimensionless and be normalized to lie between zero and one.

3. If each merit factor is a linear combination of the variables, then each variable must appear in at least two different factors. Further if one appearance is in an increasing function of that variable (positive sensitivity coefficient) then the other must be in a decreasing function.

4. The weight exponents, w_n , must be non-negative to preserve the zero to unity criterion.

Each merit factor is to be a relationship describing one aspect of the design performance or requirement. It is also assumed that the different merit factors describe conflicting requirements on the same set of independent variables. Thus it is expected that each independent variable will not only appear in both increasing and decreasing functions, but that the resulting merit function will be near zero near the boundaries of the domain of interest for each variable. This does not guarantee that an interior optimum will exist but makes it plausible that one should exist.

Since any merit factor going to zero yields a zero value for the merit function, considerable care must be exercised in choosing each merit factor. In effect, this says that no matter how well the other performance requirements are met, this particular one renders the design completely unacceptable.

Five representative functions which are suitable as merit factors are shown in Figure 4.1. For convenience, all are shown as monotonic decreasing functions of a single variable. Also shown is the effect of varying w_n on each of the functions. It is apparent in all cases that $w_n < 1$ keeps the function near unity over a larger portion of its domain than does $w_n = 1$, thus de-emphasizing that factor.

It should be noted that only the linear function, Figure 4.1(a), has both end points fixed (with the possible exception when $w_n = 0$, in which case the right hand value will be defined as unity).

Since the shape of each merit factor depends on the value judgement of the designer, it is not possible to give any rules for selecting each factor nor where to set the end points. This can only come from a thorough analysis of each application. In general though, lacking any better criteria, a good start might be with an approximate linear curve, such as shown in Figure 4.1(e). The weight exponent can then be used to alter the shape of the curve without changing the end points too drastically.

It should be emphasized that the merit factors are measures of the design performance and requirements and as such will many times be expressed in terms of functions of the independent variables. This will be more apparent in the next section when specific application will be made to the squeeze-film journal bearing problem.

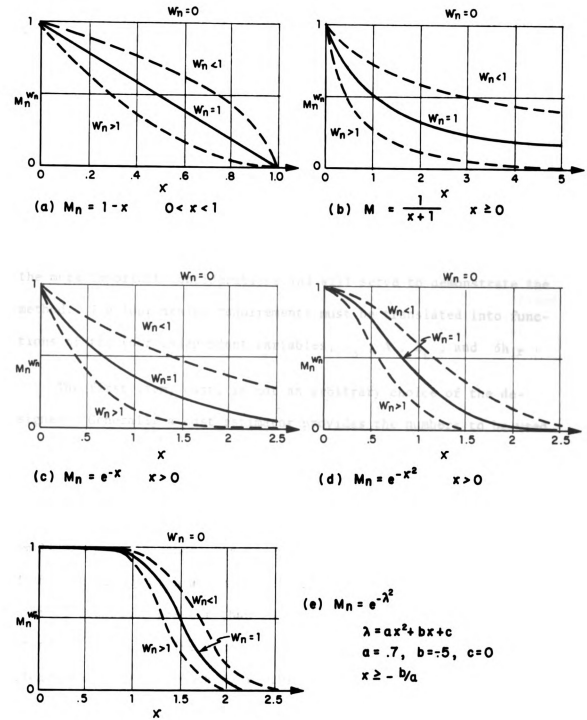

Figure 4.1 Effect of weighting exponent on representative functions

4.2 APPLICATION TO THE SQUEEZE-FILM JOURNAL BEARING

To illustrate the application of the merit function to the squeeze-film journal bearing, four different design requirements are to be considered:

1. Cost of producing the transducer.
2. Minimum eccentricity
3. Length to diameter ratio
4. Minimum power

This list is by no means exhaustive but does include some of the more important considerations and will serve to demonstrate the method. The four design requirements must be translated into functions of the four independent variables, h_o , A , Z_L , and δh_{1r} .

The first item, cost, is not an arbitrary choice of the designer. Generally a cost estimator provides the numbers to be used here. To relate cost to merit, through parameters in the gas bearing, the variable costs to produce a given nominal clearance and the increment of cost that would be necessitated by an extremely small minimum clearance were used. At one extreme, the cost to produce an assembly with a nominal clearance of 1000 microinches and a minimum clearance greater than 250 microinches was used as the standard ($M_1 = 1$). The other extreme was represented by a nominal clearance of 50 microinches, a value which present manufacturing processes are unable to produce at any reasonable cost ($M_1 = 0$). The function chosen to represent merit between the extremes was the

reciprocal of the cost function which was taken as

$$P = \frac{\frac{1}{4} h_o + 700}{h_o - 50} + e^{-(0.01c)^2} \tag{4.21}$$

where $50 < h_o \leq 1000$ and $c \geq 0$ are to be measured in microinches.

P has the value of unity at $h_o = 1000$ microinches without the additive clearance term. The clearance was put in the form given so that the small clearance requirement would have the greater effect for large values of nominal clearance. The reason for this is that when the nominal clearance is small anyway, the added requirement of small minimum clearance adds but little to the total cost. No fixed costs were considered since only differences between designs were being considered.

The first merit factor was taken as

$$M_1 = \frac{1}{P} \ . \tag{4.22}$$

Figure 4.2(a) shows that M_1 appears to be a monotonic increasing function of the nominal clearance h_o. Since M_1 is also an explicit function of the clearance, c, which in turn is a function of h_o, to prove that M_1 is monotonic increasing with h_o, it is necessary to show that $\frac{\partial M_1}{\partial h_o} \geq 0$ for all values of c. This can be done, at least for the small parameter equation, using (3.17) as the clearance equation. However, in general since c is a single-valued, continuous function of h_o, it should be possible to bound the derivative of M_1 with respect to h_o by considering the two

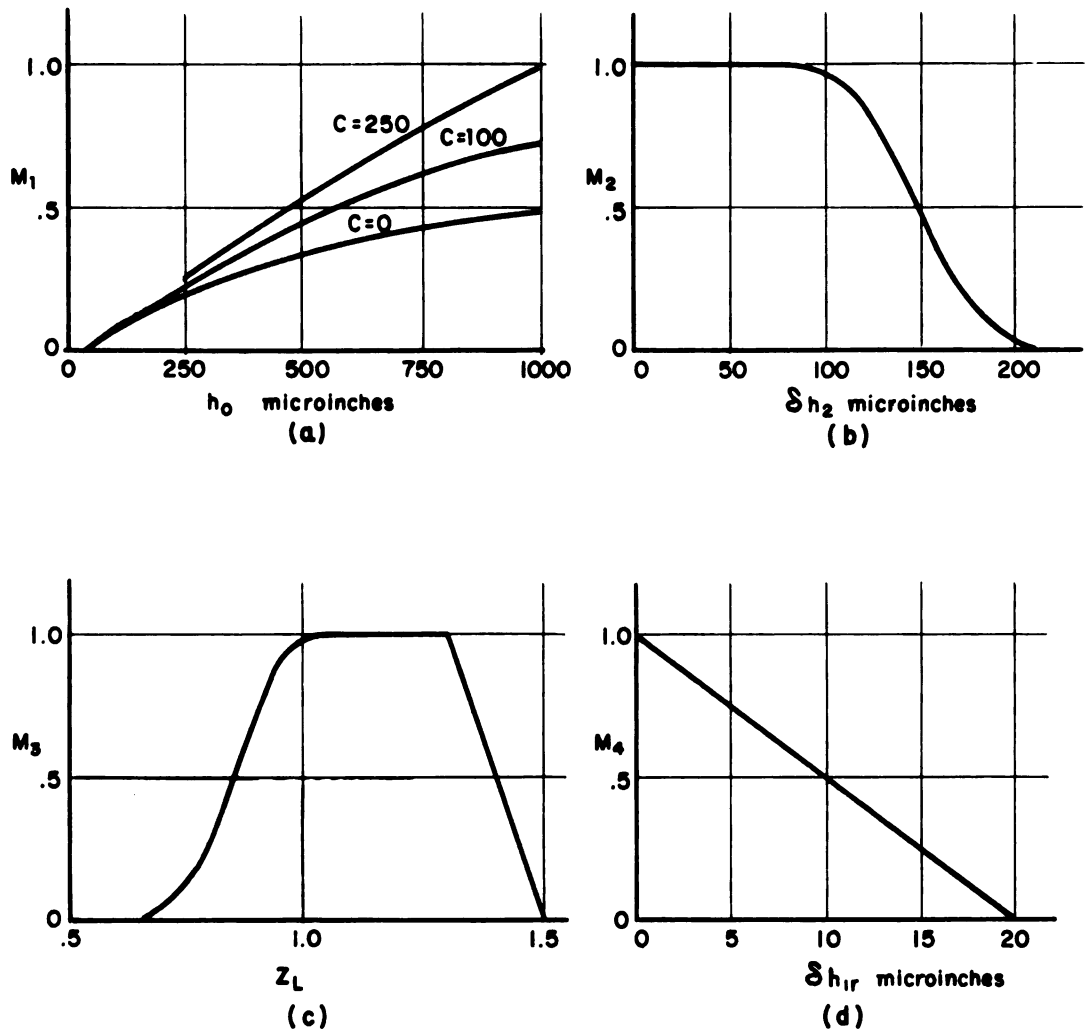

Figure 4.2 Merit factors for the squeeze-film journal bearing

extremes, $c \to \infty$ and $c = 0$. For $c \to \infty$

$$\frac{\partial M_1}{\partial h_o} = \frac{700 + \frac{50}{4}}{\left(\frac{1}{4} h_o + 700\right)^2} \tag{4.23}$$

For $c = 0$

$$\frac{\partial M_1}{\partial h_o} = \frac{650 + \frac{250}{4}}{\left(\frac{5}{4} h_o + 650\right)^2} \tag{4.24}$$

Both (4.23) and (4.24) are always positive showing that M_1 is an increasing monotonic function of h_o.

Differentiation of M_1 with respect to the other independent variables, δh_{1r}, A, and Z_L showed that, in general,

$$\frac{\partial M_1}{\partial x_i} = - 0.0002c \, e^{-(0.01c)^2} \frac{\partial c}{\partial x_i} M_1^2 \tag{4.25}$$

Equation (4.25) is positive or negative depending on the sign of $\frac{\partial c}{\partial x_i}$. In Chapter 3 it was shown that the dimensionless clearance can be optimized on the interval. Thus $\frac{\partial c}{\partial x_i}$ does change sign and M_1 is not monotonic in δh_{1r}, A, and Z_L. In Section 4 of this chapter when examining the sensitivities of the merit factors near the optimum it will be found that $\frac{\partial M_1}{\partial Z_L}$ is negative and $\frac{\partial M_1}{\partial (\delta h_{1r})}$ and $\frac{\partial M_1}{\partial A}$ are positive. This, however, is a local condition near the optimum only.

The second merit factor is a function of the radial displacement, δh_2, of the bearing. Note that δh_2 is a function of h_o, Z_L, A, and δh_{1r}, the four independent variables.

A signal transducer and forcer used in the accelerometer work best if the journal is centered (zero eccentricity). They are reasonably indifferent to radial displacements up to 100 microinches. After this point, performance degrades so that at 200 microinches the instrument is nearly useless. It was decided that the second merit factor should be an approximate linear function of the radial displacement beyond a certain minimum displacement. See Figure 4.2 (b). For this purpose the second merit factor was taken as

$$M_2 = e^{-\lambda_2^2} \tag{4.26}$$

where

$$\lambda_2 = a_2(\delta h_2)^2 + a_1(\delta h_2) + a_o$$

with

$$a_2 = 8.258\times10^{-5} \quad , \quad a_1 = 6.837\times10^{-3} \quad a_o = 0$$

The constants selected gave $M_2 = 0.98$ at $\delta h_2 = -100$ microinch and $M_2 = 0.5$ at $\delta h_2 = -150$ microinches ($M_2 = 0.024$ at $\delta h_2 = -200$ microinches). Also $M_2 = 1$ for $\delta h_2 \geq -82.8$ microinches

It can be shown from the small parameter equation that M_2 is a monotonic increasing function of A and δh_{1r} and a monotonic decreasing function of h_o. Near the optimum $\frac{\partial M_2}{\partial Z_L}$ is negative.

The third merit factor was determined from the general shape of the package desired. If the length to diameter ratio becomes either too small or too large the instrument becomes an undesirable shape. It was decided that $0.7 \leq Z_L \leq 1.5$ was the most desirable range. At the low end of the range the merit factor was chosen of the approximate linear form

$$M_3 = 1 - e^{-\lambda_3^2} \tag{4.27}$$

where

$$\lambda_3 = a_2 Z_L^2 + a_1 Z_L + a_o$$

with

$$a_2 = 5.176 \ , \ a_1 = -3.420 \ , \ a_o = 0 \ .$$

The constants selected gave $M_3 = .02$ at $Z_L = 0.7$ and $M_3 = 0.954$ at $Z_L = 1$. At the high end of the range $M_3 = 1$ for $Z_L < 1.3$ decreasing to zero at $Z_L = 1.5$. See Figure 4.2(c).

The merit function, M_3 , is a monotonic increasing function of Z_L for $Z_L < 1$ and a monotonic decreasing function for $Z_L > 1.3$. There is a discontinuity in the first derivative at $Z_L = 1.3$, however this was not removed as subsequent optimization showed that Z_L^* was always less than 1.3.

The fourth item, minimum power, is related to the drive amplitude, δh_{1r} , in that limited, unpublished experiments by W. G. Holliday[25] at Lear Siegler, Incorporated showed that the rms value

of the excursion of the transducer could be directly correlated to the input power. The fourth merit factor was taken as a simple linear relation with $M_4 = 1$ at $\delta h_{1r} = 0$ and $M_4 = 0$ at $\delta h_{1r} =$ 20 microinch rms. See Figure 4.2(d).

$$M_4 = 1 - \frac{\delta h_{1r}}{20} \tag{4.27a}$$

The total merit function for the design was then taken as the product of the four individual merit factors in the form

$$M = M_1^{W_1} M_2^{W_2} M_3^{W_3} M_4^{W_4} \tag{4.28}$$

where

$$M_1 = M_1(h_o, c(h_o, \delta h_{1r}, A, Z_L, W, V, p_a))$$

$$M_2 = M_2(\delta h_2 (h_o, \delta h_{1r}, A, Z_L, W, V, p_a))$$

$$M_3 = M_3 (Z_L)$$

$$M_4 = M_4 (\delta h_{1r})$$

Each of the merit functions is continuous, single-valued in the independent variables and, except at the high end of M_3, all the merit factors have continuous first derivatives on the interval of interest.

Although the merit factors are measures of different effects they are by no means independent in that they are various functions of the independent variables of the squeeze-film problem.

Table 4.1 summarizes the type of functional relationship which exists between each merit function and the independent variables. In most cases the relationship was derived from the small parameter equation for the gas film. Although not linear functions, as discussed earlier, each of the first three variables appears as an increasing function in at least one of the factors and as a decreasing function in one of the other factors. The exceptional case is the

TABLE 4.1 FUNCTIONAL RELATIONSHIP BETWEEN THE MERIT FACTORS AND THE INDEPENDENT VARIABLES.

	M_1	M_2	M_3	M_4
h_o	Increasing	Decreasing	Not Applicable	Not Applicable
Z_L	Decreasing*	Decreasing*	Increasing*	Not Applicable
δh_{1r}	Increasing*	Increasing	Not Applicable	Decreasing
A	Increasing*	Increasing	Not Applicable	Not Applicable

* Local condition near the optimum.

non-uniformity factor, A. The optimization, to be treated in the next section, was not, however, carried out with respect to A. The fact that M_1 and M_2 are both increasing functions of A results from the choice made for the value of A .

There does not appear to be any significance to the fact that M_1, for instance, is an increasing function of h_o , δh_{1r} and A and a decreasing function of Z_L .

4.3 OPTIMIZATION OF THE MERIT FUNCTION

With the merit function as defined in the previous section, the ability to use δh_{1r} as a normalizing parameter is gone and all computations will be done on a dimensioned basis. A convenient dimension for film thickness is the microinch which will be used exclusively for δh_{1r} , δh_2 , and h_o .

Preliminary runs of the optimization program written to solve the merit problem showed that, as with clearance, the optimum value of A is $-\frac{4}{\pi}$. However the value for A which has been physically demonstrated and which is closest to this value is A equal to -1. To reduce the number of variables, this value of A was used throughout the remainder of the work in preference to other less effective values of A which also have been demonstrated. This reduced the problem to the three independent variables (h_o , δh_{1r} , and Z_L) since again W, V, and p_a were assumed fixed in the demonstration problem. Although introduction of the weighting exponents w_n in (4.1) did, in effect bring in four new independent variables they generally were assumed equal to unity, although some limited experimentation was done varying them one at a time.

It can be shown that the merit function, M , is essentially zero at each boundary of the independent variables thus insuring an interior optimum. For instance, M_4 is zero when δh_{1r} = 20 microinches , M_2 is zero when δh_{1r} = 0 microinches ; M_1 is zero when h_o = 50 microinches; M_2 is essentially zero when h_o = 1000 microinches.

Figure 4.3 shows the merit contours computed using the augmented, small parameter gas film equation with $Z_L = Z_L^*$. Also shown on the figure are the numerically computed optima.

The optimum merit value of 0.0860 shown on Figure 4.2 may seem rather small compared to the maximum possible of unity. The main contribution to the small merit value comes from M_1. This function was selected to have a value of unity for h_o of 1000 microinches and c greater than 250 microinches. The gas film equation only allows $h_o^* = 175.6$ microinches and c = 49.3 microinches, making $M_1 = 0.149$.

The other large contributor is M_4 which linearly decreases from unity to zero as δh_{1r} goes from 0 to 20 microinches, thus at $\delta h_1^* = 7.7$ microinches, $M_4 = 0.615$. The point here is that the numerical value of the merit function evaluated at the optimum is of no consequence. The values of the parameters which gave the optimum are important.

The optimization routine was also performed using the small parameter equation to describe the gas film. The results are shown in Table 4.2 together with the results of the computation with the augmented, small-parameter equation.

It is evident from Table 4.2 that, except for the optimum drive amplitude, the answers from the two different equations agree quite well. Since the small parameter equation required much less computer time than the augmented equation it was used to generate the starting vector for subsequent optimization procedure using the augmented, small-parameter equation.

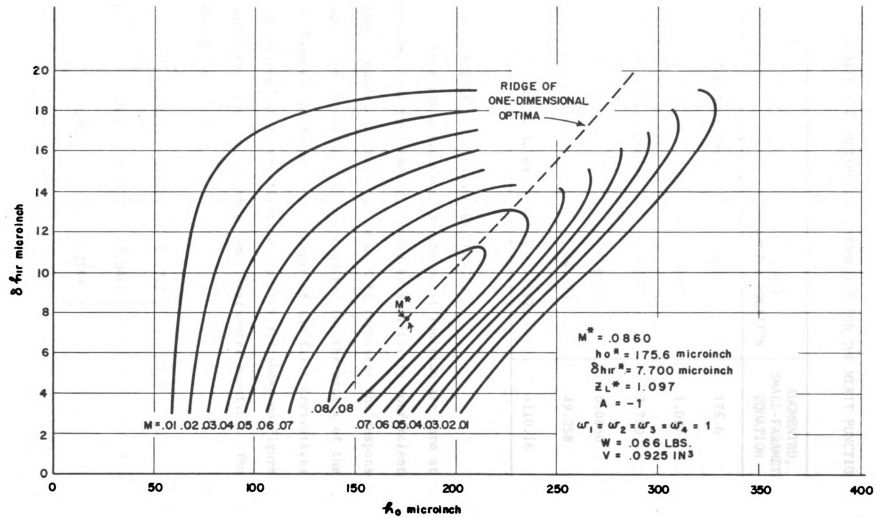

Figure 4.3 Contours of equal merit for the merit function (augmented, small-parameter equation)

TABLE 4.2 OPTIMIZING PARAMETERS FOR THE MERIT FUNCTION.

	SMALL PARAMETER EQUATION	AUGMENTED, SMALL-PARAMETER EQUATION
h_o^* microinches	167.5	175.6
Z_L^*	1.117	1.097
δh_{1r} microinches	9.527	7.700
M*	0.07122	0.0860
c microinches	44.573	49.258
δh_2 microinches	-102.92	-110.16

4.4 SENSITIVITY TO PARAMETER CHANGES

The first derivatives of the merit function are zero at the optimum, thus they cannot be used as sensitivity coefficients. But again a quadric surface can be used to represent the response surface. The second derivatives required for the matrix of the quadratic form can be found as the slopes of the first derivatives near the optimum, where the first derivatives are shown on Figure 4.4, calculated from the augmented small-parameter equation. Thus in analogy to (3.30)

$$Q = -\begin{bmatrix} 1.392 & 0.1055 & -0.5710 \\ 0.1058 & 0.3352 & -0.0460 \\ -0.5702 & -0.0456 & 0.2898 \end{bmatrix} \simeq -\begin{bmatrix} 1.4 & 0.1 & -0.57 \\ 0.1 & 0.34 & 0 \\ -0.57 & 0 & 0.29 \end{bmatrix} \tag{4.29}$$

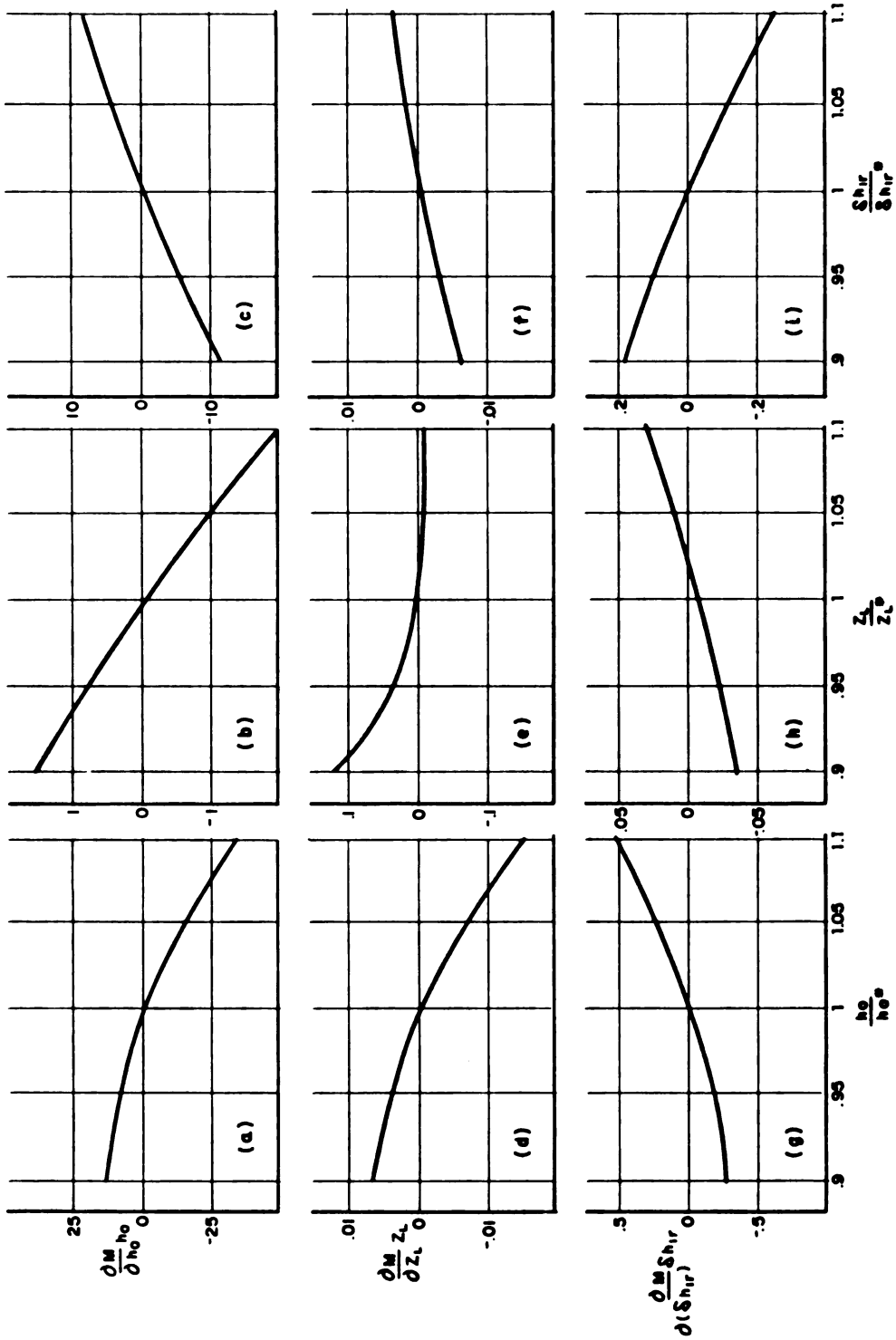

Figure 4.4 First derivatives of the merit function near the optimum (augmented, small-parameter equation)

where

$$q_{ij} = \frac{\partial^2 M}{\partial x_i \partial x_j} x_i x_j$$

with

$$\bar{x} = \left[\frac{\Delta h_o}{h_o}, \frac{\Delta Z_L}{Z_L}, \frac{\Delta\left(\delta h_{1r}\right)}{\delta h_{1r}} \right] .$$

The linear transformation

$$\bar{y} = \begin{bmatrix} 1 & 0.072 & -0.41 \\ 0 & 1 & 0 \\ 0 & 0 & 1 \end{bmatrix} \bar{x} \tag{4.30}$$

applied to (4.29) diagonalizes Q .

The deviation of the merit value from the optimum merit value may then be written

$$M - M^* = \bar{y} \begin{bmatrix} -1.4 & 0 & 0 \\ 0 & -0.333 & 0 \\ 0 & 0 & -0.058 \end{bmatrix} \bar{y}^T \tag{4.31}$$

where

$$y_1 = \frac{\Delta h_o}{h_o} + \frac{0.072\ \Delta Z_L}{Z_L} - \frac{0.41\ \Delta\delta h_{1r}}{\delta h_{1r}} \tag{4.32}$$

Equation (4.32) shows strong interaction between h_o and δh_{1r}. The ridge of one-dimensional optima which divides Figure 4.3 is also evidence of h_o - δh_{1r} interaction. The presence of the h_o - δh_{1r} interaction was also evident during the numerical optimization procedure. A steepest ascent method was used even though it was knwon that this method is inefficient for ridge systems[30]. The procedure did "zig-zag" across the ridge, eventually finding the optimum; but not without taking a great number of steps. Making the transformation of variables (4.30) would improve the efficiency of the optimization procedure; however, the transformation is not known until after the optimization has been performed. It is evident from (4.29) that the optimum is relatively insensitive to the value of Z_L .

Since the merit function is a product of merit factors, it is possible to determine sensitivity coefficients, in the sense of the classical definition, for each of the merit factors. Using (4.3), write the sensitivity coefficient in the form

$$S^M_{x_i} = \frac{x_i}{M}\frac{\partial M}{\partial x_i} = x_i \frac{\partial}{\partial x_i} \log M \qquad (i = 1, 2, \cdots I) \tag{4.33}$$

which is also

$$S^M_{x_i} = x_i \sum_{n=1}^{N} w_n \frac{\partial}{\partial x_i} \log M_n = \sum_{n=1}^{N} w_n \frac{x_i}{M_n}\frac{\partial M_n}{\partial x_i} = \sum_{n=1}^{N} w_n S^{M_n}_{x_i} \tag{4.34}$$

At the optimum, (4.34) is zero, for x_i equal to h_o , Z_L , or δh_{1r} as shown in the second column of Table 4.3. (The small residue is due to the inability of the computer to find the exact

TABLE 4.3 SENSITIVITY COEFFICIENTS OF THE MERIT FUNCTION (WEIGHT EXPONENTS EQUAL TO UNITY)

SMALL PARAMETER EQUATION					
x_i	$S^{M}_{x_i}$	$S^{M_1}_{x_i}$	$S^{M_2}_{x_i}$	$S^{M_3}_{x_i}$	$S^{M_4}_{x_i}$
h_o	-0.0067173	1.0670	-1.0737	0	0
Z_L	0.0023194	-0.0098701	-0.033910	0.045700	0
δh_{1r}	-0.00034617	0.19038	0.71582	0	-0.90967
A	0.44930	0.092708	0.35659	0	0
W	-0.46322	-0.10541	-0.35782	0	0
V	0.30909	0.070334	0.23875	0	0
AUGMENTED, SMALL-PARAMETER EQUATION					
h_o	-.0061109	1.14999	1.15589	0	0
Z_L	-0.0093814	-0.017460	-0.085965	0.094039	0
δh_{1r}	-0.0057128	0.089228	0.53106	0	-0.62602
A	0.28457	0.038712	0.24586	0	0
W	-0.31861	-0.053790	-0.26482	0	0
V	0.21176	0.035746	0.17600	0	0

optimum). However, Table 4.3 shows how the individual merit factors are affected by the parameter changes. Thus a unit change in h_o using the augmented equation, for instance, changes M_1 and M_2 by 1.15 units; whereas a unit change in Z_L changes M_1 by 0.017 units, M_2 by 0.086 units, and M_3 by 0.094 units. Thus, it is evident that Z_L does not have as great an influence as h_o or δh_{1r}.

Also shown in Table 4.3, are sensitivity coefficients with respect to the non-uniformity factor, A , the load, W , and the volume, V. These, of course, are not zero. Table 4.3 also gives the sensitivity coefficients of the merit factors for these parameters.

By chain-rule differentiation

$$S_{x_i}^{M_1} = \frac{x_i}{M_1}\frac{\partial M_1}{\partial x_i} = \left(\frac{c}{M_1}\left.\frac{\partial M_1}{\partial c}\right|_{h_o}\right)\left(\frac{\partial c}{\partial x_i}\frac{x_i}{c}\right) + \left(\frac{h_o}{M_1}\left.\frac{\partial M_1}{\partial h_o}\right|_{c}\right)\left(\frac{\partial h_o}{\partial x_i}\frac{x_i}{h_o}\right)$$

$$= \left.S_c^{M_1}\right|_{h_o} S_{x_i}^{c} + \left.S_{h_o}^{M_1}\right|_{c} S_{x_i}^{h_o} \qquad (4.35)$$

$$S_{x_i}^{M_2} = \left(\frac{\delta h_2}{M_2}\frac{\partial M_2}{\partial(\delta h_2)}\right)\left(\frac{\partial(\delta h_2)}{\partial x_i}\frac{x_i}{\delta h_2}\right) = S_{\delta h_2}^{M_2} S_{x_i}^{\delta h_2} \qquad (4.36)$$

This further reduces the sensitivity of each factor to the product of parameter sensitivities. The merit factor M_1 is an explicit function of h_o and c ; M_2 is an explicit function of δh_2 , thus three of the sensitivity coefficients in (4.35) and (4.36) are directly obtainable. The factors $S_{x_i}^{c}$ in (4.35) and $S_{x_i}^{\delta h_2}$ in (4.36)

are obtainable from the clearance equation (3.11), either analytically, using the small parameter equation, or numerically, using the augmented, small-parameter equation. The merit factors, M_3 and M_4, are explicit functions of Z_L and δh_{1r}, respectively, thus the sensitivity coefficients are obtained by direct differentiation.

Typical values of the sensitivity coefficients for the small parameter equation at the optimum are

$$S_c^{M_1}\Big|_{h_o} = 0.0002\, c^2\, M_1\, e^{-(.01c)} = .04568 \tag{4.37}$$

$$S_{h_o}^{c} = \frac{1}{c}\left(h_o + 3\,\delta h_2\right) = -3.170 \tag{4.38}$$

$$S_{h_o}^{M_1}\Big|_{c} = \frac{712.5\, M_1\, h_o}{(h_o - 50)^2} \tag{4.39}$$

$$S_{h_o}^{h_o} = 1 \tag{4.40}$$

These give

$$S_{h_o}^{M_1} = (.04568)(-3.170) + 1.211 = 1.066 \tag{4.41}$$

The second term of (4.41) shows that the explicit expression for h_o in M_1 has nearly ten times greater influence than the implicit expression for h_o. Equations (4.37) and (4.39) are constants once the expression for M_1 is selected. The parameter sensitivity

coefficient $S^{c}_{x_i}$ is different for each of the variables. This is also true in (4.36) where $S^{M}_{\delta h_2}$ is a constant for a given M_2 but the parameter sensitivity coefficient $S^{\delta h_2}_{x_i}$ changes. Typical expressions for some of the simpler parameter sensitivity coefficients from the small parameter equation, in addition to (4.38) and (4.40), are

$$S^{c}_{\delta h_{1r}} = -\frac{1}{c}\left(\frac{F(A)}{\alpha^{\frac{1}{2}}}\,\delta h_{1r} + 2\,\delta h_2\right) \tag{4.42}$$

$$S^{c}_{W} = \frac{\delta h_2}{c} \tag{4.43}$$

$$S^{c}_{V} = -\frac{2}{3}\frac{\delta h_2}{c} \tag{4.44}$$

$$\left.\begin{aligned} S^{\delta h_2}_{h_o} &= 3 \\ S^{\delta h_2}_{\delta h_{1r}} &= -2 \\ S^{\delta h_2}_{W} &= 1 \\ S^{\delta h_2}_{V} &= -\frac{2}{3} \end{aligned}\right\} \tag{4.45}$$

Thus some insight into the relative importance of the various parameters can be obtained.

Some limited experimentation was done to determine the effects of weighting exponent changes on the optimizing parameters. The results shown in Table 4.4, were obtained using the augmented,

TABLE 4.4 EFFECT OF WEIGHT EXPONENTS ON THE OPTIMIZING PARAMETERS.

w_1	w_2	w_3	w_4	M*	h_o^*	δh_{1r}^*	Z_L^*
1	1	1	1	0.0860	175.6	7.700	1.097
0.5	1	1	1	0.2458	134.5	4.0	1.112
1	0.5	1	1	0.0903	182.1	7.328	1.101
1	1	0.5	1	0.0860	179.0	8.044	1.081
1	1	1	0.5	0.1202	216.2	11.96	1.092

small-parameter equation for the gas film. No attempt was made to compute the partial derivatives with respect to the weight exponents. Rather, a significant change was made in one exponent at a time. It is probable in an application that changes would be of a similar order of magnitude. The effect of each exponent change can be visualized through the appropriate merit factor. For instance $w_1 = .5$ deemphasized the effect of h_o. As a consequence the optimizing parameters shift to a smaller value of h_o^* ; and with the smaller h_o^*, less drive is required to support the load, so δh_{1r}^* decreases.

Another aspect of sensitivity, how the optimizing parameters change with load changes, is deferred to the next chapter. There a merit function weighted by the expected load to be applied will be developed.

CHAPTER 5

WEIGHTED FIGURE-OF-MERIT

5.1 WEIGHTED MERIT FUNCTION

The merit function developed in the previous chapter is capable of further extension which may be of great value when one of the parameters, previously assumed constant, is permitted to vary. In particular, the load to be carried by the squeeze-film journal bearing has been treated as a constant. However, in many aerospace design problems, as in the demonstration problem, this load is the maximum at which the instrument is expected to perform. The actual load applied at any moment can be described by a probability function.

A common practice is to design for the maximum load with the philosophy, "if it works at the maximum, it will surely work at all lesser loads." The argument with this philosophy is that it tends to create a heavy, bulky, more costly design than is necessary in order to have the reserve for the occasional maximum load. This is especially true if the merit function has been optimized for the maximum load.

What is proposed is a figure-of-merit function, weighted in some suitable fashion by a probability function which describes the load. Such a weighted merit function may be created as follows:

1. Optimize the merit function of a number of competing designs by evaluating at different load values up to the maximum to be expected.

2. Using the optimizing parameters found in step 1, evaluate each competing design at a number of values over the range of expected loads. Call these values $M_{d,s}$ where d is the fraction of the maximum load at which the design was optimized and s is the fraction of the maximum load at which the design is being evaluated.

3. Evaluate the integral

$$\bar{M}_d = \int_0^1 M_{d,s}\, \phi\, ds \qquad (5.1)$$

where ϕ is the weighting function to be selected.

It is then a simple matter to select the design having the maximum $\bar{M}_d$ value.

This procedure should be approached with some caution, though, since it is possible to select a weight function which will so minimize the effect of large load values, that the design with the optimum $\bar{M}_d$ will not function at the maximum load. This could be treated by constraining the optimum design in such a fashion to insure an acceptable level of performance at the maximum load. In any case, it is desirable to check at the maximum load to insure acceptable,

though no larger optimum, performance at the maximum load.

Although application of the weighted merit function is being made to the load, it should be remembered that other parameters could be used as well.

5.2 APPLICATION TO SQUEEZE-FILM BEARING

The procedure described in the preceding section was applied to the squeeze-film journal problem, with W_{max} = .066 pounds and A = -1. Unless otherwise noted the weighting exponents, w_n, in the merit function were all set equal to unity.

The results of the first step, the determination of the optimizing parameters for a number of competing designs at loads, d, less than the maximum, is shown in Figure 5.1. It is immediately apparent that Z_L is not an important parameter and in the final program to optimize $\overline{M}_d$, Z_L was fixed at its first computed value and only h_o and δh_{lr} were used in the optimization program.

Figure 5.2 shows how the merit value, clearance and radial displacement vary when the maximum load is applied to each of the competing designs. Evidently a design optimized for a load of less than .3 of maximum cannot be used as the merit is rapidly approaching zero. This appears to be mainly due to the radial displacement approaching the undesirable region of 200 microinches.

The path followed by the optimizing parameters is shown in Figure 5.3 (a) in the δh_{lr}-h_o plane superimposed on contours of constant merit and in Figure 5.3 (b) superimposed on constant clearance

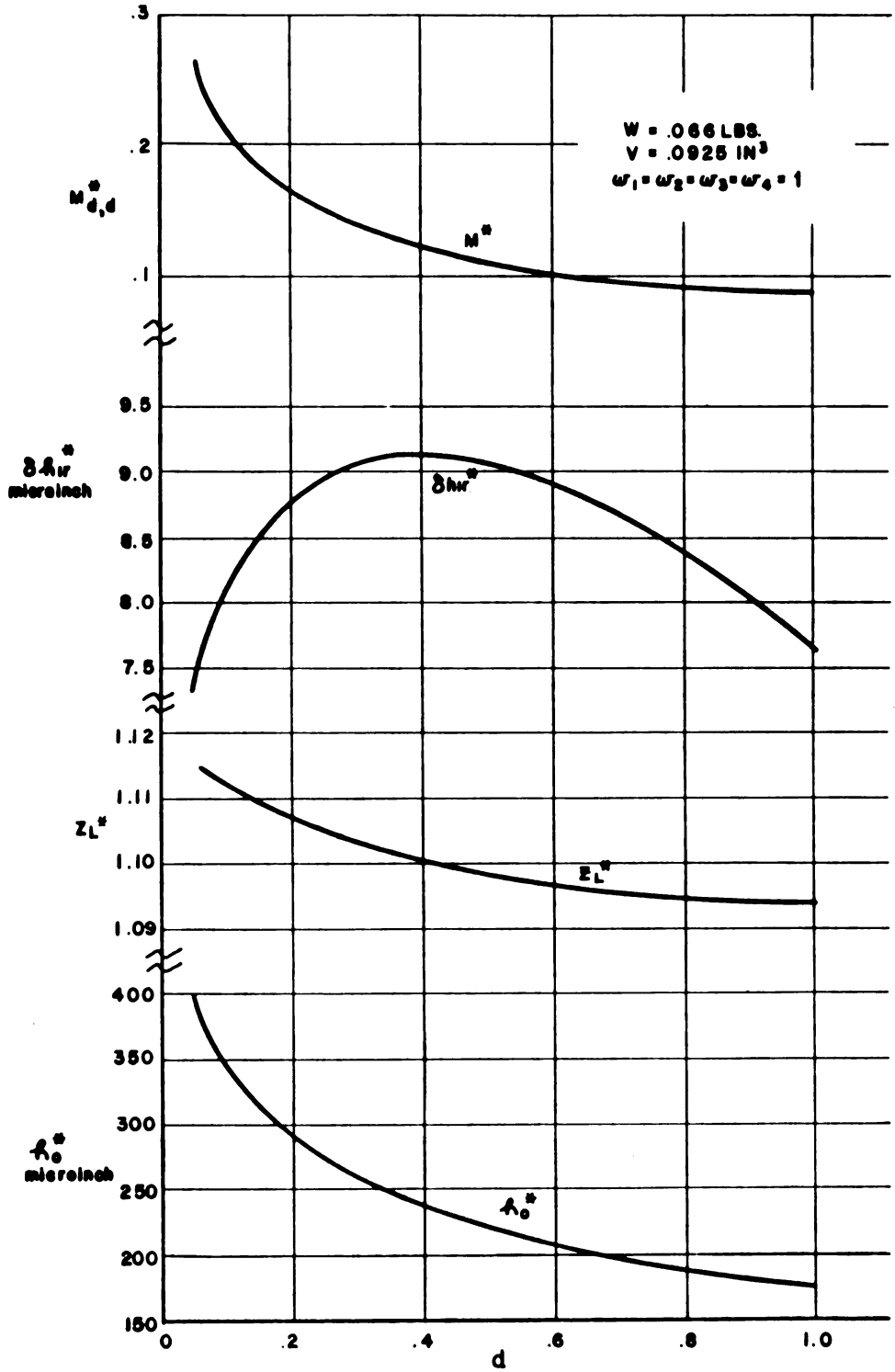

Figure 5.1 Optimizing parameters as functions of load

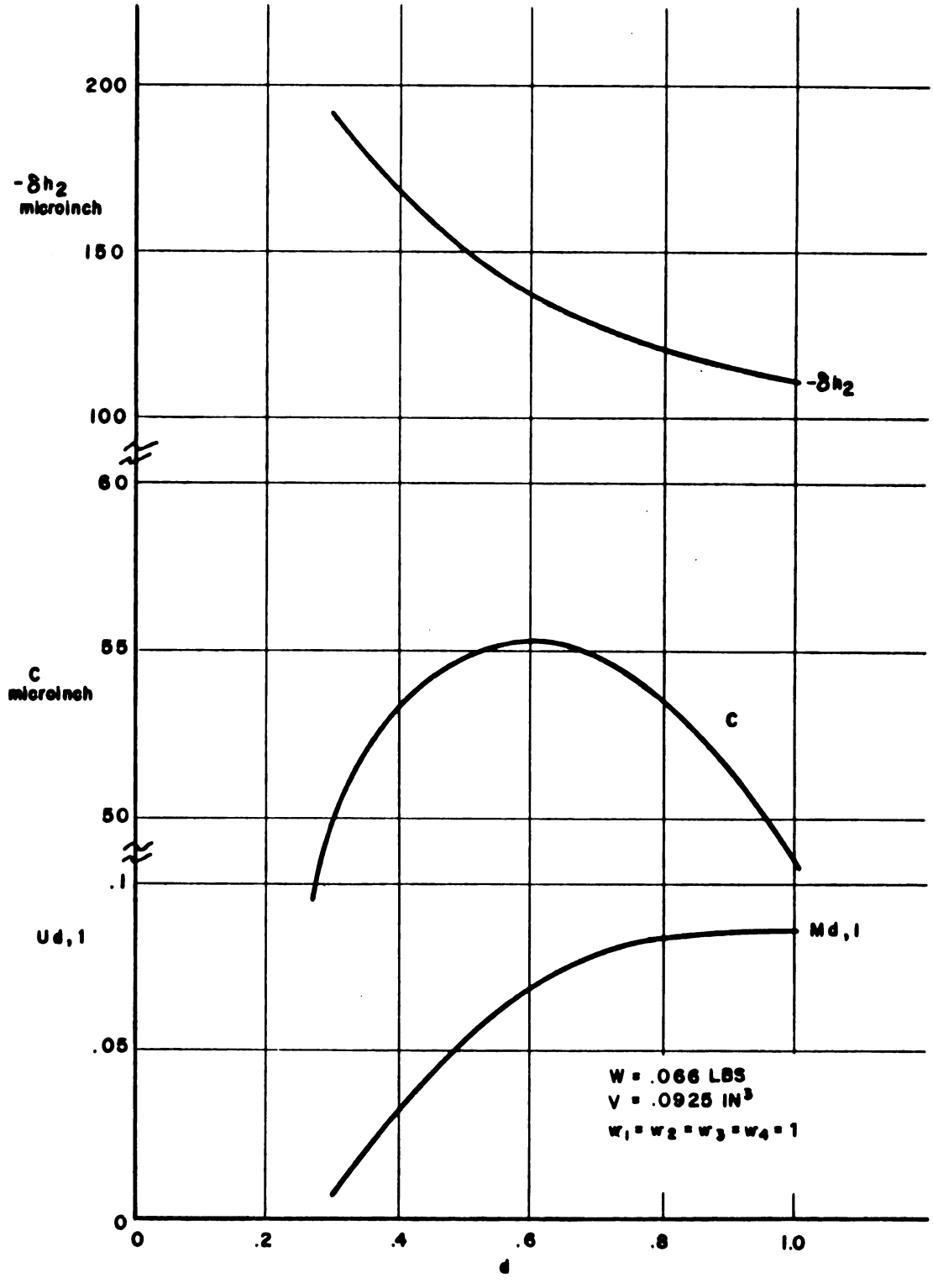

Figure 5.2 Performance of designs optimized at lesser loads when loaded at maximum load

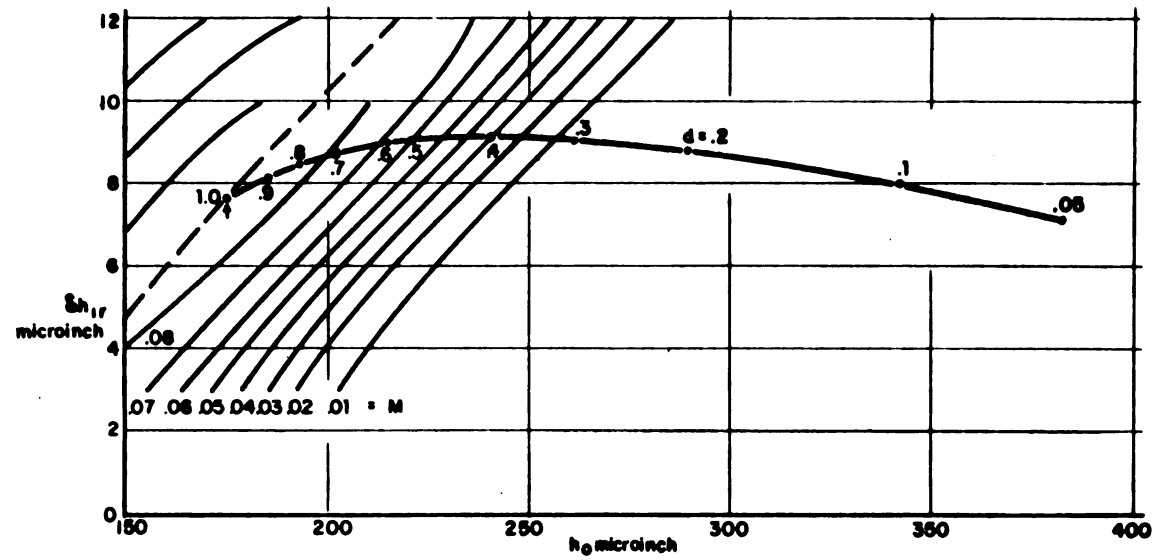

(a) Merit contours

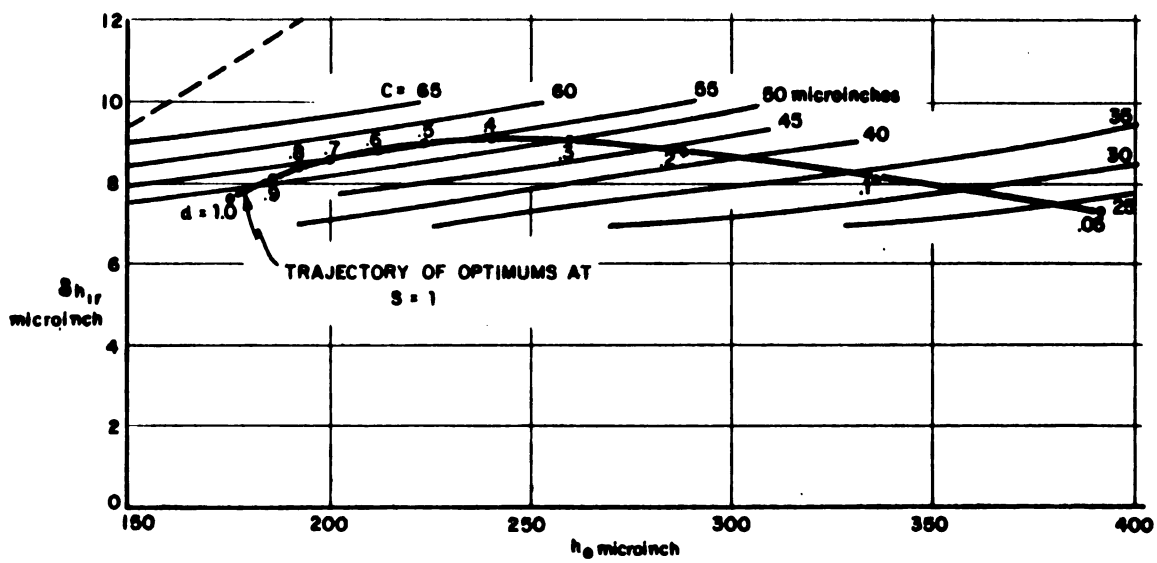

(b) Clearance contours

Figure 5.3 Trajectory of optimums on contour maps

contours in the same plane.

Figure 5.4 illustrates the results of the second step, the evaluation of each competing design over the load range. Again it can be seen that a design optimized at a design load of less than .3 is near failure at the maximum load. On the other hand, the merit rating of a design optimized at the maximum load changes very little over the load range. It is clear that if the design value is very small ($d \to o$) the area under the curve goes to zero. It is not evident that there is a maximum area under one of the design curves, other than the one for $d = 1$.

The third step in the optimization of the weighted merit function is to evaluate the integral given in (5.1). For this problem the weighting function was chosen to be the normal (Gaussian) distribution,

$$\phi = \frac{1}{\sqrt{2\pi}} e^{-\frac{s^2 \sigma^2}{2}} \tag{5.2}$$

where σ is the standard deviation of the load-frequency distribution.

There is equal probability that a given load will be applied in any radial direction leading to the maximum load being ± 30 g in the coordinate plane originally defined. Thus the mean value of the load-frequency distribution was taken as zero.

Figure 5.4 Merit values as function of load for optimum designs

Numerical integration of (5.1) was performed for different values of sigma, with the results shown in Figure 5.5. The value of σ = o corresponds to a weight of one, or all ordinates equally weighted. This has its maximum at d = .6. As sigma increases, the effect is to de-emphasize the larger load values and the maximum shifts to smaller d values. A sigma value of three indicates that the maximum load would be applied approximately 0.3 percent of the time, thus strongly de-emphasizing the importance of the maximum load; in fact, any larger value for sigma says that the probability of this maximum load being applied is vanishingly small.

Considering a reasonable value of sigma to be two, i.e., there is a 5 percent probability of the maximum load being applied at any instant, the optimum weighted merit value corresponds to a design at d = 0.45. It is interesting in Table 5.1 to compare the optimum parameters for this design with those for the design at d = 1.

TABLE 5.1 COMPARISON BETWEEN DESIGN OPTIMIZED AT MAXIMUM LOAD (d = 1.0) AND DESIGN OPTIMIZED AT THE WEIGHTED OPTIMUM (d = 0.45)

d	1.0	0.45
h^*_o	175.6 microinches	230 microinches
δh^*_{1r}	7.7 microinches	9.1 microinches
Z^*_L	1.094	1.098
$M^*_{d,d}$	0.0860	0.1166
$\overline{M}_d$	0.0232	0.0269

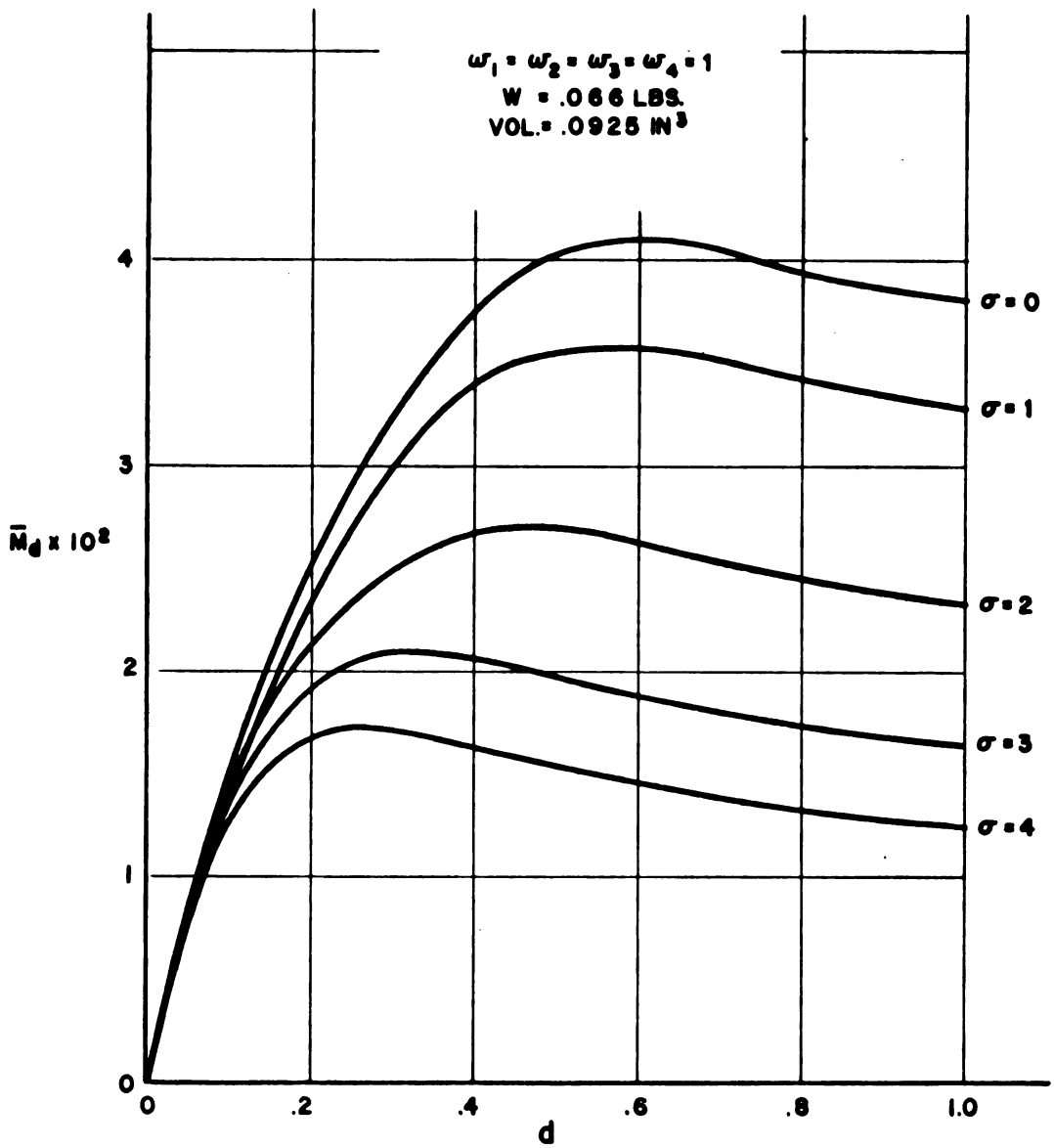

Figure 5.5 Weighted merit as function of design

Although the improvement in $\bar{M}_d$ is only 16 percent, the improvement in the individual $M^*_{d,d}$ is 36 percent.

The results, of course, will be different for a different set of merit functions and for a different problem. The squeeze-film journal bearing example has been carried out in considerable detail. The reason has been to illustrate the merit function and the weighted merit function technique on a concrete example. It should be evident that the merit function approach to a problem allows the selection of an optimum design after a designer analytically specifies his preferences; and, when applicable, the weighted merit function technique further sharpens the choice of optimums.

5.3 STABILITY CONSIDERATIONS

Since all compressible fluid bearings exhibit potential instabilities, this is a matter which must be investigated during the design of any gas bearing. Beck and Strodtman[16] first investigated the stability of a journal bearing when no flow along the axis is permitted (infinite journal). Nolan[17] enlarged this investigation to include Z axis flow (finite journal). Although neither work is directly applicable except when A = 0 (uniform excursion), Nolan's results can be used to indicate whether stability might be a problem in the present case.

Figure 5.6 is a combination of Figures 20 and 21 of Nolan's thesis. A design is considered stable if its parameters (β,ε_2) fall below the appropriate ε_1 curve. The parameter β is the dimensionless "mass" parameter,

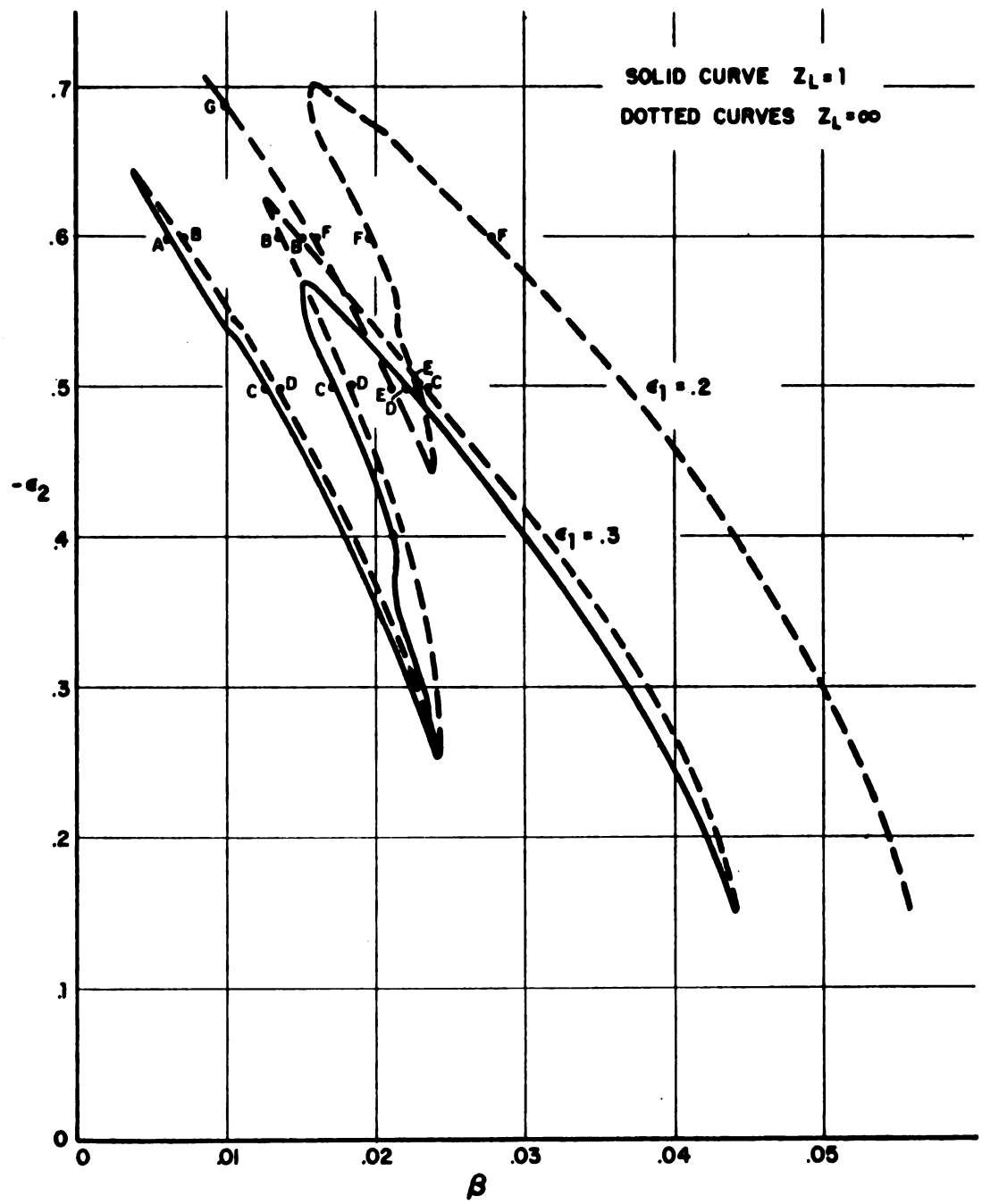

Figure 5.6 Stability map adapted from reference [17]

$$\beta = \frac{p_a RL}{m\omega^2 h_o} \tag{5.3}$$

In the demonstration problem, β has a value of .007 for a drive frequency of 80,000 Hertz, Z_L of unity, and a nominal clearance of 176 microinches. At the optimum of Figure 4.3, h_o = 176 microinches, δh_{1r} = 7.7 microinches, Z_L = 1.097, A = -1, and the radial displacement is 111 microinches. This corresponds to ε_2 = -0.6 and ε_{1r} = 0.0436. At β = 0.007, ε_1 = -0.6, the stability boundary of Figure 5.6 is crossed at ε_1 approximately 0.3. If all the above parameters were to hold for A = 0 (where $\varepsilon_1 = \varepsilon_{1r}$) then, the optimum values give a design which is well removed from the stability boundary

For values of A other than zero it can be argued that the equivalence between ε_{1r} and ε_1 at the stability boundary can be established by the value of the static load support at the boundary. The basis for this argument lies in Figure 5.6, on the two curves for ε_1 = 0.3. One curve is for the infinite journal, the other for a finite journal, yet the stability boundaries practically coincide. A point such as C represents a static load support, W', of 0.27 whereas D represents a load support of 0.155. We can then bound the load support represented by the point E by interpreting ε_1 in two ways (1) as the maximum boundary excursion or (2) as the root-mean-square value of the excursion. Using interpretation (1) the static load support at point E for A = -1 is 0.062 and for interpretation (2) it is 0.016. Similarily point F represents either 0.090 or 0.022.

The optima of Figure 4.3 give a load support of 0.018 at ε_2 = -0.63 and ε_{1r} = 0.0436. The point (0.007, - 0.63) falls well to the left of the worst F (0.016, - 0.6) representing a load support between 0.022 and 0.090.

The weighted optimum design for sigma of two, i.e., for design load of 0.45 maximum load, had h_o = 230 microinches, and δh_{1r} = 9.15 microinches, and gave δh_2 = 158 microinches when loaded at the maximum load equivalent to ε_2 = -0.69, ε_{1r} = 0.040. For the new value of h_o = 230 microinches, β has the new value of 0.0053. The load support required at the maximum load is 0.018 as before. Point G (0.01, -0.69) of Figure 5.6 represents a load support either 0.024 or 0.11. The design value of (0.0053 - 0.69) is still on the stable side; however, under the worst interpretation of G as representing a load support of 0.024, the design is very near the stability boundary.

It would appear that the locations of the stability boundaries for non-uniform excursion should be the subject for future investigation in order to put this matter on a firm basis.

CONCLUSIONS AND RECOMMENDATIONS

One of the objectives of this thesis was to show that the proper choice at variables would maximize the minimum clearance in the bearing under the constraint of fixed load weight and load volume. A second objective was to develop a technique for design optimization. Both objectives have been met.

In meeting the primary objectives, a number of other tasks were accomplished. A method of treating non-uniform driver excursion by means of its root-mean-square value and a non-uniformity factor was developed. Although, in this thesis, the non-uniform excursion was treated as a sinusoidal function in the axial direction, the treatment is general enough to accommodate other shape functions which may be encountered.

The asymptotically-derived partial differential equation describing the squeeze-film bearing was expanded in an asymptotic series of powers of the radial displacement. It was shown that separation of variables on the resulting series of partial differential equations could be accomplished. It was found that the resulting series solution including the third order term was of sufficient accuracy that a slower, alternating-direction, implicit, numerical solution of the squeeze-film differential equation was not required

for this problem. If desired, further improvement in accuracy is possible by following the pattern shown to be present in the series of partial differential equations, to develop higher order terms.

It was found, using only first order terms in the small parameter equation, that explicit optimization of the minimum clearance could be accomplished. A gradient method was used to optimize the clearance using the augmented, small-parameter equation. The optimum nominal clearance was found to be well within the range of values used in the squeeze-film bearings built to date. The optimum length-diameter ratio was considerably less than has usually been used. The optimum non-uniformity factor appeared to be constant regardless of whether the small parameter or the augmented equations were used.

A study of the response surface near the optimum showed that, of the variables treated, the most important variables are the non-uniformity factor and the dimensionless nominal clearance-drive amplitude ratio. The length-diameter ratio did not appear to be an important variable.

By varying the load on the bearing, it was found that the optimum nominal clearance-drive amplitude ratio varied in an especially simple fashion with the change on load.

The concept of a figure-of-merit function as introduced in Chapter 4 should be applicable to a wide range of design problems. Its main forte is its ability to treat dissimilar quantities without

reducing each to a "cost" function. It was shown that a cost factor, a displacement factor, a length-diameter ratio factor, and a drive amplitude factor could be combined into a merit function. It was then possible to optimize the resulting merit function, which was done numerically by a gradient method.

The merit function was further improved by the introduction of the weighted merit function in Chapter 5. The weighted merit function showed that if one of the constraints, such as load, was described by a probability function, the weighted merit function produced an optimum at less than maximum load. The design optimized at this weighted optimum had a merit value 36 percent greater than that of the design optimized at the maximum load.

Among the problems left unanswered or at least which need additional work are the following:

(1) A more complete set of rules for the formation of the merit factors is needed. This was explored to some extent in Chapter 4 and some rules were given.

(2) The treatment of stability of the journal bearing when the excursion is non-uniform is needed. Some arguments were advanced in Chapter 5 based on previous work which treated uniform excursion only [17].

(3) The effect of certain manufacturing errors on the optimization of clearance and on the merit function should be treated. Such errors include taper in the nominal clearance along the longitudinal axis, out-of-roundness or taper in the nominal clearance on the angular direction, and non-uniform excursion on the angular direction.

LIST OF REFERENCES

LIST OF REFERENCES

1. Gross, W. A., Gas Film Lubrication, John Wiley and Sons, New York, 1962.

2. Hirn, G., "Sur les principaux phénomenès qui présentent les frottementes médiats," Société industrielle de Mulhouse. Bulletin 26, 1854, pp. 188-277.

3. Kingsbury, A., "Experiments with an Air Lubricated Journal," Journal of the American Society of Naval Engineers, Vol. 9, 1897, pp. 267-292.

4. Harrison, W. J., "The Hydrodynamical Theory of Lubrication with Special Reference to Air as a Lubricant," Transactions of the Cambridge Philosophical Society, Vol. 22, 1913, pp. 39-54.

5. Taylor, G. I., and Saffman, P. G., "Effects of Compressibility at Low Reynolds Numbers," Journal of the Aeronautical Sciences, Vol. 24, 1957, pp. 553-562.

6. Reiner, M., "Researches on the Physics of Air Viscosity," Technical Report, Technion Research and Development Foundation, Haifa, Israel, 1956.

7. Langlois, W. E., "Isothermal Squeeze Films," Quarterly of Applied Mathematics, Vol. 20, 1962, pp. 131-150.

8. Salbu, E. O. J., "Compressible Squeeze Films and Squeeze Bearings," Journal of Basic Engineering, Transactions ASME, Series D, Vol. 86, No. 2, June, 1964, pp. 355-364.

9. Malanoski, S. B. and Pan, C. H. T., discussion of E. O. J. Salbu's paper "Compressible Squeeze Films and Squeeze Bearings," Journal of Basic Engineering, Transactions ASME, Series D, Vol. 86, No. 2, June, 1964, pp. 364-366. Erratum, Journal of Basic Engineering, Transactions ASME, Series D, Vol. 86, No. 3, Sept., 1964, p. 638.

10. Pan, C. H. T., "On Asymptotic Analysis of Gaseous Squeeze-Film Bearings," Journal of Lubrication Technology, Transactions ASME, Series F, Vol. 89, No. 3, July, 1967, pp. 245-253.

11. Pan, C. H. T., Malanoski, S. B., Broussard, P. H., Jr., and Burch, J. L., "Theory and Experiments of Squeeze-Film Bearing, Part 1, Cylindrical Journal Bearings," Journal of Basic Engineering, Transactions ASME, Series D, Vol. 88, No. 1, March, 1966, pp. 191-198.

12. Beck, J. V., and Strodtman, C. L., "Load Support of the Squeeze-Film Journal Bearing of Finite Length," Journal of Lubrication Technology, Transactions ASME, Series F, Vol. 90, No. 1, Jan., 1968, pp. 157-161.

13. Chiang, T., Malanoski, S. B., Pan, C. H. T., "Spherical Squeeze-Film Hybrid Bearing with Small Steady-State Radial Displacement," Journal of Lubrication Technology, Transactions ASME, Series F, Vol. 89, No. 3, July, 1967, pp. 254-262.

14. Beck, J. V. and Strodtman, C. L., "Load Support of Spherical Squeeze-Film Gas Bearings," Paper No. 68-LubS-3. Presented at the Lubrication Symposium, Las Vegas, Nev., June 17-20, 1968, of The American Society of Mechanical Engineers.

15. Pan, C. H. T., and Broussard, P. H., Jr., "Squeeze-Film Lubrication," Paper No. 12, Gas Bearing Symposium on Design Methods and Applications, University of Southampton, Department of Mechanical Engineering, April, 1967.

16. Beck, J. V. and Strodtman, C. L., "Stability of a Squeeze-Film Journal Bearing," Journal of Lubrication Technology, Transactions ASME, Series F, Vol. 89, No. 3, July, 1967, pp. 369-374.

17. Nolan, J. E., Analytical Investigation of Stability of Squeeze-Film Journal Bearings, Ph.D. thesis, Michigan State University, Department of Mechanical Engineering, 1966.

18. Elrod, H. G., Jr., "A Differential Equation for Dynamic Operation of Squeeze-Film Bearings," Contribution A, Gas Bearing Symposium on Design Methods and Applications, Contributions and Discussions, University of Southampton, Department of Mechanical Engineering, April, 1967.

19. Pan, C. H. T., and Chiang, T., "Dynamic Behaviour of Spherical Squeeze-Film Hybrid Bearing," Paper No. 68-LubS-37. Presented at the Lubrication Symposium, Las Vegas, Nev., June 17-20, 1968, of The American Society of Mechanical Engineers.

20. DiPrima, R. C., "Asymptotic Methods for an Infinitely Long Slider Squeeze-Film Bearing," Journal of Lubrication Technology, Transactions ASME, Series F, Vol. 90, No. 1, Jan., 1968, pp. 173-183.

21. Pan, C. H. T., and Chiang, T., "On Error Torques of Squeeze-Film Cylindrical Journal Bearings, Journal of Lubrication Technology, Transactions ASME, Series F, Vol. 90, No. 1, Jan., 1968, pp. 191-198.

22. Beck, J. V., Holliday, W. G., Strodtman, C. L., "Experiment and Analysis of a Flat Disk Squeeze-Film Bearing Including the Effects of Supported Mass Motion," Paper No. 68-LubS-35. Presented to the Lubrication Symposium, Las Vegas, Nev., June 17-20, 1968, of The American Society of Mechanical Engineers.

23. Sage, Andrew P., Optimum Systems Control, Prentice-Hall, Inc., Englewood Cliffs, New Jersey, 1968.

24. Starr, Martin Kenneth, Product Design and Decision Theory, Prentice-Hall, Inc., Englewood Cliffs, New Jersey, 1968.

25. Holliday, William G., Personal Communication, 1967.

26. Kuo, Benjamin C., Automatic Control Systems, Prentice-Hall, Inc., Englewood Cliffs, New Jersey, 1962.

27. Box, G. E. P., "The Exploration and Exploitation of Response Surfaces: Some General Considerations and Examples," Biometrics, Vol. 10, 1954, pp. 16-60.

28. Von Neumann, John and Morgenstern, Oskar, Theory of Games and Economic Behaviour, Princeton University Press, 1953.

29. Luce, R. Duncan and Raiffa, Howard, Games and Decisions, John Wiley and Sons, 1957.

30. Wilde, Douglass J. and Beightler, Charles S., Foundations of Optimization, Prentice-Hall, Inc., Englewood Cliffs, New Jersey, 1967.

APPENDIX A

APPENDIX A

AUGMENTED, SMALL-PARAMETER SOLUTION OF THE SQUEEZE-FILM EQUATION

A.1 SERIES EXPANSION

The squeeze-film equation, for the journal bearing of finite length, derived on the basis of infinite squeeze number is

$$\frac{\partial}{\partial\theta}\left[\frac{\bar{H}}{2}\frac{\partial T}{\partial\theta} - T\frac{\partial\bar{H}}{\partial\theta}\right] + \frac{\partial}{\partial Z}\left[\frac{\bar{H}}{2}\frac{\partial T}{\partial Z} - T\frac{\partial\bar{H}}{\partial Z}\right] = 0 \qquad (A.1)$$

with the boundary conditions

$$T\left(\pm Z_L,\theta\right) = \left.\frac{\overline{H^3}}{\bar{H}}\right|_{\pm Z_L} \qquad (A.2)$$

$$\frac{\partial T(Z,\theta)}{\partial\theta} = \frac{\partial T(Z,\pi)}{\partial\theta} = 0 \qquad (A.3)$$

For the case considered in this thesis, where only displacement in the radial direction is permitted,

$$H = 1 - \varepsilon_2 \cos\theta - \varepsilon_1 f_1 \sin t \; . \qquad (A.4)$$

Equation (A.1) becomes

$$\frac{\partial}{\partial\theta}\left[\frac{1-\varepsilon_2\cos\theta}{2}\frac{\partial T}{\partial\theta} - T\,\varepsilon_2\sin\theta\right] + \frac{\partial}{\partial Z}\left[\frac{1-\varepsilon_2\cos\theta}{2}\frac{\partial T}{\partial Z}\right] = 0 \qquad (A.5)$$

and the boundary conditions (A.2) become

$$T\left(\pm Z_L,\theta\right) = \left(1-\varepsilon_2 \cos\theta\right)^2 + \frac{3}{2} f_1^2\left(\pm Z_L\right)\varepsilon_1^2 \qquad (A.6)$$

An approximation to T may be made by expanding T in a power series of ε_2, the eccentricity of the bearing,

$$T = \sum_{n=o}^{\infty} \varepsilon_2^n T_n \qquad (A.7)$$

Putting (A.7) into (A.5) yields

$$\sum_{n=o}^{\infty}\left[\left(\varepsilon_2^n-\varepsilon_2^{n+1}\cos\theta\right)\frac{\partial^2 T_n}{\partial\theta^2} - \varepsilon_2^{n+1}\sin\theta\,\frac{\partial T_n}{\partial\theta} - 2\,\varepsilon_2^{n+1}\cos\theta\,T_n\right.$$

$$\left. + \left(\varepsilon_2^n-\varepsilon_2^{n+1}\cos\theta\right)\frac{\partial^2 T_n}{\partial Z^2}\right] = 0 \qquad (A.8)$$

Substitution of (A.7) into (A.6) gives the boundary conditions

$$\sum_{n=o}^{\infty}\varepsilon_2^n T_n\left(\pm Z_L\right) = \left(1-\varepsilon_2\cos\theta\right)^2 + \frac{3}{2} f^2\varepsilon_1^2 \qquad (A.9)$$

where

$$f = f_1\left(\pm Z_L\right)$$

The derivative boundary conditions (A.3) take the form

$$\frac{\partial}{\partial\theta}\sum_{n=o}^{\infty}\varepsilon_2^n T_n\left(Z,0\right) = \frac{\partial}{\partial\theta}\sum_{n=o}^{\infty}\varepsilon_2^n T_n\left(Z,\pi\right) = 0 \qquad (A.10)$$

Expanding (A.8), (A.9) and (A.10) into the indicated series and collecting coefficients of like powers of ε_2 gives the series of partial differential equations and boundary conditions,

n = 0

$$\frac{\partial^2 T_o}{\partial \theta^2} + \frac{\partial^2 T_o}{\partial Z^2} = 0 \tag{A.11}$$

$$T_o\left(\pm Z_L\right) = 1 + \frac{3}{2} f^2 \varepsilon_1^2 \tag{A.12}$$

$$\frac{\partial T_o(Z,O)}{\partial \theta} = \frac{\partial T_o(Z,\pi)}{\partial \theta} = 0 \tag{A.13}$$

n = 1

$$- \cos\theta \frac{\partial^2 T_o}{\partial \theta^2} - \sin\theta \frac{\partial T_o}{\partial \theta} - 2 T_o \cos\theta + \frac{\partial^2 T_1}{\partial \theta^2} + \frac{\partial^2 T_1}{\partial Z^2} - \cos\theta \frac{\partial^2 T_o}{\partial Z^2} = 0 \tag{A.14}$$

$$T_1\left(\pm Z_L\right) = - 2 \cos\theta \tag{A.15}$$

$$\frac{\partial T_1(Z,O)}{\partial \theta} = \frac{\partial T_1(Z,\pi)}{\partial \theta} = 0 \tag{A.16}$$

n = 2

$$- \cos\theta \frac{\partial^2 T_1}{\partial \theta^2} - \sin\theta \frac{\partial T_1}{\partial \theta} - 2 T_1 \cos\theta + \frac{\partial^2 T_2}{\partial \theta^2} + \frac{\partial^2 T_2}{\partial Z^2} - \cos\theta \frac{\partial^2 T_1}{\partial Z^2} = 0 \tag{A.17}$$

$$T_2\left(\pm Z_L\right) = \cos^2\theta = \frac{1}{2}\left(1 + \cos 2\theta\right) \tag{A.18}$$

$$\frac{\partial T_2(Z,0)}{\partial\theta} = \frac{\partial T_2(Z,\pi)}{\partial\theta} = 0 \tag{A.19}$$

n = 3

$$- \cos\theta \frac{\partial^2 T_2}{\partial\theta^2} - \sin\theta \frac{\partial T_2}{\partial\theta} - 2\, T_2 \cos\theta + \frac{\partial^2 T_3}{\partial\theta^2} + \frac{\partial^2 T_3}{\partial Z^2}$$

$$- \cos\theta \frac{\partial^2 T_2}{\partial Z^2} = 0 \tag{A.20}$$

$$T_3\left(\pm Z_L\right) = 0 \tag{A.21}$$

$$\frac{\partial T_3(Z,0)}{\partial\theta} = \frac{\partial T_3(Z,\pi)}{\partial\theta} = 0 \tag{A.22}$$

The same pattern that is evident in (A.14), (A.17), (A.20) continues for higher values of n, and all boundary values are zero.

A.2 SOLUTION FOR T_o AND T_1

The solution of (A.11) is

$$T_o = 1 + \frac{3}{2} f^2 \epsilon_1^2 \tag{A.23}$$

Putting this value of T_o into (A.14) gives

$$\frac{\partial^2 T_1}{\partial\theta^2} + \frac{\partial^2 T_1}{\partial Z^2} - 2\, T_o \cos\theta = 0 \tag{A.24}$$

The variables may be separated in (A.24) by assuming a solution of the form

$$T_1 = h_1(Z) \cos\theta \tag{A.25}$$

giving

$$h_1'' - h_1 = 2\,T_o \tag{A.26}$$

with the requirement from the boundary conditions (A.15)

$$h_1\Big|_{\pm Z_L} = -2 \tag{A.27}$$

The solution of (A.26) is

$$h_1 = -2\left[T_o + \left(1-T_o\right)\frac{\cosh Z}{\cosh Z_L}\right] \tag{A.28}$$

giving

$$T_1 = -2\cos\theta\left[T_o + \left(1-T_o\right)\frac{\cosh Z}{\cosh Z_L}\right] \tag{A.29}$$

A.3 SOLUTION FOR T_2

Putting (A.25) for T_1 into (A.17) gives the partial differential equation for T_2 ,

$$\frac{\partial^2 T_2}{\partial\theta^2} + \frac{\partial^2 T_2}{\partial Z^2} - \left(h_1 + h_1''\right)\cos^2\theta + h_1 \sin^2\theta = 0 \tag{A.30}$$

Assume a product solution of (A.30) of the form

$$T_2 = g_o(Z) + g_1(Z) \cos \theta + g_2(Z) \cos 2\theta \tag{A.31}$$

Putting (A.31) into (A.30) gives

$$\left(g_o'' - \frac{h_1''}{2}\right) + \left(g_1'' - g_1\right) \cos \theta + \left(g_2'' - 4g_2 - h_1 - \frac{h_1''}{2}\right) \cos 2\theta = 0 \tag{A.32}$$

with the boundary conditions from (A.18)

$$g_o\left(\pm Z_L\right) = \tfrac{1}{2} \tag{A.33}$$

$$g_1\left(\pm Z_L\right) = 0 \tag{A.34}$$

$$g_2\left(\pm Z_L\right) = \tfrac{1}{2} \tag{A.35}$$

Since the terms in 1, cos θ, cos 2θ, $\cdots$ cos $n\theta$ are orthogonal, each coefficient of (A.32) must be zero thus leading to the differential equations

$$g_o'' - \frac{h_1''}{2} = 0 \tag{A.36}$$

$$g_1'' - g_1 = 0 \tag{A.37}$$

$$g_2'' - 4g_2 - h_1 - \frac{h_1''}{2} = 0 \tag{A.38}$$

Equation (A.36) is

$$g_o'' + \left(1 - T_o\right) \frac{\cosh Z}{\cosh Z_L} = 0 \tag{A.39}$$

which can be integrated twice to get

$$g_o = -\left(1 - T_o\right)\frac{\cosh Z}{\cosh Z_L} + C_1 Z + C_2 \qquad (A.40)$$

The boundary values (A.33) require that

$$C_1 = 0 \qquad \text{and} \qquad C_2 = \frac{3}{2} - T_o$$

giving the solution

$$g_o = -\left(1 - T_o\right)\frac{\cosh Z}{\cosh Z_L} + \frac{3}{2} - T_o \qquad (A.41)$$

Equation (A.37) has the solution

$$g_1 = C_1 e^{Z} + C_2 e^{-Z} \qquad (A.42)$$

but the boundary values (A.34) are only satisfied if

$$C_1 = C_2 = 0$$

therefore

$$g_1 = 0 \qquad (A.43)$$

Equation (A.38) can be written

$$g_2'' - 4g_2 = -2\,T_o - 3\left(1 - T_o\right)\frac{\cosh Z}{\cosh Z_L} \qquad (A.44)$$

The solution of the homogenous part of (A.44) is

$$g_{2H} = C_1 e^{2Z} + C_2 e^{-2Z} \tag{A.45}$$

A particular solution of (A.44) is

$$g_{2p} = \left(1 - T_o\right) \frac{\cosh Z}{\cosh Z_L} + \frac{T_o}{2} \tag{A.46}$$

The general solution with consideration of the boundary values (A.35) is then

$$g_2 = \left(1 - T_o\right)\left(\frac{\cosh Z}{\cosh Z_L} - \frac{\cosh 2Z}{2 \cosh 2Z_L}\right) + \frac{T_o}{2} \tag{A.47}$$

The solution of the partial differential equation (A.30) for T_2 is then

$$\begin{aligned} T_2 = {} & \frac{3}{2} - T_o - \left(1 - T_o\right) \frac{\cosh Z}{\cosh Z_L} \\ & + \left[\left(1 - T_o\right)\left(\frac{\cosh Z}{\cosh Z_L} - \frac{\cosh 2Z}{2 \cosh 2Z_L}\right) + \frac{T_o}{2}\right] \cos 2\theta \end{aligned} \tag{A.48}$$

It was hoped that this additional term would be enough to give answers of acceptable accuracy for large values of ε_2 ; however comparison to the numerical solution, though showing a significant improvement due to this term, was still not good enough.

A.4 SOLUTION FOR T_3

Writing

$$T_2 = g_o(Z) + g_2(Z) \cos 2\theta$$

then (A.20) can be put in the form

$$\frac{\partial^2 T_3}{\partial \theta^2} + \frac{\partial^2 T_3}{\partial Z^2} + \left(2g_2 - \frac{g_2''}{2} - 2g_o - g_o''\right) \cos \theta - \frac{g_2''}{2} \cos 3\theta = 0 \tag{A.49}$$

The variables in (A.49) may be separated by assuming a solution of the form

$$T_3 = k_o(Z) + k_1(Z) \cos \theta + k_2(Z) \cos 2\theta + k_3(Z) \cos 3\theta \tag{A.50}$$

Putting (A.50) into (A.49) gives

$$k_o'' + \left(k_1'' - k_1 + 2g_2 - \frac{g_2''}{2} - 2g_o - g_o''\right) \cos \theta + \left(k_2'' - 4k_2\right) \cos 2\theta + \left(k_3'' - 9k_3 - \frac{g_2''}{2}\right) \cos 3\theta = 0 \tag{A.51}$$

Putting (A.50) into the boundary values (A.21) gives

$$k_o\left(\pm Z_L\right) = k_1\left(\pm Z_L\right) = k_2\left(\pm Z_L\right) = k_3\left(\pm Z_L\right) = 0 \tag{A.52}$$

Again orthogonality of the series in cos $n\theta$ gives the differential equations

$$k_o'' = 0 \tag{A.53}$$

$$k_1'' - k_1 + 2g_2 - \frac{g_2''}{2} - 2g_o - g_o'' = 0 \qquad (A.54)$$

$$k_2'' - 4k_2 = 0 \qquad (A.55)$$

$$k_3'' - 9k_3 - \frac{g_2''}{2} = 0 \qquad (A.56)$$

The only solutions of (A.53) and (A.55) which satisfy the boundary conditions are

$$k_o = 0 \qquad (A.57)$$

$$k_2 = 0 \qquad (A.58)$$

The solutions of (A.54) and (A.56) proceed in a straight forward fashion and eventually lead to

$$k_1 = \left(1 - T_o\right)\left[\frac{9Z_L \tanh Z_L \cosh Z - 9Z \sinh Z + 12\left(\cosh Z - \cosh Z_L\right)}{4 \cosh Z_L}\right] \qquad (A.59)$$

and

$$k_3 = -\left(1 - T_o\right)\left[\frac{\cosh Z}{16 \cosh Z_L} - \frac{\cosh 2Z}{5 \cosh 2Z_L} + \frac{11}{80}\frac{\cosh 3Z}{\cosh 3Z_L}\right] \qquad (A.60)$$

The expression for T_3 is now completely determined by substituting (A.57), (A.58), (A.59) and (A.60) into (A.50)

Additional terms could be found in the same manner but subsequent tests showed that terms including those to ε_2^3 gave sufficient accuracy.

APPENDIX B

APPENDIX B

COMPARISON OF THE AUGMENTED, SMALL-PARAMETER SOLUTION TO THE NUMERICAL SOLUTION

In order to show that the augmented equation had sufficient terms to be an acceptable solution, the load support computed by using T from the finite-difference method was compared to the load support computed by using T from the augmented, small-parameter solution with the ε_2^3 term. In both cases, the integration of the load support equation was performed numerically using Simpson's rule.

It was known that an error existed in the direct numerical method due to the finite grid size used. Since the answers computed by this method were to be used as a standard, the error must be reduced to a minimum. The numerical method approximated the derivatives in the squeeze-film equation by central differences, of second order accuracy, thus it was expected that the error in T would be proportional to the square of the mesh spacing in both the Z and θ directions. If M and N are the number of nodes in the Z and θ directions respectively, then $m = \frac{1}{M-1}$ and $n = \frac{1}{N-1}$ are the respective mesh spacings.

One method of improving the accuracy would be to increase the number of nodes in the two directions, this however, would certainly increase the computer time needed for a solution and, if carried to extremes, might well increase the truncation and roundoff errors to

unacceptable levels. The computations were to be performed on an IBM System/360-50, which in single precision, carries six hexadecimal digits (equivalent to approximately 7.2 decimal digits) thus roundoff error could rather quickly reach unacceptable levels.

An investigation was made to determine if an extrapolation to zero mesh size, based on the assumed error being $0(m^2)$ and $0(n^2)$, would be effective. It was assumed that the domain of interest for the independent variables was

$$0 < \varepsilon_1 \leq 0.5$$

$$-1 \leq A \leq 0$$

$$0.6 \leq Z_L \leq 1.5$$

$$-0.8 \leq \varepsilon_2 \leq 0$$

A sampling was made using mesh sizes ranging from 9 x 9 to 17 x 41 at the extremes of the above domain. It was quickly apparent that the effect of mesh size was greatest for small values of ε_1, for large absolute values of ε_2, for $A = -1$, and for large values of Z_L. It also appeared that the N mesh spacing (θ direction) was more critical than the M spacing (Z direction). The worst combination of values which was found is shown in Table B.1, and plotted versus n in Figure B.1.

It appears from Figure B.1 that the points lie on a straight line ($N = 9$ appears to be a slight exception) and that the error is $0(n^2)$. It also appears that an answer extrapolated from the 9 x 9

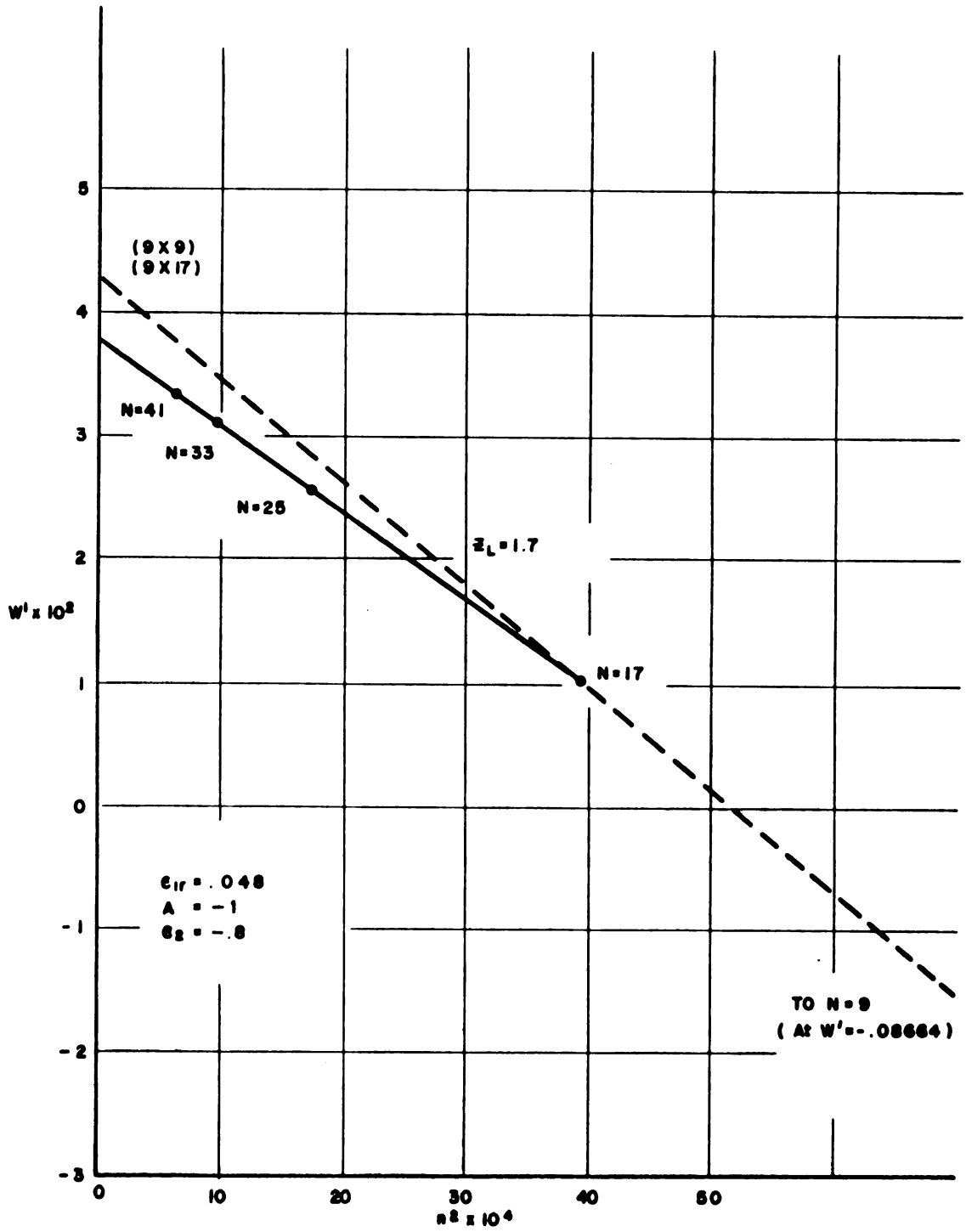

Figure B.1 Load support as a function of mesh spacing in the axial direction

TABLE B.1 COMPARISON OF THE EFFECT OF THE NUMBER OF NODES ON LOAD SUPPORT CALCULATIONS. (ε_{1r}=0.048, ε_2 = - 0.8, A = - 1)

M	m^2	N	n^2	W' AT Z_L = .5	W' AT Z_L = 1.7
9	.0156	9	.0156	.025626	-.086639
9	.0156	17	.00391	.062890	.010319
9	.0156	25	.00174	.069058	.025852
9	.0156	33	.000977	.071179	.031138
9	.0156	41	.000625	.072168	.033602
17	.00391	17	.00391	.062717	.0092033
17	.00391	25	.00174	.068907	.024931
17	.00391	33	.000977	.071035	.030282
17	.00391	41	.000625	.072029	.032778

grids (W' = 0.04253) is closer to the answer extrapolated from 9 x 17 and 9 x 24 (W' = 0.03831) than is the single computation at 9 x 41 (W' = 0.033602). It appears that extrapolation from two coarse grids gives a better answer than that from one fine grid. Using grid size as a measure of computer time, the 9 x 9 and 9 x 17 combination should be nearly twice as fast as a single 9 x 41 grid. In all other cases checked the slope of the extrapolation curve was less than that of Figure B.1 indicating that the accuracy of the answer extrapolated from the coarse grids was proportionately better.

At the other extreme of large values of ε_1 and small absolute values of ε_2 it was found that the slope of the curve of W' versus n^2 was essentially zero but that W' plotted versus m^2 now had a significant slope. Thus in one case extrapolation on n^2 improves the answer; in the other case extrapolation on m^2 is

necessary. To cover both cases then, extrapolation is necessary in the m^2 - n^2 plane rather than linear extrapolation on either m^2 or n^2 although the greatest improvement is made by n^2 extrapolation. The final result was that the computation was performed three times with meshes of 9 x 17, 9 x 25, and 17 x 17 respectively, with extrapolation of a plane to zero mesh size in both the m^2 and n^2 directions.

A short investigation was also made to determine if the Simpson's rule integration for W' was introducing any measureable error. This was done by computing the T values for a given mesh (say 17 x 17) then using quadratic interpolation to generate the missing values in a mesh with twice the number of intervals (33 x 33). Each set of values was integrated and the final answers compared. There was no significant difference between the two computations. Consider the case when T in (2.23) is given by

$$T = \hat{T}\left[1 + O(\Delta\theta)^2 + O(\Delta Z)^2\right] \tag{B.1}$$

where $\hat{T}$ is the exact value. Then

$$T^{\frac{1}{2}} = \hat{T}^{\frac{1}{2}}\left[1 + O(\Delta\theta)^2 + O(\Delta Z)^2\right] \tag{B.2}$$

All other terms in the integrand of (2.23) can be expressed exactly. Since the error in Simpson's rule is of the order of the fourth power of the mesh spacing, this error is evidently insignificant compared to the $O(m^2)$ or $O(n^2)$ of the T computation itself.

An error analysis performed on the finite difference equations

for small absolute values of ε_2 showed that the magnitude of the error is approximately

$$\left|\eta\right|_{max} = \varepsilon_2\left[\frac{m^2}{12} + \frac{5n^2}{6}\right] \qquad (B.3)$$

bearing out the observation that the n interval (θ direction) is more important than the m interval (Z direction).

Finally, the finite difference computation for W' was compared to the augmented, small-parameter solution. The results of this comparison are shown in Figure B.2 for the worst case. (Worst in that the augmented equations are exact in ε_1, so that the maximum error should be associated with small ε_1 and large absolute values of ε_2.) In the range of interest of $0.7 \leq Z_L \leq 1.5$ the maximum difference for the augmented equation including terms to ε_2^3 was at $Z_L = 0.7$ and amounted to less than 10%. The error for the augmented equation to including terms to ε_2^2 however was an unacceptable 28%.

It was concluded that the augmented equation with terms to ε_2^3 gave answers which would be more than accurate enough for the present investigation. Further, when only load support is needed in any future work the augmented equation will suffice. The computer time for the finite-difference equation is approximately 20 seconds per load support computation compared to less than 4 seconds for the augmented equation when using the IBM System/360-50.

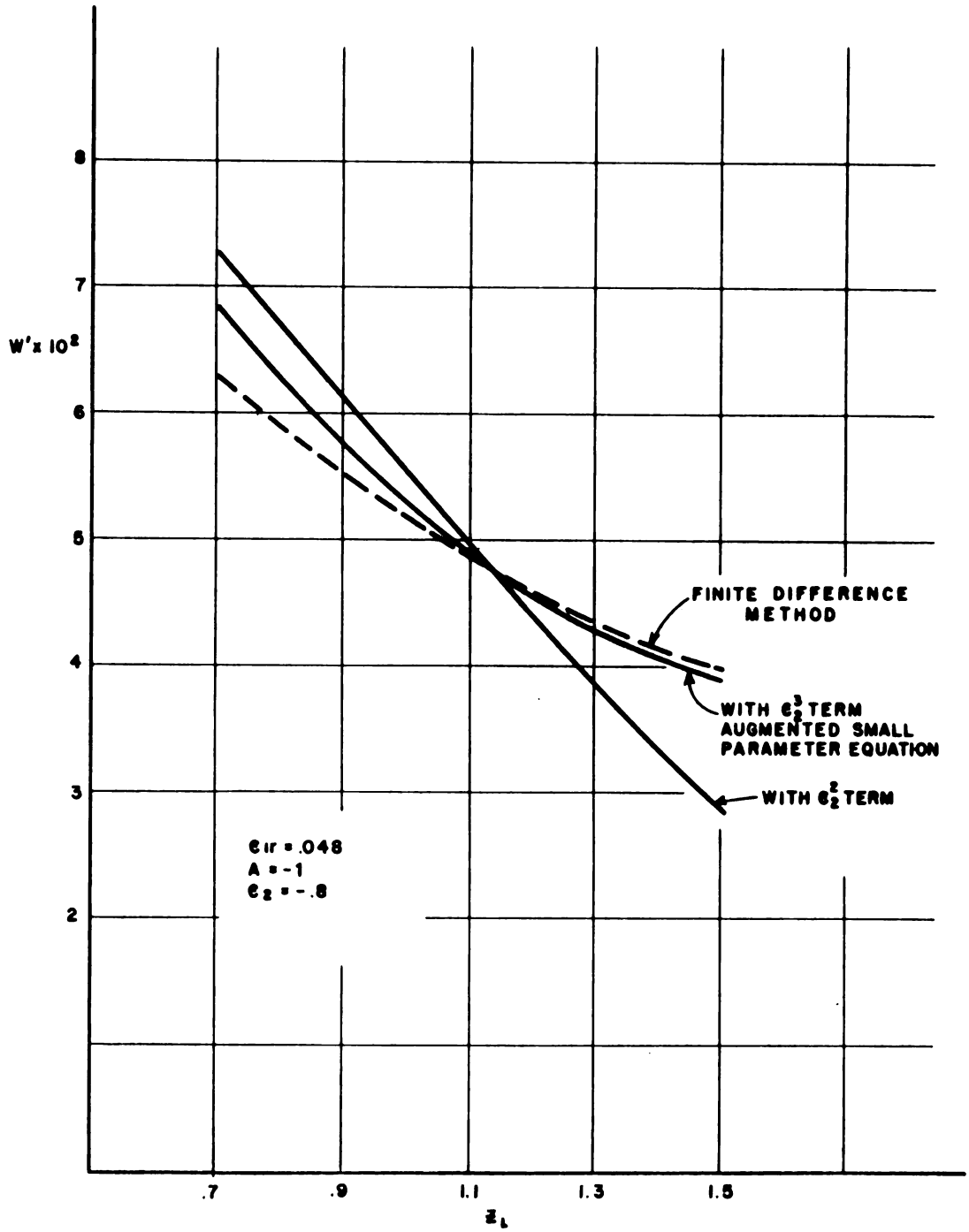

Figure B.2 Comparison between finite difference solution and augmented, small-parameter equation.